Projecting the Impact of Electrification of the Uinta Basin Oil and Gas Fields on Air Quality

March 15, 2022

A STEP project prepared for PacifiCorp

By:

Marc Mansfield
Liji David
Huy Tran
Seth Lyman

Robert Hammer
Xin Qiu

Bingham Research Center
Utah State University Uintah Basin

SLR International

TABLE OF CONTENTS

EXECUTIVE SUMMARY

Emissions of ozone precursors, namely, nitrogen oxides (NO_x) and volatile organic compounds (VOC), need to be reduced in the Uinta Basin to meet air quality standards for ozone pollution set by the Clean Air Act. The oil and gas industry in the Basin contributes significant amounts of these emissions, through the use of internal combustion engines and other equipment. In principle, such emissions could be reduced if equipment were switched to electric power. All the following emissions categories could be mitigated through electrification:

- Pumpjack engine NO_x and VOC emissions
- Separators and heaters NO_x emissions
- Pneumatic controller VOC emissions
- Pneumatic pump VOC emissions
- Storage tank VOC emissions
- Drilling and completions NO_x and VOC emissions

Recent independent measurements indicated that existing estimates of emissions by pumpjack engines and drilling and completions were unreliable, and so we developed improved emissions estimates for these two categories. These new estimates combined with previous estimates developed by the Utah Division of Air Quality (UDAQ) indicate that pumpjack engines, separators and heaters, and drilling and completions are the most important emission sources.

We developed computer models to predict the impact of NO_x and VOC reductions on winter ozone concentration. These models indicate that ozone concentrations will respond about equally to reductions in either NO_x or VOC. The computer models also suggest that elimination of all pumpjack engines, separators, and heaters through electrification will produce a reduction of 24 ppb in peak ozone concentrations. The additional elimination of NO_x and VOC emissions from drilling and completions will produce a further reduction of 4 ppb.

We also examined the engineering and implementation aspects of electrification, including (1) the existing Uinta Basin transmission grid, (2) beneficial infrastructure changes, (3) existing infrastructure development plans, (4) characteristics and emissions of existing internal combustion engines, (5) challenges faced by electrification expansion, (6) reliability of electrification, and (7) complimentary emission reductions that might result from electrification.

We considered four separate geographical regions within the Uinta Basin (regions A through D defined in the map in Figure 29) and examined how the existing power grid could be expanded to each of the four regions. The oil fields to the north of US Highway 40, region A, are already electrified. The eastern portion of the basin, region B, is dominated by natural gas production, so electrification would have a small impact on air quality. Region C appears to be the most favorable region for electrical development for several reasons, especially proximity to existing or planned transmission lines. Region D, containing the most pumpjacks, would also benefit, but extension throughout this larger, more remote region would be more costly.

We examined the economic and social costs and benefits to electrification. The cost of constructing utility distribution lines is estimated at around $50,000 to $90,000 per mile. [Cook et al. 2017a] Existing powerplant production would probably not be adequate to cover the higher demand. Costs of switching from internal combustion engines to electric motors must also be considered. Onsite generation of electricity is economically advantageous in many regions but is problematic in the Uinta Basin since internal combustion engines are still required. On the other hand, the oil and gas industry is the economic lifeblood of the Uinta Basin: Between 2010 and 2019, 18% of Uinta Basin jobs and 31% of Uinta Basin wages were directly related to the industry, and many Basin residents faced significant economic hardships when the industry declined in 2015. If the only way to satisfy the demands of the Clean Air Act is to curtail that industry, then the societal costs will also prove to be enormous.

I. INTRODUCTION

I. A. Project overview

A program, the Sustainable Transportation and Energy Plan (STEP), administered by PacifiCorp and funded by the Utah State Legislature, has been developed to foster sustainable energy solutions for the State of Utah. Early in 2021, The Bingham Research Center of Utah State University (USU) and SLR International Corp., an environmental consulting firm, applied for STEP funding. The USU/SLR project, "Projecting the Impact of Electrification of the Uinta Basin Oil and Gas Fields on Air Quality," was approved by the Utah Public Service Commission and work commenced in July 2021.

The oil and natural gas fields of the Uinta Basin in Duchesne and Uintah Counties, Utah, provide most of the oil and natural gas produced in the state. A large portion of the oil and gas fields are not electrified, and many pieces of equipment contribute to the winter ozone problem in the Basin. For example, there are thousands of artificial lift or "pumpjack" engines in the Basin that pump oil out of wells. In most of the Basin, these are powered by natural-gas-fueled engines that emit ozone precursors. Electrification of all pumpjacks would remove this emission source. Other equipment that could be electrified include other engines, pneumatic pumps and controllers, heaters, separators, storage tanks, and well drilling and completion activities. The goal of the USU/SLR project has been to better understand the more important emitter classifications to better understand the impact that electrification would have on Uinta Basin air quality.

I. B. Ozone formation in the Uinta Basin

Ozone is a very reactive form of oxygen with three atoms per molecule, O_3, unlike ordinary oxygen with two atoms, O_2. Important concentrations of ozone are found in the atmosphere both at higher elevations in the stratosphere, about 15 to 35 km above sea level, and in the troposphere at the surface of the Earth. Stratospheric ozone (the "ozone layer") screens out a large fraction of solar ultraviolet radiation and is necessary for life at the surface. [Seinfeld & Pandis, *pp* 138 *ff*] However, ozone at the surface where we all live and breathe is harmful at high concentrations, especially to children, the elderly, and individuals with compromised respiratory function. [Seinfeld & Pandis, *pp* 52 *ff*] Surface ozone production occurs when two classes of compounds, collectively known as ozone precursors, are present, and when the atmosphere is illuminated by ultraviolet radiation from the sun. [Seinfeld & Pandis, *pp* 235 *ff*] The two classes of compounds are usually designated VOC and NO_x:

(1) VOC, or "volatile organic compound," literally is any organic (carbon-containing) molecule found in the gas phase, although usually carbon monoxide and carbon dioxide are not included in the definition. Also, because it has a low ozone reactivity, methane and ethane are often excluded. Nevertheless, in this report methane and ethane are counted as

a VOC, unless explicitly stated otherwise. VOC sources are engine exhaust, infrastructure leakage, storage tanks, etc.

(2) Two oxides of nitrogen, nitrogen oxide, NO, and nitrogen dioxide, NO_2, are important in atmospheric chemistry. In the sun-lit atmosphere, the two molecules interconvert so rapidly that the two act as a single entity, nitrogen oxides, $NO_x = NO + NO_2$. [Seinfeld & Pandis, pp 209 ff] NO_x results from the oxidation of nitrogen in any process that heats air, and internal combustion engines and other flames are the most significant NO_x sources.

Surface ozone concentrations usually follow a diurnal pattern. They begin to rise at sunrise, grow throughout the morning, peak in the afternoon, and decline again over night. The Environmental Protection Agency (EPA) has established the "National Ambient Air Quality Standard," (NAAQS) for ozone to be 70 parts per billion (ppb). Any day during which the eight-hour running-average ozone concentration exceeds the NAAQS constitutes one "exceedance" of the ozone standard. Legislative and regulatory restrictions come into play whenever the exceedance count in any one calendar year gets too high.

The Uinta Basin experiences ozone both in summer and winter, and the root causes differ in the two seasons. As far as we know, high concentrations of ozone in winter are very rare, occurring only in the Uinta Basin and in the Upper Green River Basin of western Wyoming. It is rare elsewhere because the low-lying winter sun cannot provide enough ultraviolet radiation. However, in the Uinta Basin, three ingredients combine in a perfect storm (Figure 1): One, persistent (i.e., multi-day) thermal inversions act to trap ozone precursors in a shallow boundary layer (about 200 m thick) adjacent to the ground, with the bowl-shaped basin topography contributing to inversion formation. Two, the high surface albedo (reflectivity) of the snowpack has two roles: It nearly doubles the amount of solar radiation available for photochemical reactions and it stabilizes and intensifies thermal inversions. Three, the chemical makeup of the precursor mix generated by the oil and natural gas industry is well-suited for ozone production. (Typical urban precursor mixes do not stimulate ozone, even with snow and inversions.)

Summer ozone in the Basin usually occurs in conjunction with wildfires. Wildfire-generated precursors can blow into the Basin from anywhere in western North America and the summer sun provides adequate solar radiation. Because the summer atmosphere is rarely inverted, local precursors, either from the oil and gas industry, from traffic, or from vegetation, do not accumulate enough to make a significant contribution.

Historically, summer ozone has not been as important as winter ozone. One or two exceedances of the NAAQS, usually in the range of 70 to 80 ppb, are seen each summer, while winters when all the necessary ingredients are present have been known to produce dozens of exceedances, sometimes in the range of 100 to 120 ppb or more.

Winter ozone measurements in the Basin began in 2010 and have shown a statistically significant decline ever since. [Mansfield & Lyman, 2021] Two contributing factors have been first, the decline in oil and gas drilling and production which has occurred over the previous decade, and second, pollution control measures that have come online.

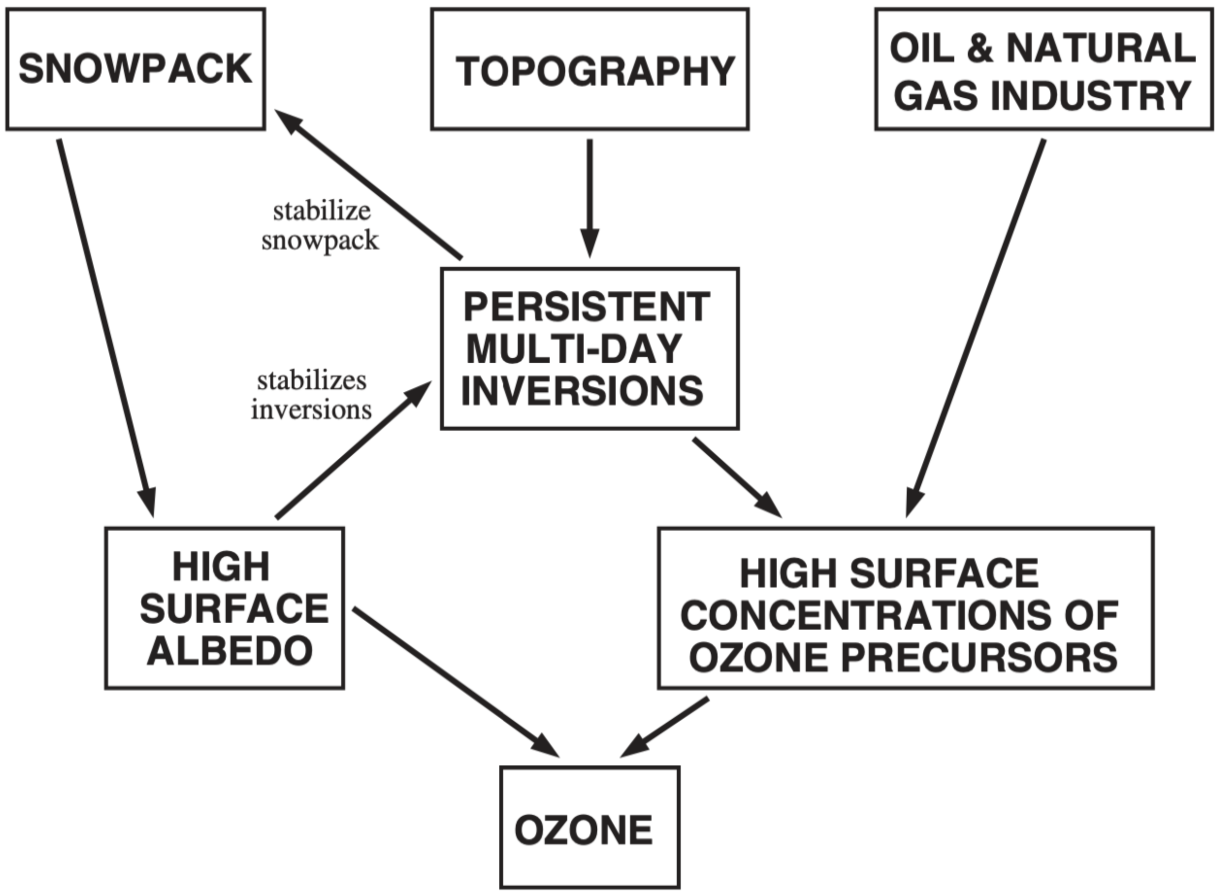

Figure 1. Winter ozone requires several ingredients: A basin topography helps stabilize persistent thermal inversions, an active oil and natural gas extraction industry generates ozone precursors that become concentrated at the surface, a snowpack reflects most incoming solar radiation which triggers the photochemical production of ozone.

I. C. Ozone sensitivity to NO_x and VOC precursors; the photochemical regime

Not all ozone precursors have the same impact on ozone formation. In any given air mass, ozone formation may be more sensitive either to NO_x or to VOC, i.e., ozone concentrations respond more strongly to reductions in one rather than the other. We will use the expressions "NO_x-sensitive regime," "VOC-sensitive regime," and generically, the "photochemical regime" to describe this behavior. (Other terms have the same meaning: "NO_x-limited," "NO_x-controlled," etc.) NO_x-sensitivity usually results when there is so much VOC that adding or subtracting more has no impact, and vice versa. If you want to bake cakes and have twenty pounds of flour but only two eggs, then you are "egg-limited:" The number of eggs, not the amount of flour, is the controlling factor in the number of cakes you can bake. An air mass might also be in an intermediate photochemical regime, being sensitive to both NO_x and VOC.

Knowing the photochemical regime of a given region is important. It would be wasteful to apply expensive NO_x controls, for example, if the air is mostly VOC-sensitive. In fact, it could make matters worse. An occasional characteristic of VOC-sensitivity is that reducing NO_x can generate *more* ozone. [Shi & Brasseur, 2020] (NO_x in the atmosphere can react to generate or deplete ozone. Net ozone formation depends on the balance between these two trends.) Determining the photochemical regime of any particular region is non-trivial, requiring accurate modeling.

Mainly because of deficiencies in the existing models, the photochemical regime of the Uinta Basin in winter has never been definitively determined. At the beginning of this study, we believed that available evidence indicated NO_x control, along with some VOC dependence. However, our group has steadily improved the models, and they now point to a mixed regime, indicating that controlling either for NO_x or VOC will reduce ozone concentrations.

VOC compounds also have very different ozone reactivities. This is the problem of VOC "speciation," or of determining the precise chemical mix of VOC compounds in the air mass. VOCs emitted by the oil-and-gas sector are very different from the typical urban mix, which is not conducive to winter ozone. Our measurements have found many more ozone-reactive VOC compounds in the Uinta Basin ambient air than are found in urban settings. Default speciations usually used in modeling are based on these urban emissions. However, All the models used in this project relied on the most recent speciation measurements rather than any of the defaults.

I. D. Federal, state, and tribal air quality regulations and enforcement

Depending on land ownership, several different agencies, including the Environmental Protection Agency (EPA), the Bureau of Land Management (BLM), the Utah Division of Air Quality (UDAQ) and the Ute Tribe, are responsible for monitoring and regulating atmospheric emissions in the Basin. Duchesne and Uintah counties have been assigned "marginal ozone non-attainment" status since 2018 under the Clean Air Act, and should, in all likelihood, advance soon to "moderate" non-attainment. Under moderate non-attainment, EPA, UDAQ, and the Ute Tribe will be required to develop "State" and "Federal Implementation Plans" (SIPs and FIPs) spelling out actions to bring the Basin into compliance. Uinta Basin oil has a tighter profit margin than many other crude oils, and costly pollution abatement scenarios will further tighten the margin. Since the industry completely underpins the Basin economy, it will be important to find ozone abatement scenarios that permit the industry to continue to operate.

I. E. Atmospheric modeling techniques employed in this study

I. E. 1. "Box" modeling techniques for modeling atmospheric chemistry

We used the "Framework for 0-D Atmospheric Modeling" (F0AM) platform developed by Wolfe and coworkers in one part of the study. [Wolfe et al. 2016] It is what atmospheric modelers call a "box" model. More sophisticated models are required when one wants to account for topography and geographically distributed emissions. Box models are appropriate when we want to focus attention only on chemical processes isolated from meteorology or topography. A good way to think about box models is that they represent chemical reactions in a smog chamber in the laboratory, when the effects of temperature, humidity, pressure, ultraviolet light intensity, precursor concentrations, etc., are under the control of the experimenter and the reactions are carried out in isolation from the environment.

The chemical processes in any model are represented by a chemistry module or "mechanism." The chemistry module consists of a list of molecular species and a list of chemical reactions that occur among the species. It also includes specifications for calculating the rate of each reaction as a function of temperature, pressure, ultraviolet light intensity, etc. Several different modules have been developed. Our box-model work employed a subset of the "Master Chemical Mechanism," MCM v3.3.1, [Jenkin et al. 2003; Jenkin et al. 2015; Saunders et al. 2003; Zong et al. 2018; MCM 2022] including about 3,400 different molecular species and 17,000 different reactions.

I. E. 2. Definitions of ozone sensitivity to VOC and NO_x

There are a number of ways to quantify the sensitivity of an ozone model to VOC or NO_x concentrations. We have employed two. One considers sensitivities to small or incremental changes in VOC or NO_x concentrations, the other to large (40%) reductions.

To simplify the notation in the following definitions, let *x* and *y* represent, respectively, VOC and NO_x concentrations, and let *z* represent the ozone concentration. Mathematically, a box model defines *z* as a function of *x* and *y*. Let *dz* represent a small change in the ozone concentration resulting from a small change, *dx* or *dy*, in the VOC or NO_x concentration. Then fractional changes in any of the variables are

$$\frac{dx}{x}, \qquad \frac{dy}{y}, \qquad \frac{dz}{z} \qquad \text{(Eq. 1)}$$

Define incremental sensitivities of ozone to either VOC or NO_x as the following ratios of fractional changes:

$$S_i(VOC) = \frac{dz}{z} \Big/ \frac{dx}{x} = \frac{x}{z}\,\frac{dz}{dx} = \frac{d\ln z}{d\ln x}$$

(Eq. 2)

$$S_i(NO_x) = \frac{dz}{z} \Big/ \frac{dy}{y} = \frac{y}{z}\frac{dz}{dy} = \frac{d\ln z}{d\ln y}$$

(Eq. 3)

S_i is unitless, and is the slope of the *z* vs. *x* or *z* vs. *y* curve on a log-log plot. If we bring about a 1% reduction in VOC (or in NO_x) concentration, and if $S_i(VOC)$ = W [or $Si(NO_x)$ = W], then we produce a W% reduction in ozone concentration.

We can also define sensitivities to large changes in precursor concentrations. Here we consider the fractional reduction in ozone when *x* or *y* is decreased by 40%.

$$S_{60}(VOC)\ or\ S_{60}(NO_x) = \frac{z(100\%) - z(60\%)}{z(100\%)}$$

(Eq. 4)

Here, $z(100\%)$ represents the original ozone concentration predicted by the model, and $z(60\%)$ represents the ozone concentration when either *x* or *y* is set at 60% of its original value.

1. E. 3. Three-dimensional photochemical grid techniques

In contrast to box models, models to simulate ozone formation in an actual geographic region that take into account the topography and meteorology, are called "three-dimensional photochemical grid models." The air space is divided into a three-dimensional array of grid cells. In all our models, grid resolution in horizontal directions, i.e., along east-west and north-south axes, has been set at 1.3 km. Vertical grid resolution is not constant but varies with altitude: The models are better able to capture the dynamics of the atmosphere when grids near the surface are thinner than grids aloft. Higher grid resolution is always desirable, but the 1.3-km resolution already strains the capabilities of present-day high-performance computers.

To simulate chemical processes such as ozone formation, each grid cell executes the same algorithm as the box models discussed above, with the added complexity that matter and energy, in the form of air flow, pollutant concentration, heat, etc., are exchanged between adjacent cells according to established laws of physics. A 3D photochemical grid model can be thought of as a large set of box models, each exchanging matter and energy with its neighbors. These models are much more demanding of computer resources. We run box models on our laptops; while we run the 3D grid models on high-performance computational clusters. USU and SLR both have access to high-performance computational facilities, and the computer resources required for this project were donated by USU and SLR.

A 3D grid model must be developed in three stages: first, meteorological modeling; second, emissions modeling; and third, the actual 3D grid model.

I. E. 3. i. Meteorological modeling (WRF)

Any 3D grid model requires specification of meteorological conditions (temperature, pressure, wind speed and direction, relative humidity, etc.) in each grid cell. Observational data are available from airports and other meteorological stations, but not in every grid cell. To obtain the necessary meteorological inputs, we used the Weather Research and Forecasting (WRF) tool maintained by the National Center for Atmospheric Research (NCAR). [UCAR 2022] It is a popular system used both for atmospheric research and for weather forecasting. One way of thinking about the WRF platform is it lets us interpolate and extrapolate from any available observational data to estimate hour-by-hour meteorological conditions in each grid cell of the model according to established physical laws.

I. E. 3. ii. Emissions modeling (SMOKE)

An important distinction between box models and 3D grid models is that pollutant inputs to the box model are usually in the form of concentrations – we specify the initial concentrations of NO_x and VOC and the system calculates how those concentrations change with time. With a 3D grid model we normally specify emissions. Over one time-step of the simulation, a predetermined amount of each chemical compound is injected into each grid cell to simulate all emissions from all sources in the cell. The modeling platform applies the laws of physics and chemistry to calculate concentrations of compounds in each cell as they evolve over time.

We used a tool known as the Sparse Matrix Operator Kernel Emissions Modeling System (SMOKE), maintained by the Community Modeling and Analysis System (CMAS) community, to organize all emissions data. [CMAS 2022] There are thousands of independent emissions sources (e.g., each pumpjack engine) distributed in time and space emitting many different chemical compounds. The SMOKE tool is used to organize all the emissions data for input into the 3D grid model.

I. E. 3. iii. 3D grid modeling (CAMx)

To execute the 3D grid models, we used the Comprehensive Air Quality Model with Extensions (CAMx) platform maintained by Ramboll, an international engineering consultancy firm. [CAMx 2022] As the chemistry module, we used version 6 of the Carbon Bond Mechanism (CB6). [Yarwood 2020]

I. F. Evidence originally suggested that the Uinta Basin airmass is under NO_x control.

Based on available data, we hypothesized at the beginning of the project that the Uinta Basin airmass in winter is primarily under NO_x control, meaning that controlling NO_x emissions would have a bigger air-quality impact than controlling VOC emissions. However, the models developed in this study, which employed the best available data for VOC speciation, indicate that the system is about equally sensitive to VOC and NO_x, meaning that both types of controls should be sought for. The original hypothesis was based on several lines of evidence that we now discuss in light of the newer modeling results. In Section III.B, we present the new box model.

I. F. 1. The Edwards et al. box model

A box model [Edwards et al. 2014] suggested that the Uinta Basin air mass is more sensitive to NO_x, with limited VOC sensitivity. Based on Figure 3 of Edwards et al., the model predicted these sensitivities:

$$\begin{aligned} S_i(NO_x) &\approx 0.41 \\ S_i(VOC) &\approx 0.12 \\ S_{60}(NO_x) &\approx 0.21 \\ S_{60}(VOC) &\approx 0.11 \end{aligned} \qquad \text{(Eq. 5)}$$

and the relative sensitivities were predicted to be:

$$\frac{S_i(NO_x)}{S_i(VOC)} \approx 3.4$$

$$\frac{S_{60}(NO_x)}{S_{60}(VOC)} \approx 1.9 \qquad \text{(Eq. 6)}$$

As explained in Section I.F.2, we expected that the above relative values would hold near the beginning of the peak ozone season and become even stronger for NO_x as the peak season progressed. The difference may be a result of chemical changes that have occurred over time. In section III.A, we show that the more accurate VOC speciation data give these values for the sensitivities:

$$\begin{aligned} S_i(NO_x) &\approx 0.22 \\ S_i(VOC) &\approx 0.25 \\ S_{60}(NO_x) &\approx 0.12 \\ S_{60}(VOC) &\approx 0.12 \end{aligned} \qquad \text{(Eq. 7)}$$

with the ratios:

$$\frac{S_i(NO_x)}{S_i(VOC)} \approx 0.9$$

$$\frac{S_{60}(NO_x)}{S_{60}(VOC)} \approx 1.0$$

(Eq. 8)

Moreover, as explained in I.F.2, we expected these ratios to hold near the end of peak ozone season, and to be somewhat lower earlier in the season. NO_x and VOC reductions are now predicted to be essentially equivalent.

I. F. 2. Measurements of the ozone production efficiency

A quantity known as the ozone production efficiency (OPE), so named because it represents the number of ozone molecules generated for each NO_x consumed, can be calculated if the concentrations of ozone and certain nitrogen compounds have been measured. Interestingly, the OPE also serves as an indicator of the photochemical regime. [Sillman, 1995; Sillman et al., 1998; Sillman, 1999; Sillman & He, 2002; Seinfeld & Pandis, 2006, pp 215 ff] Larger values indicate a shift towards relatively higher NO_x sensitivity and vice versa.

We measured the OPE in the Uinta Basin [Lyman et al. 2013 & 2018] and observed that the value changes over the course of the winter, implying that the two ratios

$$\frac{S_i(NO_x)}{S_i(VOC)} \text{ and } \frac{S_{60}(NO_x)}{S_{60}(VOC)}$$

also increase as the winter progresses. The peak ozone season in the Uinta Basin is February. The Edwards et al. box model was designed to represent an ozone episode between Jan. 31 and Feb. 6, 2013, around the beginning of the peak season. Therefore, the Edwards et al. model combined with this seasonality trend suggests that the ratio of incremental sensitivities would be 3.6 or larger throughout the peak ozone season. On the other hand, the new model reported below represents an ozone episode culminating on Feb. 27, 2019, around the end of peak ozone season which implies that the ratio will be slightly less than 1 during the peak season.

Similar seasonality trends have been observed in Beijing and Shenandoah National Park, Virginia, [Chou et al. 2009, Jacob et al. 1995] suggesting that such trends in the OPE may be a global phenomenon. Our preliminary modeling results imply that temperature, absolute humidity, and solar zenith angle all drive these seasonal trends.

I. F. 3. Correlations between NO_x and ozone concentrations

As we discussed elsewhere, [Mansfield & Lyman, 2021] ambient wintertime ozone concentrations during seasons with adequate snow cover appear to be more strongly correlated with NO_x concentrations than with VOC. This suggests that the airmass is more sensitive to NO_x. On the other hand, VOC measurements have been less extensive, making it harder to detect VOC-ozone correlations. VOC concentrations can also be sensitive to localized sources. Finally, the interplay between ozone and NO_x formation chemistry can probably account for at least some of the VOC-NO_x correlation.

II. MEASUREMENTS AND ESTIMATES OF OZONE PRECURSOR EMISSIONS

A basic hypothesis of this study was that electrification of the Uinta Basin oil and gas fields would lead to important reductions in ozone precursor emissions. Obviously, any models need accurate measurements or estimates of current emissions. This section describes measurements and estimates of emissions from artificial lift, a.k.a. "pumpjack" engines, and from well drilling and completions. We concentrated on these two emissions sources because there were indications that existing estimates were inaccurate.

An independent study, (The USU Engine Study [Lyman et al 2022]), found that pumpjack engines are *not* significant NO_x emitters. Our own internet research confirmed this study. But the study also found that VOC emissions by pumpjacks are much greater than previously believed. Therefore, since our modeling now indicates that the Uinta Basin airmass is sensitive both to NO_x and to VOC, electrification of the pumpjacks should still be beneficial, eliminating a large VOC source.

New well development consists of "drilling and completions." In industry jargon, well drilling is the process of boring a new well while well completion includes all the processes, including fracking, required to prepare a new well to start producing oil or gas. As we have already shown, ozone concentrations in any winter with a snowpack are correlated with drilling and completion activities. [Mansfield & Lyman, 2021] Satellite measurements discussed below also indicate that NO_2 concentrations are correlated with drilling and completion activities. Drilling and completion activities rely on large internal combustion engines and are expected to be an important NO_x source.

II. A. Official inventories of emissions from the Uinta Basin oil and gas sector

Every three years, the Utah Division of Air Quality (UDAQ) performs official inventories of emissions by the oil and gas sector in each county. Well owners and operators are required to submit emissions data which are then compiled by UDAQ. The latest complete inventory covered the calendar year 2017 and was released in 2021 [UDAQ 2021]. These inventories are also submitted to EPA and become part of the official National Emissions Inventory (NEI). The Uinta Basin oil and gas fields lie entirely within Duchesne and Uintah counties. Below all basin-wide data reported from the inventory are the sum of estimates for these two counties.

NOx compounds are emitted to the atmosphere when ordinary nitrogen, N_2, in the air is heated in an engine or flame. It is oxidized at these high temperatures to NO and NO_2. A significant fraction of the crude oil produced in the Uinta Basin is raised to the surface by over 3,000 pumpjacks, powered by natural-gas-fueled engines. (Most of the artificial lifts north of US Highway 40 are powered by electric motors.) Table 1 displays emissions data taken from the UDAQ inventory, including three important NO_x sources accounting for nearly 70% of all NO_x emissions in the inventory: pumpjacks, drilling and completions, and separators and heaters. The UDAQ inventory [UDAQ 2021] and an independent estimate by Gorchov Negron et al. [2018] both peg the NO_x emission from pumpjack engines at about 5,000 ton/year or 41% of all oil-and-gas NO_x emissions. Drilling and completion emissions, although only 6% of NO_x in 2017, were much larger in the early years of the decade.

Table 1. Estimates of emissions of the indicated pollutant from the indicated source as a fraction of the estimate of the total emission from the oil-and-gas sector for calendar year 2017.

	Pumpjack engine emissions		
	UDAQ inventory	Revised	
NO_x	41%	1-2%	
VOC	2%	21%	
	Drilling and completion emissions		
	UDAQ inventory	Revised, tier 2 assumption	Revised, tier 4 assumption
NO_x	6%	19%	8%
VOC	< 1%	< 1%	< 1%
	Separators and heaters		
	UDAQ inventory	Revised, tier 2	Revised, tier 4
NO_x	22%	33%	37%
VOC	< 1%	< 1%	

II. B. Actual measurements of pumpjack emissions indicate that the official estimates are very inaccurate.

II. B. 1. Utah State University Engine Study

Under an independent contract from UDAQ, our colleagues at Utah State University measured emissions from 58 pumpjack engines in the Basin between January and May 2021, with a few follow-up measurements in January 2022. [Lyman et al., 2022] Hereafter, we refer to the Lyman et al. 2022 study as the "USU Engine Study." Of the 58 engines studied, the average NO_x emission was only 9% of the UDAQ estimate for the same 58 engines, while the VOC emission was 15 times higher. Revision in light of the new data is also shown in Table 1: NO_x from pumpjacks falls to less than 2% of all oil-and-gas NO_x emissions; VOC from pumpjacks jumps to 17%. With the effective elimination of pumpjack NO_x contributions, drilling and completion contributions suddenly become much more important. Electrification of pumpjacks will still have an impact, because of their large VOC emission.

II.B.2. Internet search: NO_x emissions by pumpjack engines

As part of the PacifiCorp project, we have performed an internet search and subsequent estimations to better understand why UDAQ's pumpjack NO_x estimate [UDAQ 2021] is so different from the results of the USU Engine Study. The results of the Engine Study are confirmed by these independent measurements.

Engine emissions are usually reported as the "specific emission rate," SER, i.e., the emission in g/hr normalized by the engine load in hp, resulting in units of g/(hp-hr). This definition can be confusing, because it is often not clear from the context whether the emission has been normalized by the engine's horsepower rating as reported by the manufacturer, or by the actual load on the engine at the moment that the emission was measured. The SER also implicitly suggests that the emission is proportional to the load, which as we show below, is far from correct, at least for the natural-gas-fueled engines used to pump oil.

Engine emissions are normally measured indirectly. Three different measurement protocols will be cited in this report and are summarized in Table 2. The USU Engine Study used the Exhaust Velocity protocol. To interpret results from the literature, we sometimes used the Ideal Gas protocol. Most other measurements used the Wyoming protocol. Because its assumptions are not totally valid, the Ideal Gas protocol is used here as a last resort. Lyman et al. [2022] report systematic differences between the Exhaust Velocity and Wyoming protocols. Here, we avoid direct comparisons between protocols to the extent possible.

Table 2. Different protocols for estimating the emission rate in g/hr or in g/(hp-hr) from pumpjack engines.

Protocol	Description
Exhaust Velocity	The product of the concentration in the exhaust, g/m^3; the exhaust velocity, m/s; and the cross-sectional area of the stack, m^2. Yields g/hr.
Ideal Gas	Assumptions: 1. At the moment the fuel-air mixture is drawn into the cylinder it is an ideal gas at standard temperature and pressure; heating and pressure change do not begin until after the valves close. 2. The combustion process does not change the total number, *n*, of ideal gas moles present. (This is a good assumption when CO_2 is the dominant combustion product: $$CH_4 + O_2 \rightarrow CO_2 + 2\, H_2O;\ \ \Delta n = 0;$$ but becomes less so as more of the product appears as CO: $$CH_4 + \frac{3}{2}\, O_2 \rightarrow CO + 2\, H_2O;\ \ \Delta n = 0.5.)$$ The flow rate is calculated given the displacement of the piston and the engine speed. Yields g/hr.
Wyoming	The emission rate in g/(hp-hr) is determined directly from NO_x and O_2 exhaust concentrations using a correlation equation recommended by the State of Wyoming. Yields g/(hp-hr) [WAQD 2006]

Laboratory measurements [Varde et al. 1995, Griffin 2015, Griffin and Jacobs 2015, Brown 2017] indicate that NO_x emissions by pumpjack engines are highly non-linear functions of the load on the engine. We display this in two ways. In Figure 2, the average NO concentration in the exhaust, measured by Griffin, [2015] is shown. In Figure 3(d), the distribution of NO_x emissions measured by Brown [2017] (calculated from engine speed and exhaust concentration data by the Ideal Gas protocol) in 44 different experiments with different operating conditions (load, speed, and spark advance) are shown and compared against other measured or estimated distributions. In both cases, note the strong dependence on engine load, spanning nearly two orders of magnitude. The Varde et al. paper [1995] also includes measurements of VOC emissions and supports the results of the USU Engine Study with regard to VOC.

Federal “quad-J” regulations require that pumpjack engines installed after 2008 undergo emissions field testing, with results on file with the State of Utah. [CFR 2022] Such tests almost always employ the Wyoming protocol. We extracted about one hundred NO_x SER values from these results and display the distributions in Figure 4. These data emphasize that SER values in the field vary widely, even for engines of the same make and model, and are usually much smaller than the values used in preparing the inventories.

We consulted a few other inventories prepared for Oklahoma, Texas, Minnesota, and the Western Regional Air Partnership [ODEQ 2012, TCEQ 2010, WRAP 2009, MPCA 2021]. All follow the same approach to estimating pumpjack engine emissions. They use a SER value appropriate at 100% load, thereby ignoring the non-linear dependence on the load documented above. Some inventories apply a load factor, but this is equivalent to using the blue line in Figure 2. This load factor is commonly assumed to be around 70%, [TCEQ 2010] but according to calculations reported below, this is also an overestimate. During February 2017, over one-half of the Uinta Basin pumpjacks lifted less than 14 barrels of water and oil per day, with, according to our calculations, a time-averaged power requirement of 1 to 2 hp or less, using engines rated between 25 and 65 hp. A majority of the pumpjack engines are operating at the far left of Figure 2 and are not working very hard. Figures 3a, 3b, and the blue bars in Figure 4 indicate the impropriety of the assumptions currently employed to estimate pumpjack NO_x emissions.

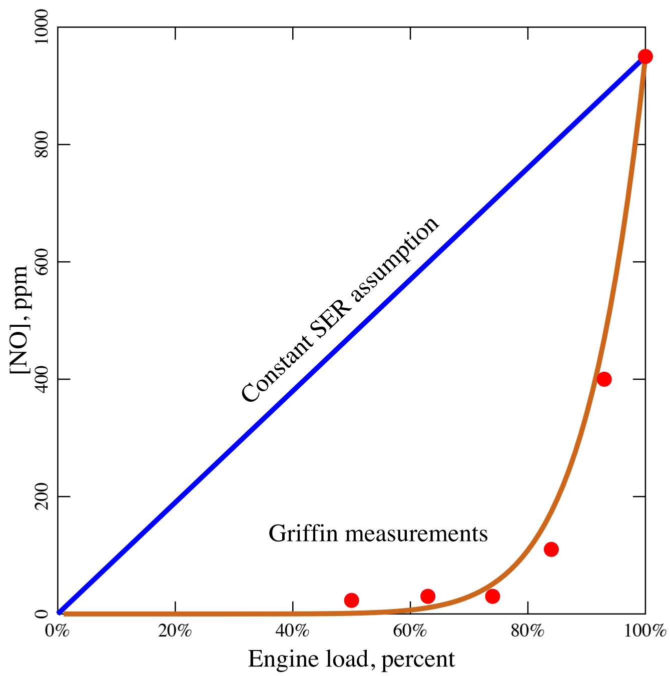

Figure 2. NO concentration in engine exhaust as a function of engine load for an Ajax E-565 engine at 450 revolutions per minute (rpm). NO concentration is highly non-linear in the load. The blue diagonal represents the expected concentration from an assumption of constant SER. Adapted from Griffin [2015], Figure 19.

We have been unable to find a definitive explanation for this strong non-linearity in the NO_x emission. It only seems to be a property of natural-gas powered engines, and since NO_x formation is a strong function of temperature, it presumably arises because the engine temperature is also a strong function of the load. Griffin [2015] speculates that it may be the result of poor scavenging leading to exhaust gas recirculation at lower loads.

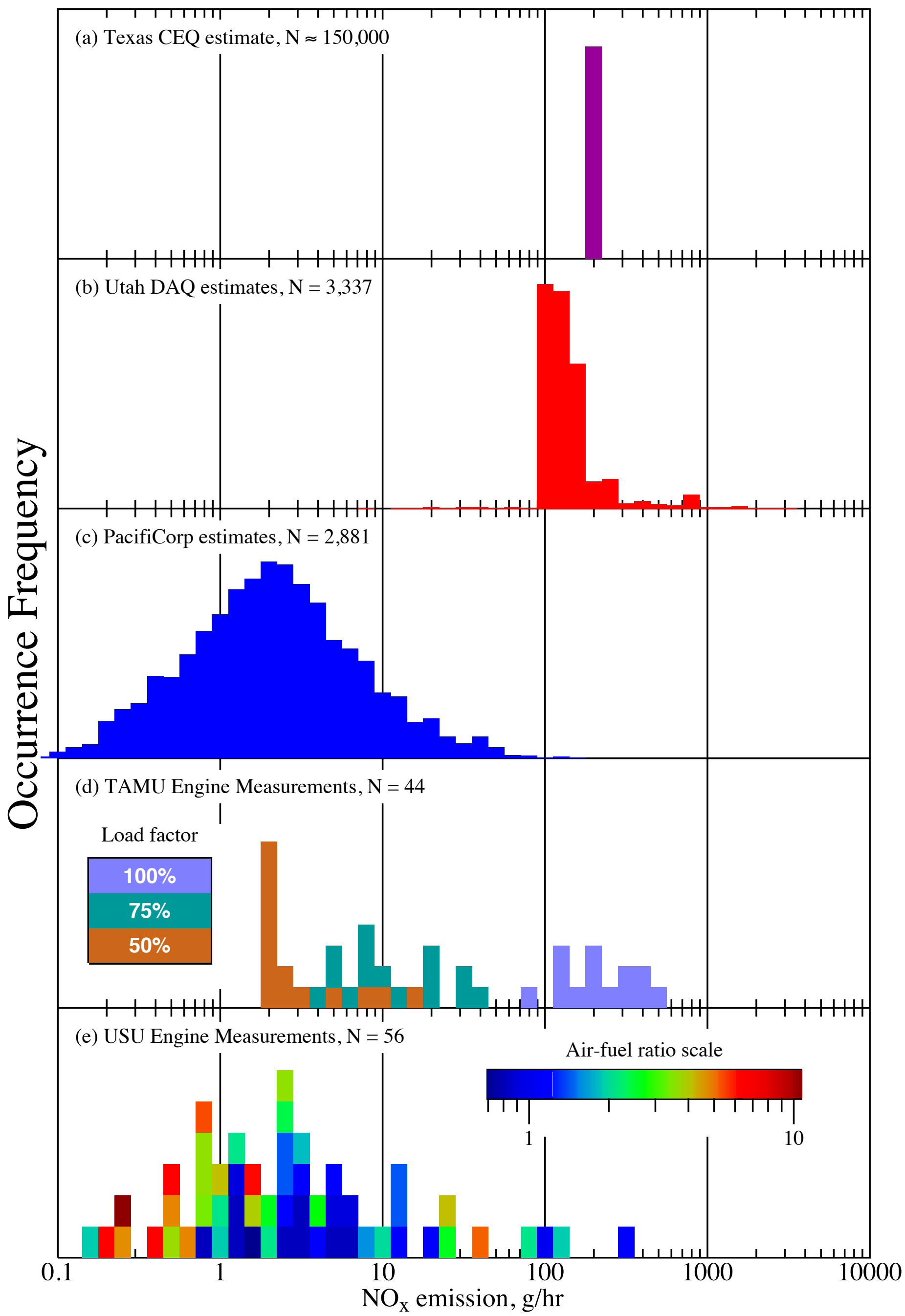

Figure 3. NO_x emissions from pumpjack engines, either estimates or measurements. N is the number of engines or independent measurements. (a) An emissions inventory for the Texas Commission on Environmental Quality [TCEQ] applies a blanket average 215 g/hr to all engines in the inventory. (b). The distribution of NO_x emission estimates from pumpjack engines from the UDAQ 2017 inventory. [UDAQ 2017] (c). Distribution of estimates used in our study. (d). Laboratory results from Texas A&M University for NO_x emissions from an Ajax E-565 engine, broken down by engine load. [Brown 2017] (e). Measurements by Utah State University in the Uinta Basin, color code indicates the air/fuel ratio (λ).

The strong dependence on engine load documented here is significant. When a well is new, operators must install an engine capable of lifting the fluids produced. However, the production from a well declines significantly after about a year, but the engines typically are not switched out. Therefore, after about a year, most engines operate well below their rated horsepower capacity, are following the tan trace in Figure 2 rather than the blue, and their NO_x emissions are significantly overestimated in the inventory. Note that the right-most edges of the empirical distributions in Figures 3 and 4 agree well with the inventories. The implication is that the emissions inventories employ estimates appropriate to new wells.

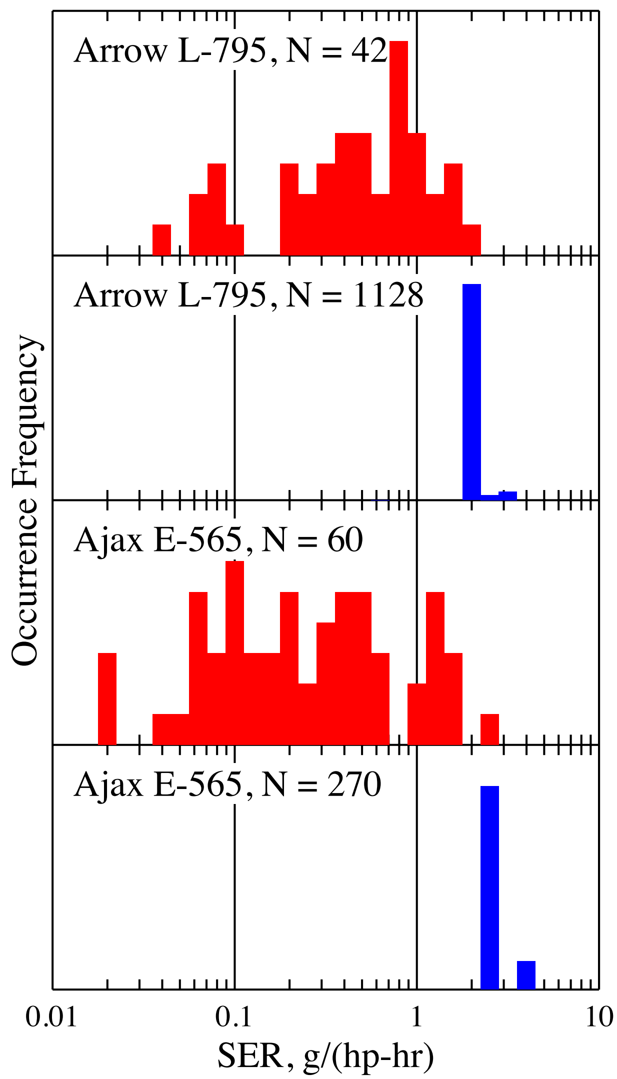

Figure 4. Distribution in NO_x SER values for the indicated engine make and model. Red bars are the results from a random selection of JJJJ-mandated field tests, blue bars indicate the SER values used to develop the UDAQ inventory.

II. B. 3. Modified estimates of NO_x emissions by pumpjack engines

To avoid these severe over-estimates of pumpjack engine emissions, and to inform the models discussed below, we have developed our own method for estimating NO_x emissions from pumpjack engines. The pumping rate of the engine, measured as the average number liquids (water or oil) lifted per day (LL), is an important variable. For each well, we calculated the liquids lifted (LL) in barrels per day by extracting from the Utah Division of Oil, Gas, and Mining database [UDOGM 2021a] the total days of operation, total barrels of produced oil, and total barrels of produced water for February 2017. The UDAQ emissions inventory included about 3400 engines, but about 500 were reported to have produced no oil or water in February 2017. Figure 5 shows the distribution in LL over the remaining 2888 engines. There were a few very high producing wells, while the mode, mean, and median of the distribution are respectively ≈ 10, 28.12, and 13.75 bbl/day. Other statistics for this distribution are reported in Appendix C, Table C1.

Estimates of the engine load (L) were based on the industry-standard software product Echometer QRod 3.1. [Echometer, 2021] Appendix B provides details on several QRod calculations. Important input variables to QRod are the daily barrels of liquids lifted (LL) and two efficiencies, the surface unit efficiency ε_1 and the pump volumetric efficiency ε_2. It was infeasible to run QRod on each of the wells in the inventory. Rather, we performed enough runs to obtain the following calibration formulas that provide good approximations to the QRod results.

$$\frac{L}{hp} = 10^P \times \left[\frac{LL}{(bbl/day)}\right]^S \qquad (Eq. 9a)$$

$$P = -1.03944 - 0.6699\,(\varepsilon_1\varepsilon_2 - 0.9025) \qquad (Eq. 9b)$$

$$S = 1.0473 + (0.013)(\varepsilon_1\varepsilon_2 - 0.9025) \qquad (Eq. 9c)$$

Appropriate values of ε_1 and ε_2 are not available. The assumption

$$\varepsilon_1 \approx \varepsilon_2 \approx \frac{2}{3} \qquad (Eq. 9d)$$

seems reasonable and provides excellent agreement between the distribution in Figure 3(c) and the empirical distribution in Figure 3(e).

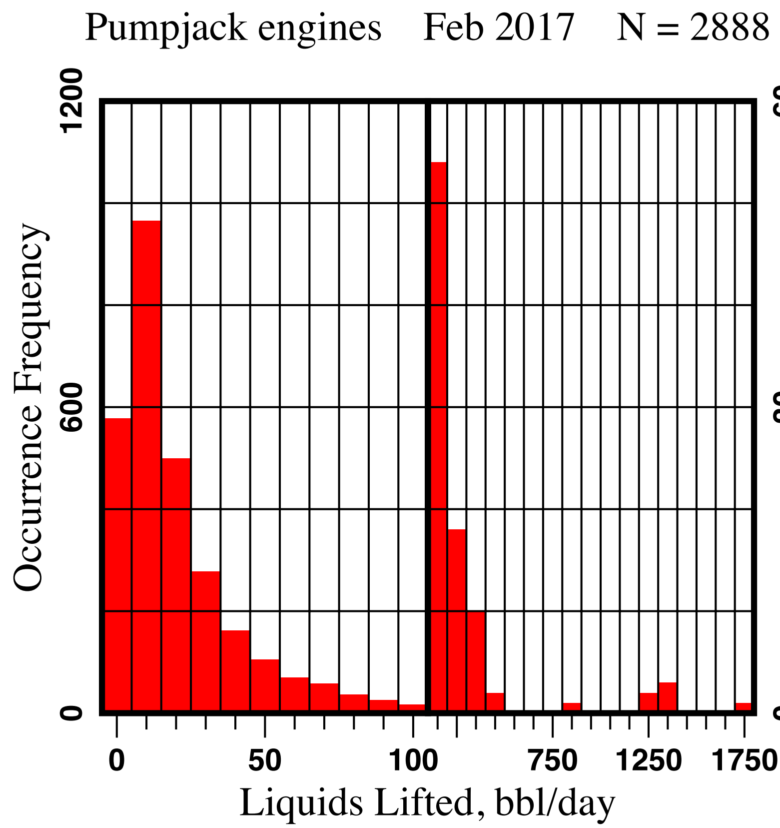

Figure 5. Distribution in liquids lifted, bbl/day, by pumpjack engines. Note that the right side of the diagram is greatly expanded relative to the left. It only accounts for about 3% of the wells.

Figure 6 shows the distribution in loads for the 2888 engines estimated in this way. The mode, mean, and median of this distribution are ≈ 1, 5.22, and 2.39 hp, respectively. Additional statistics on this distribution are reported in Appendix C, Table C3.

We suggest that a selection bias accounts for some of the differences between our estimates and others. When industry technicians report that most engines operate at 70% load, they may inadvertently be discounting older, lower-producing wells, whereas our distributions include all wells reported to have produced any liquids at all.

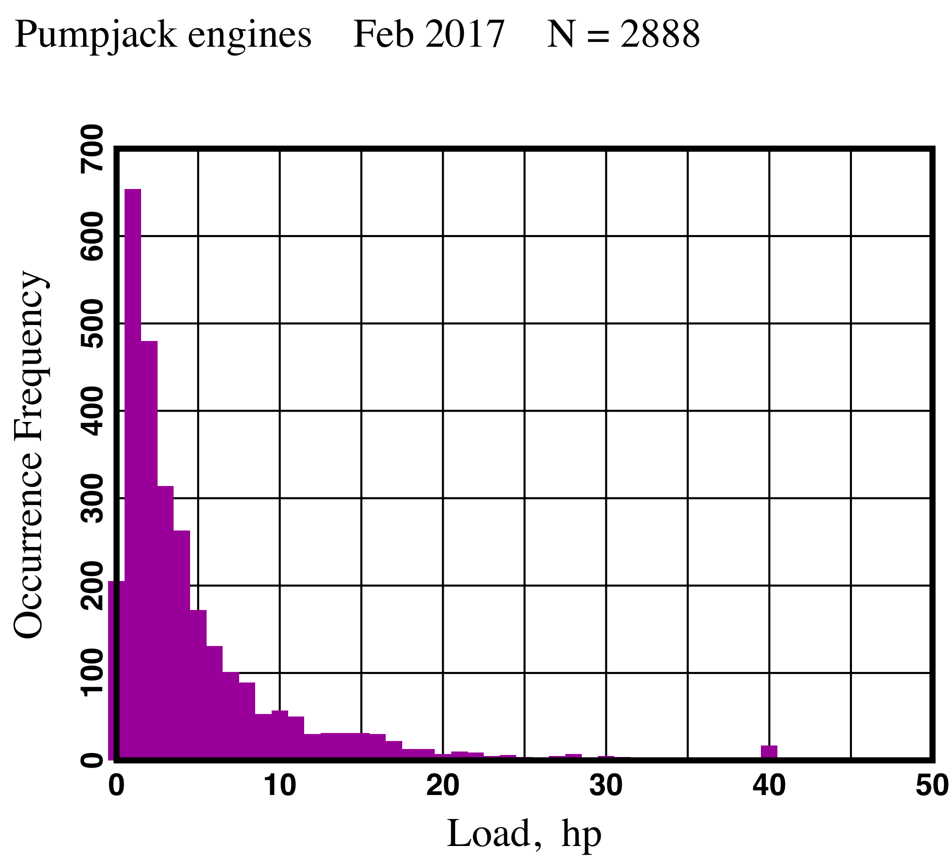

Figure 6. Distribution in the estimated pumpjack engine loads. There are 13 outliers appearing off-scale to the right: 1 at 55 hp, 8 at 65 hp, 1 at 66 hp, and 2 at 96 hp.

We used the following formula to estimate the engine emission:

$$\left[NOx\ emission, \frac{g}{hr}\right] = \left[SER, \frac{g}{hp \cdot hr}\right] \times [L, hp] \qquad (Eq. 10)$$

where SER is the specific emission rate in g/(hp-hr) and L is the load in horsepower. We applied two different approaches to estimate SER values. Starting in 2008, federal regulations ("quad-J" or "JJJJ" regulations) mandated the installation of cleaner pumpjack engines. [CFR 2022] For pre-JJJJ-era engines, we used the same SER value employed in the original inventory. For post-JJJJ engines, we were guided by the results of the JJJJ certification tests displayed in Figure 4, assuming that the appropriate SER was correlated with the manufacturer's horsepower rating of the engine, and interpolated or extrapolated from the average values for the Ajax E-565 and Arrow L-795 engines.

The distribution in the NO_x emissions calculated in this way are shown in Figure 3(c). The total estimated emission over all 3393 engines is 13 kg/hr. In contrast, the total emission estimate from these 3393 engines in the UDAQ inventory was 586 kg/hr, a factor of 45 times larger.

New wells are high producers, represented by the far right of Figures 3 and 4, and they must be fitted with engines capable of lifting large volumes. Production declines after about a year, but the engines are not replaced. The result is that most engines run at partial loads. Older wells producing fewer than 10 bbl/day or so, have very low average loads, amounting only to a few horsepower. According to our QRod calculations, productions of 10 bbl/day or less correspond to stroke times of a minute or longer. Such engines must spend a lot of time idling. Undoubtedly, peak loads over the cycle are larger.

Table 3 compares per-engine NO_x emissions from several measurements and from our estimates. In terms of averages, the RMP estimates align more closely with the 50% load measurements from Brown. The USU Engine Study aligns best with the 75% load measurements. This may be another manifestation of the selection bias mentioned above. There was undoubtedly a tendency to skip over low-producing wells during the study, whereas with the RMP estimates, we endeavored to include all producing wells. Table 3 also illuminates the fallacy of assuming that a single SER can be applied at all values of the load.

Table 3. Average NO_x emissions, either measurements or estimates, per engine

Description	Load	SER	Average NO_x emission	
	hp	g/(hp-hr)	Hourly (g/hr)	Annual (kg/y)
Brown @ 50% Ajax E-565	20	0.20	4.1	36
Brown @ 75% Ajax E-565	30	0.49	14.6	128
Brown @ 100% Ajax E-565	40	6.05	242	2118
USU Engine Study			14.77	129
Estimate for RMP project			4.595	40

II. C. Estimates of drilling and completion emissions

As documented in Table 1, With pumpjack NO_x emissions revised down, drilling and completion emissions are now recognized to be important. NO_x is produced because large diesel engines are used. We have also developed new estimates of NO_x emissions from drilling and completion activities in the Uinta Basin during February 2017.

Diesel engines are ranked according to "tiers" that correspond to their potential to emit pollutants. Tier 1 engines are older, have fewer pollution controls, and pollute more than tier 2, etc. The engines currently used for drilling and completions in the Uinta Basin are all tier 2, 3 or 4. There are no available data on the tier rating of engines used in the Basin. Therefore, we have made two separate estimates, one assuming all engines are tier 2, the other that they are all tier 4. The two estimates are expected to bracket the actual behavior. Wells are classified as horizontal or vertical. Primarily because of the added length, horizontal well drilling and completion take longer.

Our calculations of NO_x emissions are based on Table 4, which gives an estimate of the total NO_x emissions for both activities, assuming both tier 2 and tier 4 engines, and for both horizontal and vertical wells. Table 4 is derived from software used to prepare general conformity permit applications to the Bureau of Land Management (BLM).

Table 4. Estimates of per-well emissions from drilling and completions in ton/well.

	Drilling Vertical	Completions Vertical	Drilling Horizontal	Completions Horizontal
NO_x Tier 2	2.13	2.98	5.82	6.95
NO_x Tier 4	0.231	1.65	0.638	3.85
VOC Tier 2	0.112	0.157	0.306	0.366
VOC Tier 4	0.0659	0.0930	0.180	0.217
CO	1.23	1.72	3.35	4.01
PM 10	0.226	0.0192	0.191	0.229
PM 2.5	0.0133	0.0186	0.186	0.222
SO_2	0.0765	0.107	0.209	0.249

The UDOGM database records the date at which drilling started (the “spud” date) and the date at which completion ended (the “completion” date). [UDOGM 2021a] For several reasons, the completion process often does not occur immediately after the drilling process, and dates at which drilling ends and completion begins are not recorded. Therefore, additional assumptions are required to distribute the total NO_x tonnage listed in Table 4 across the time between the spud and completion dates. Because drilling and completion crews have reputations for alacrity, an appropriate assumption is that a flurry of activity begins at the spud date, pauses after the well is drilled, starts up again when the completion phase commences, and continues forward until the completion date. We have assumed a standard duration of D days, listed in Table 5, for each activity. Then, we assume that drilling ends D days after the spud date and that completion starts D days before the completion date, with no emissions allocated to the intervening days. The second assumption is that the total NO_x tonnage listed in Table 4 is distributed uniformly over the D days.

Table 5. Average duration of the indicated activity.

		Days
Vertical	Drilling	D = 10
	Completion	D = 4
Horizontal	Drilling	D = 28
	Completion	D = 9

Applying these assumptions for the month of February 2017 produces Figure 7. A five-day running average is also shown. Tier 2 estimates tend to be more than twice those of tier 4. Total emissions for the month are estimated at between 35 tons (tier 4) and 86 tons (tier

2). For comparison with the UDAQ inventory, Table 6 displays total emissions estimated in this way for all of 2017. Our estimates bracket the UDAQ estimate, which lies closer to our tier 4 calculation.

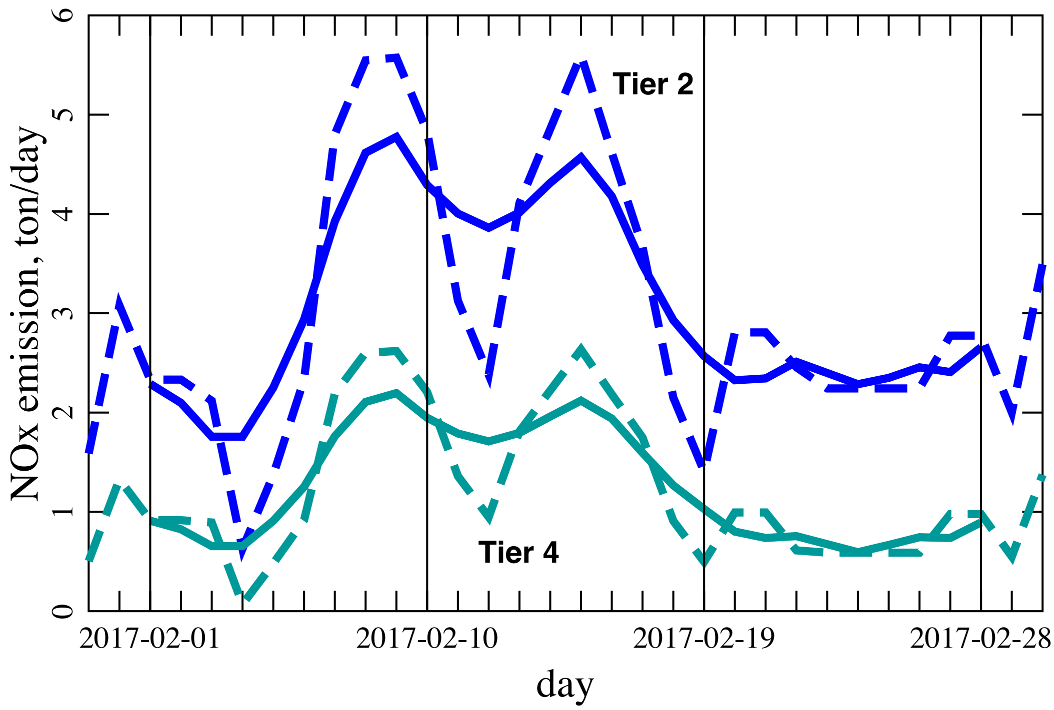

Figure 7. Estimated daily NO_x emissions from drilling and completion activity in the Uinta Basin for February 2017. Dashed traces are calculated as explained in the text, solid traces are five-day running averages.

Table 6. Comparison between our estimates and those of UDAQ for drilling and completions.

	Monthly (02/2017), ton/mo	Annual (2017), ton/y
UDAQ	N/A	740
Current calculation, tier 2	86	1590
Current calculation, tier 4	35	580

The results of the same calculation for every month since 2000 are shown in Figure 8, assuming tier 2 engines. The tier-4 assumption generates a similar plot but on a lower scale, topping out at around 0.2 to 0.3 tonne/hr. An abrupt decline in drilling and completions, triggered by declining global markets, paralleled an abrupt decline in estimated NO_x emissions in 2015. A partial rebound has occurred, but the high emissions seen in the early years of the decade have not returned. 2013-2014 highs have fallen almost 80% by 2017/2018. This result correlates with ozone concentrations observed over the last decade, suggesting that drilling and completion activities may contribute significantly to high ozone. [Mansfield & Lyman, 2021] Based on these estimates, as shown in Table 1, NO_x emissions from drilling and completions now appear to be about 10 to 20% of the total in 2017.

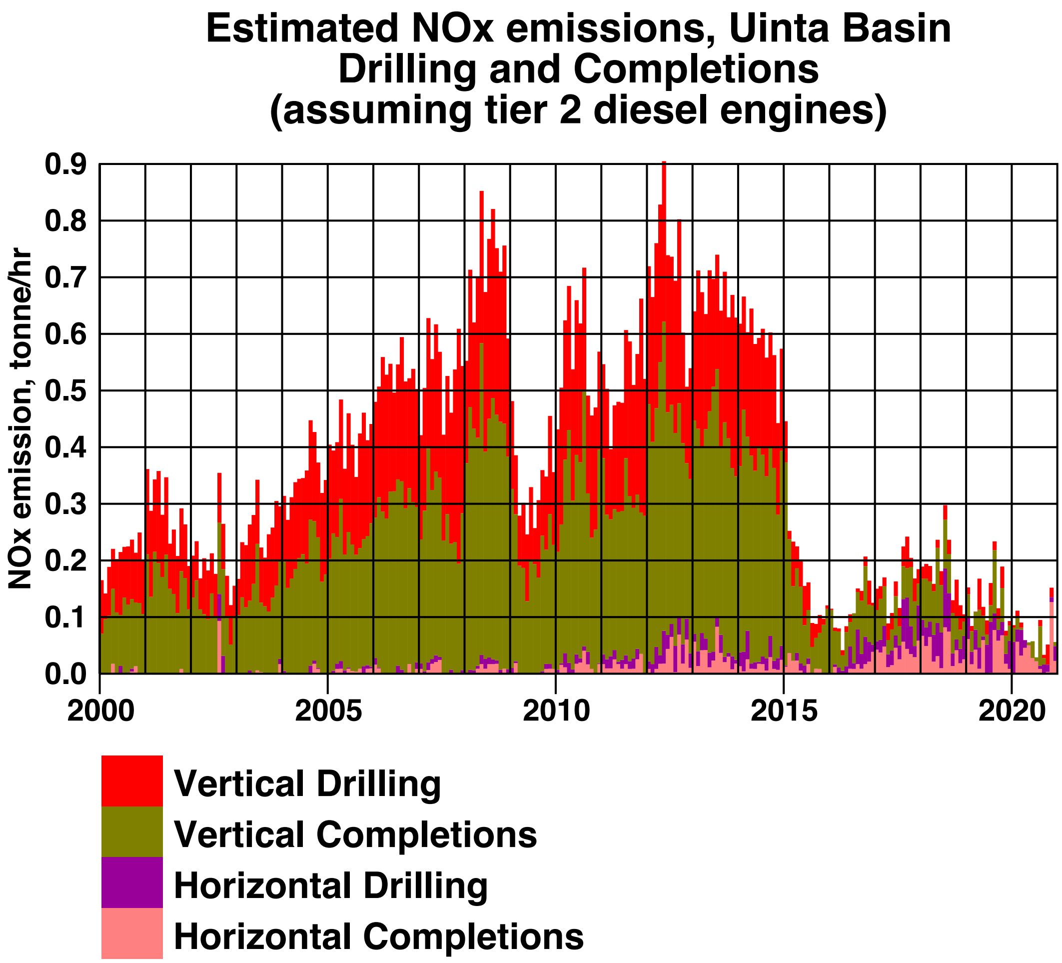

Figure 8. Estimate of NO_x emissions from drilling and completion of oil and gas wells, assuming tier 2 engines.

II. D. Historical trend analyses

II. D. 1. Uinta Basin oil and water production data

The UDOGM database [UDOGM 2021a] tabulates monthly water and oil production statistics from each well in the basin, shown in Figure 9. These data reached a peak in late 2014 and early 2015 of about 11 million barrels per month and declined to about 8 million per month in 2016. Note the sharp decline at the beginning of 2016 which lags the sharp decline in Figure 8 by one year, confirming the statement that oil production remains high for the first year of production. The percent decline in produced fluids from 2014/2015 to 2018/2019 is only about 20%, compared with about 80% in estimated NO_x emissions from drilling and completions. Of course, this is consistent with the fact that most wells continue to produce over many years.

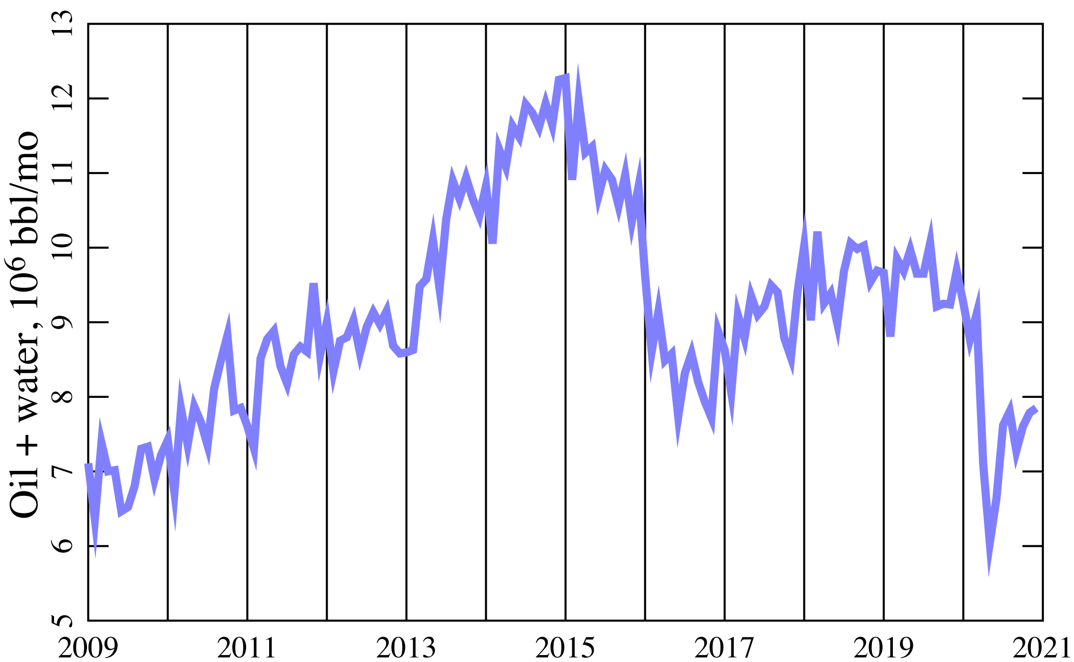

Figure 9. Monthly production of oil and water from all wells in the Uinta Basin.

II. D. 2. Correlations between NO_x measurements and oil and gas activity

We accessed NO_2 data from the Aura satellite, [NASA 2021] available as the "NO_2 column," or the total concentration of NO_2 molecules along the line of sight between the satellite and the ground. Ground-based sensors measure the NO_2 concentration at the surface, and so are not directly comparable to the NO_2 column. Nevertheless, the column still provides a basis for comparison.

Any emissions or concentrations, including the NO_2 column, that are associated with creating a new well should correlate more strongly with Figure 8; while those associated with ongoing production should correlate more strongly with Figure 9. Since one trace drops off much more precipitously than the other, analysis of the NO_2 column data allows us to make tentative source attributions. (Note that the baseline of Figure 8 drops all the way to zero, but not Figure 9.) The more the historical NO_2 column declines in a fashion similar to Figure 8, the more likely it is that NO_x emissions can be attributed to drilling and completions. On the other hand, if the decline is more similar to Figure 9, then NO_x emissions can be attributed to on-going production activities. [See Dix et al 2019 for a similar application of the NO_2 column in source attribution.]

The actual NO_2 column data display interesting seasonal trends, correlating more strongly with drilling and completion data in winter, and production data in summer. We show this in Figures 10 and 11. In January, February, and March, NO_2 columns are more sensitive to (higher slopes), and correlate more strongly with (higher R^2), the drilling and completion NO_x emission than in other months. For ease of reference, R^2 values in each month are displayed in Figure 12. There are several challenges related to comparing the NO_2 column directly to a NO_x emission. The NO_2/NO ratio in any given concentration of NO_x shifts to higher values when UV radiation is less abundant, [Seinfeld & Pandis 2006, p. 210] while the column is subject to dispersal by wind action. The overall strength of the response, indicated by the slope in each month, is apparently responding to both effects: Available sunlight and wind dispersal action are both typically lower in January. Moreover, in the winter months without snow cover (2012, 2015, 2018) the NO_2 column is particularly large.

Figure 11 shows scatter plots of the variation in the NO_2 column relative to the monthly oil and water production data. The monthly R^2 values also appear in Figure 12. Interestingly, the NO_2 column is not correlated with production data in January or February, but it is in other months, particularly September and October. Of course, the NO_x source or sources responsible for this early-fall correlation are any engines or flares correlated with, but not necessarily related to, oil and water production. For example, this could be a reflection of increased vehicular traffic.

Because of the interplay between insolation, wind action, and NO_x chemistry, all the aspects of these monthly trends have not been explained. However, the lack of correlation in the January panel of Figure 11 is consistent with our finding that NO_x emissions from pumpjacks do not contribute to winter ozone in the basin, while the correlation in the January panel of Figure 10 suggests that drilling and completions may have been an important NO_x source during the early years of the decade.

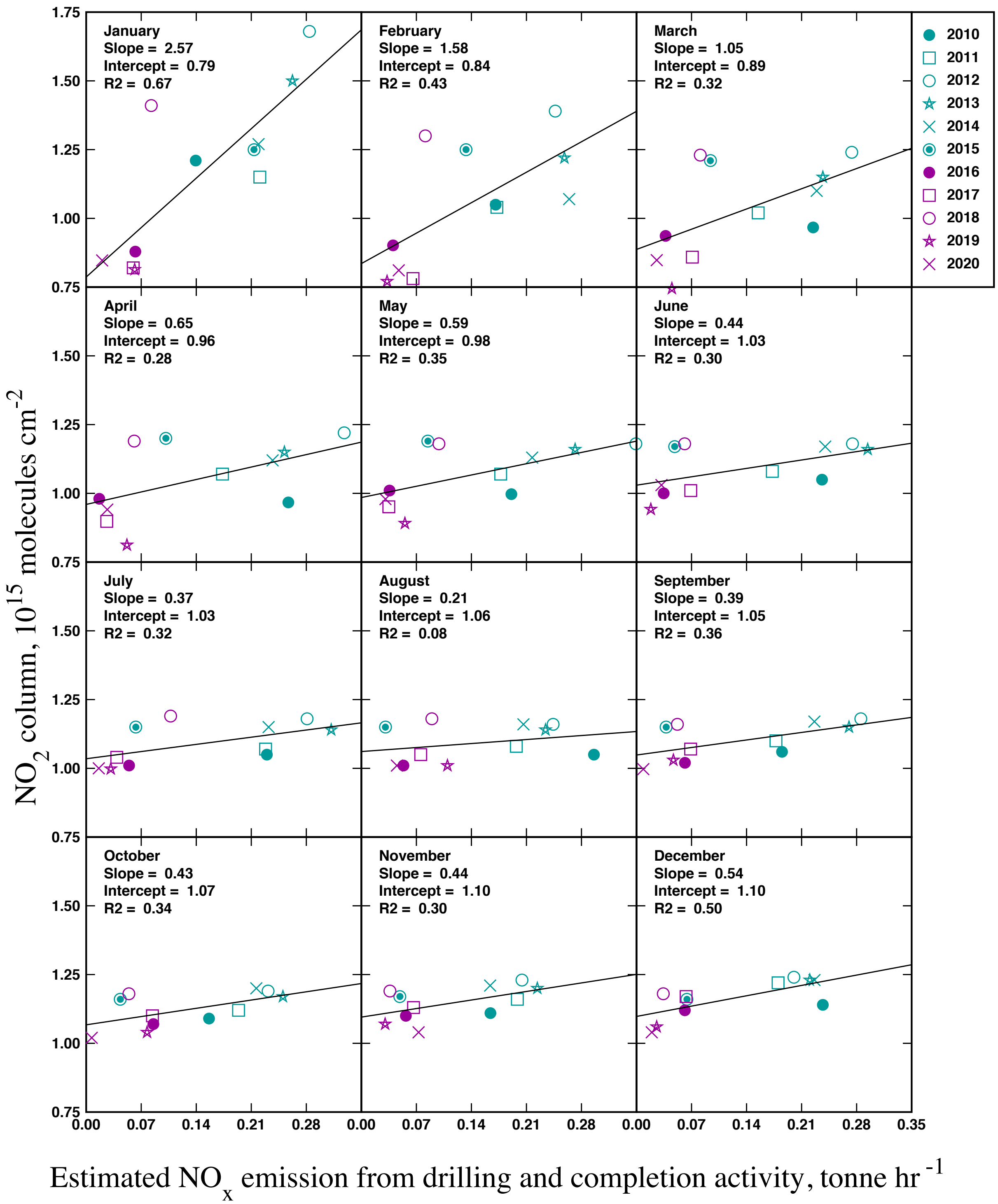

Figure 10. Scatter plot of the NO_2 column vs. the estimated NO_x emission from drilling and completions. Monthly data from each year since 2010 are shown.

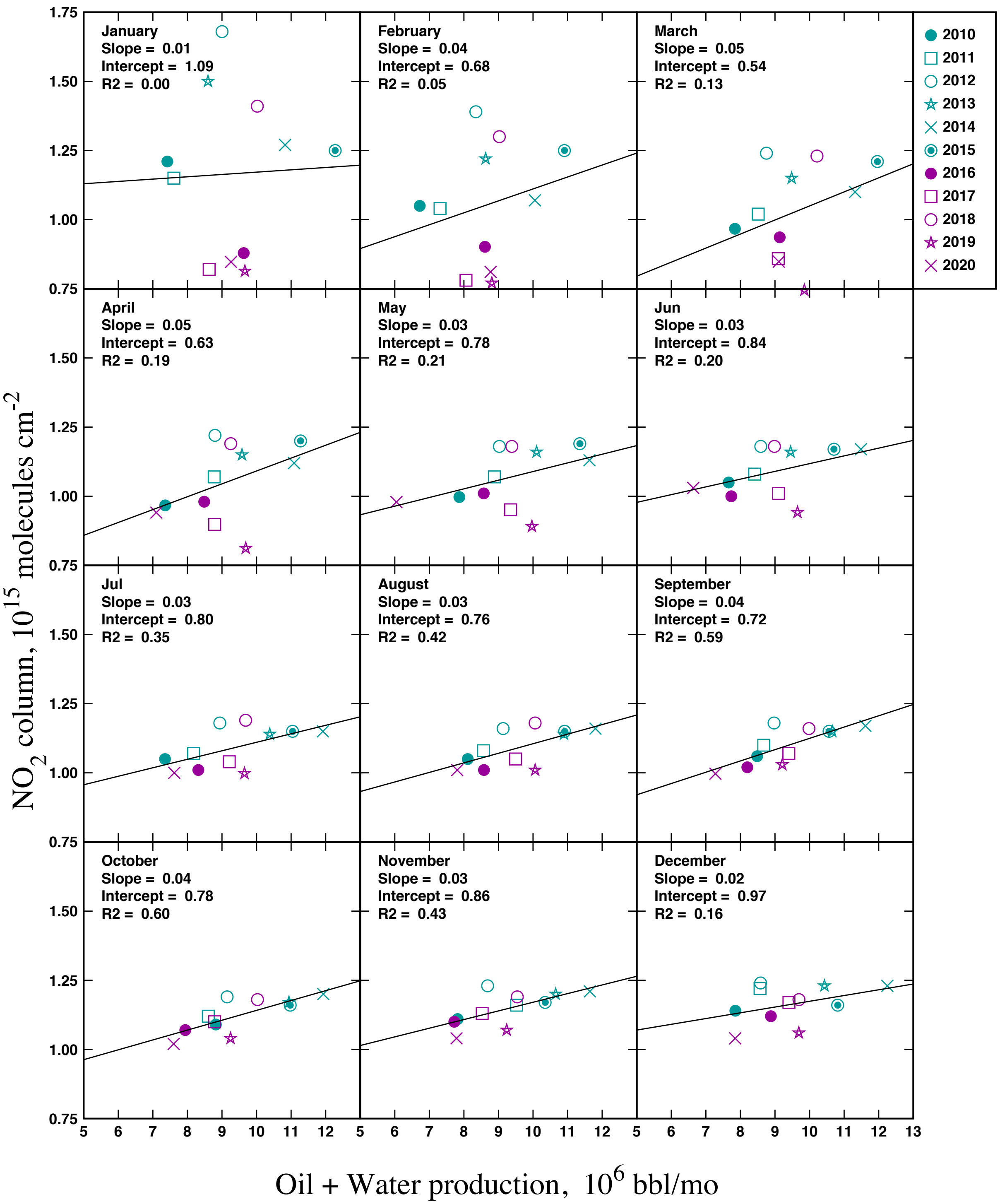

Figure 11. Scatter plots of the NO_2 column vs. the total barrels of oil produced in any one month.

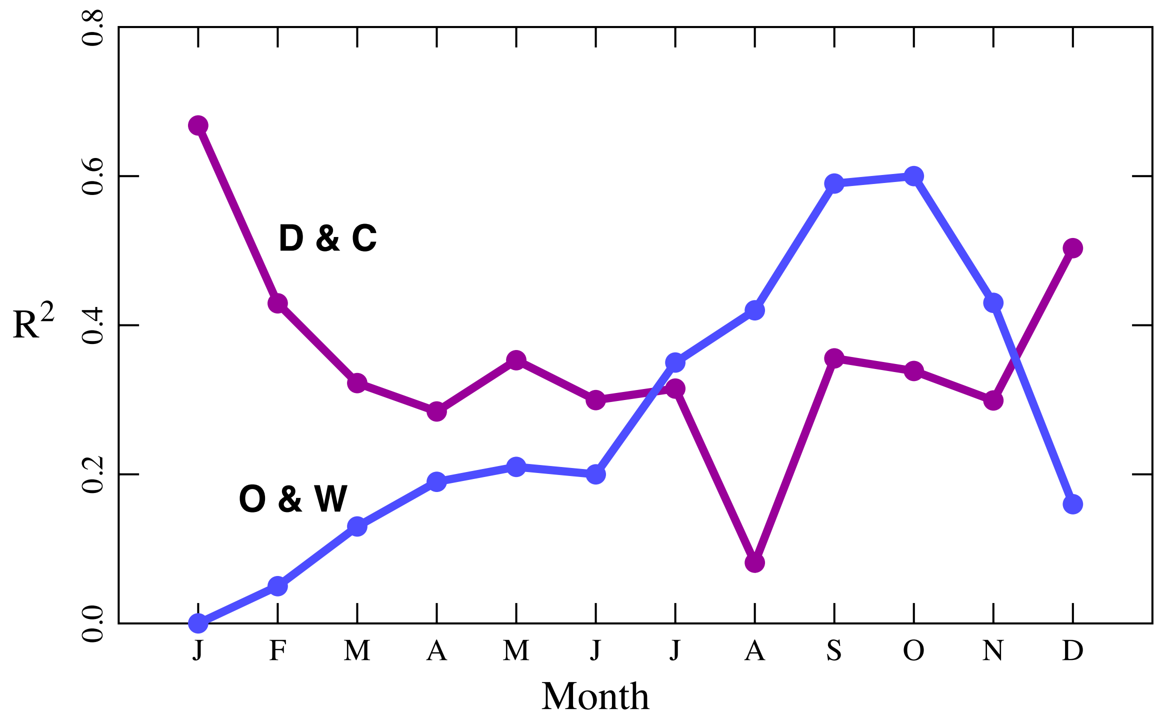

Figure 12. Correlation coefficients for each of the scatter plots displayed in Figures 10 and 11. O & W (oil and water) are the coefficients from Figure 11, D & C (drilling and completions) are the coefficients from Figure 10.

III. MODELING RESULTS

III. A. F0AM box model results. Nearly equivalent NO_x and VOC sensitivity.

The F0AM box model used to probe VOC and NO_x sensitivity was based on an ozone event that culminated on February 27, 2019 with a daily maximum ozone concentration of about 100 ppb at the Horsepool monitoring station in central Uintah County. We modeled ozone formation over a four-day period. Because input concentrations of some compounds are initialized at zero, three days of "spin-up" are needed so that on the fourth day of modeling, the concentrations of all important compounds have climbed to reasonable values. Figure 13 shows the comparison between simulated and measured ozone concentrations. The input VOC concentrations were distributed among molecular species according to the best available speciation data summarized in Table 7. [Lyman et al. 2021] A single "unit" of input VOC corresponds to the 40 compounds with the concentrations listed in Table 7. The input NO_x concentrations of the base model varied by the hour and were selected to agree with the measured hourly NO_x concentrations averaged over the four days of the episode (February 24 to 27), Figure 14, which constitutes one "unit" of NO_x. The input VOC concentrations of the base model were adjusted until the maximum day-4 ozone concentrations (*ca*. 100 ppb) were in agreement. VOC and NO_x inputs to the base model were 0.75 and 1 units, respectively.

We then calculated the maximum day-4 ozone concentration as we varied NO_x and VOC concentrations relative to the base model. Figure 15 shows a contour plot or "ozone isopleth diagram" of the results. The symbol ⊗ indicates the base model at slightly more than 100 ppb ozone concentration. The two × symbols indicate that the ozone concentration drops to slightly less than 90 ppb when either the NO_x or the VOC concentration is decreased by 40%. The other symbols will be explained below. The sensitivities for the base model are nearly the same for both NO_x and VOC:

$$S_i(NO_x) \approx 0.22$$
$$S_i(VOC) \approx 0.25$$
$$S_{60}(NO_x) \approx 0.12$$
$$S_{60}(VOC) \approx 0.12$$

(Eq. 11)

These are the ratios of sensitivities:

$$\frac{S_i(NO_x)}{S_i(VOC)} \approx 0.9$$

$$\frac{S_{60}(NO_x)}{S_{60}(VOC)} \approx 1.0$$

(Eq. 12)

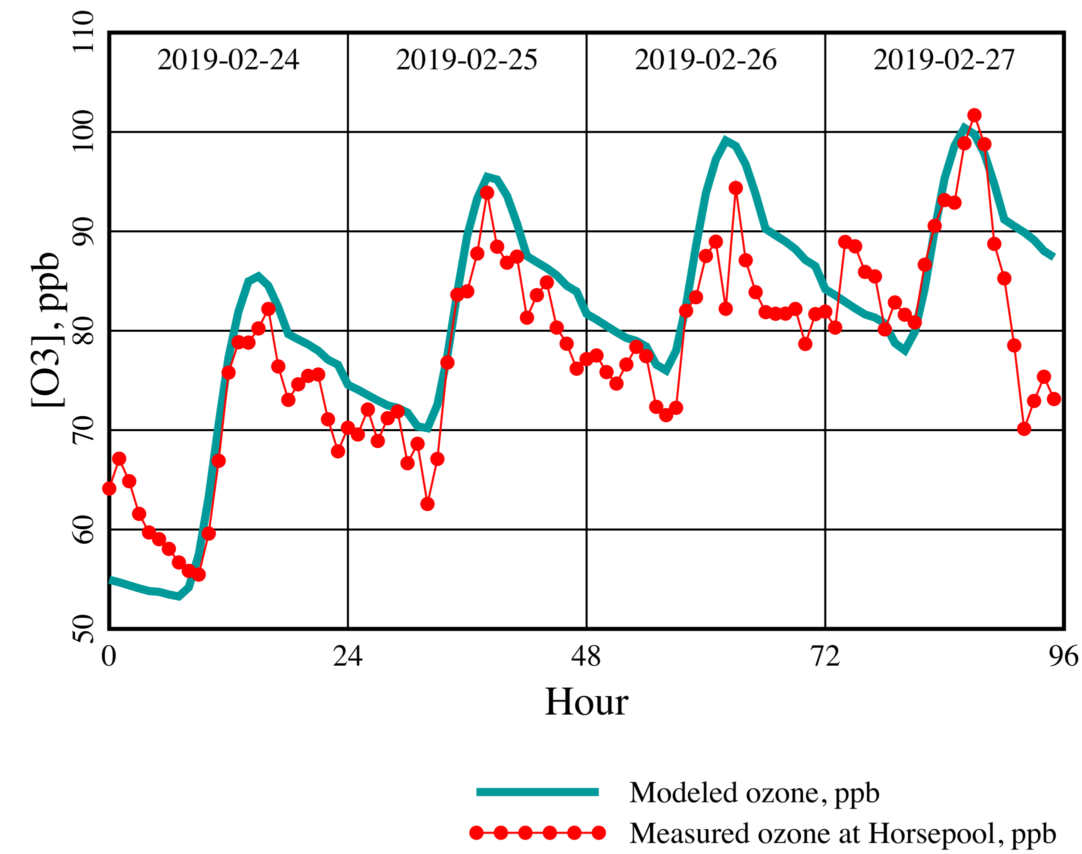

Figure 13. Comparison between measured and modeled ozone concentrations in the F0AM model.

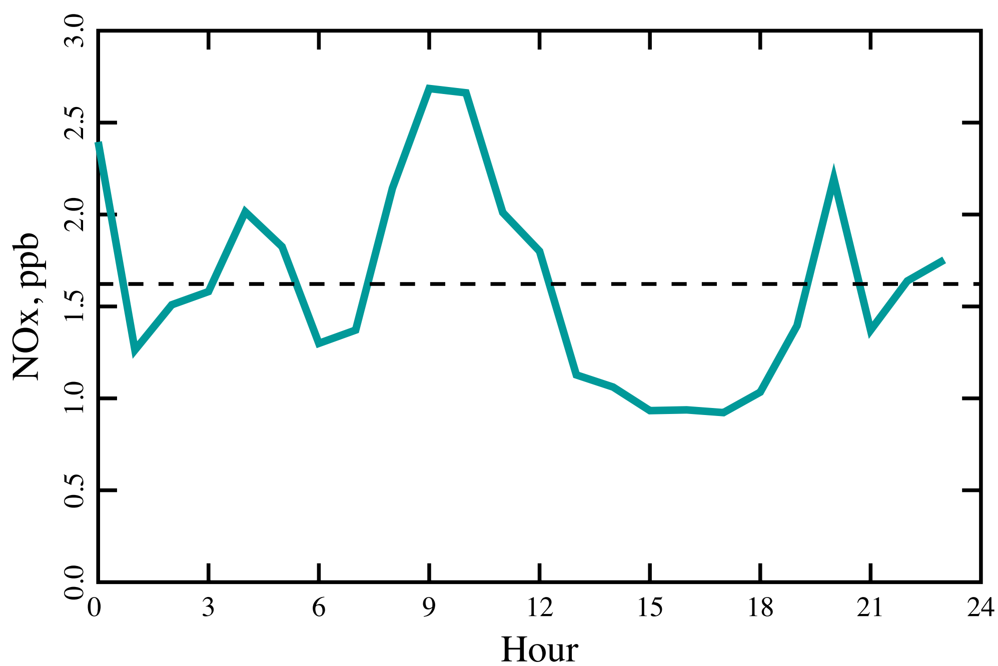

Figure 14. Input NO_x concentrations to the F0AM model. This concentration profile, with an average of 1.62 ppb, constitutes one "unit" of input NO_x.

Table 7. VOC concentrations in the F0AM box model. The concentrations listed here constitute one "unit" of VOC in the model.

Methane		Total
methane	4920.0 ppb	4920.0 ppb
Non-methane alkanes		Total
ethane	123.0 ppb	264.8 ppb
propane	63.0	
n-butane	25.0	
Isobutane	15.0	
n-pentane	10.0	
Isopentane	11.0	
n-hexane	4.0	
2-methylpentane	3.0	
3-methylpentane	2.0	
2,2-dimethylbutane	0.3	
2,3-dimethylbutane	1.6	
n-heptane	1.9	
2-methylhexane	0.8	
3-methylhexane	1.2	
n-octane	0.8	
n-nonane	0.2	
n-decane	0.2	
cyclohexane	1.8	
Alkenes and Alkynes		Total
ethylene	1.1 ppb	3.0 ppb
propylene	0.1	
acetylene	1.8	
Aromatics		Total
benzene	1.2 ppb	3.0 ppb
toluene	1.2	
o-xylene	0.1	
m-xylene	0.2	
p-xylene	0.1	
ethylbenzene	0.1	
1,2,3-trimethylbenzene	0.1	
Alcohols		Total
methanol	10.0 ppb	12.6 ppb
ethanol	0.3	
isopropanol	2.3	
Carbonyls		Total
formaldehyde	6.5 ppb	21.0 ppb
acetaldehyde	2.9	
butyraldehyde	1.3	
acrolein	1.6	
methacrolein	0.6	
benzaldehyde	4.4	
acetone	3.0	
methyl ethyl ketone	0.7	

Figures 16 and 17 show how S_i(VOC) and S_i(NO_x) vary with input NO_x and VOC concentrations. Again, the symbol ⊗ indicates the base model, and the two × symbols represent a 40% decrease in NO_x or VOC concentration. The other symbols will be explained below. S_i(NO_x) goes negative in a wedge in the upper left; S_i(VOC) goes negative in a sliver along the lower right. Negative sensitivities correspond to a domain in which decreasing NO_x or VOC produces an *increase* in ozone concentration.

Figure 18 displays a contour plot of the relative incremental sensitivities, i.e., the ratio

$$\frac{S_i(NO_x)}{S_i(VOC)}$$

The ratio for the base model is ≈ 0.9.

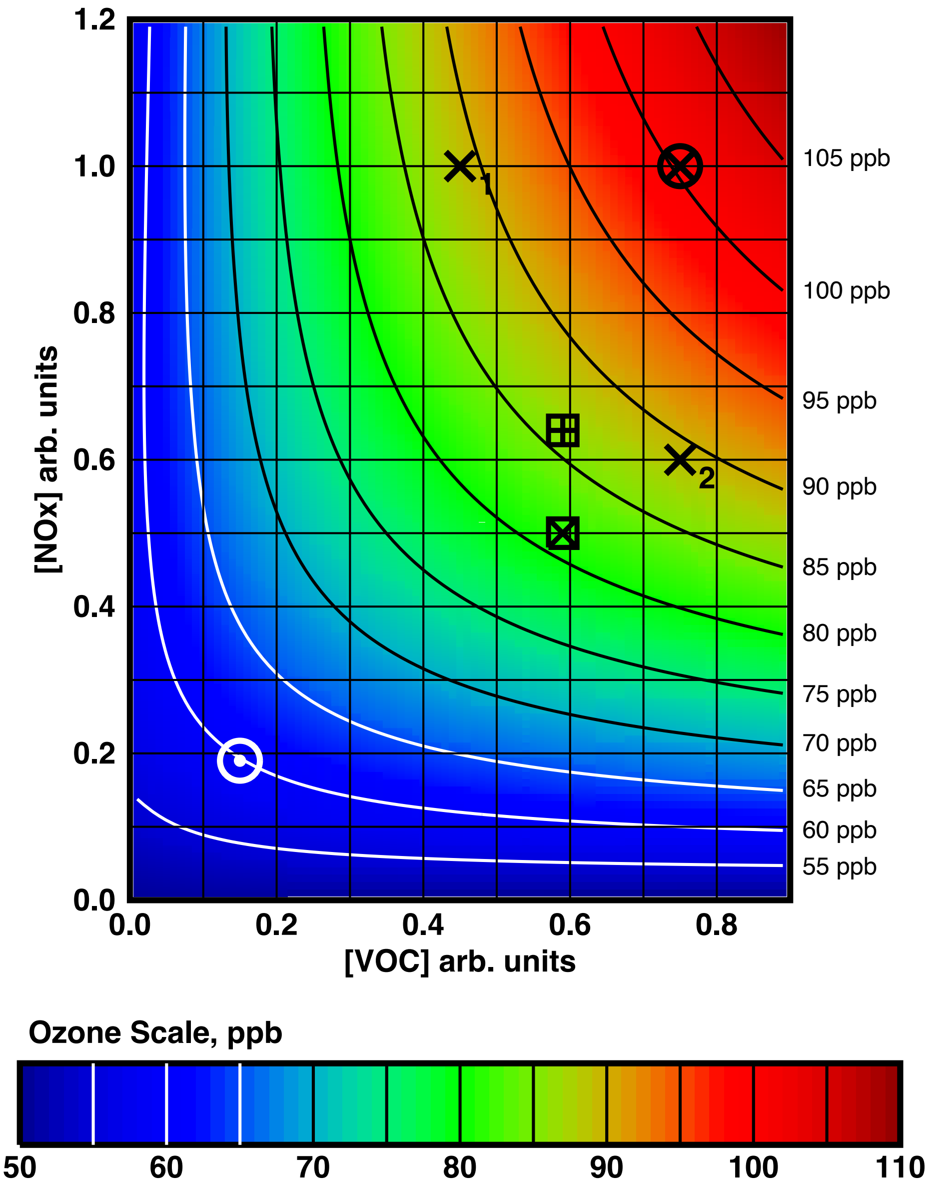

Figure 15. Contour plot showing results of the F0AM box model. Concentration of simulated ozone as a function of input VOC and NO_x concentrations. Values at the indicated points: Base model, $\otimes = 100.4$ ppb; 40% reduction in VOC, $\times_1 = 88.7$ ppb; 40% reduction of NO_x, $\times_2 = 88.8$ ppb; base model without pumpjacks, separators, heaters, $\boxplus = 86.2$ ppb; base model without pumpjacks, separators, heaters, and drilling and completion emissions, $\boxtimes = 81.5$ ppb; highly diluted CAMx model, $\odot = 59.9$ ppb.

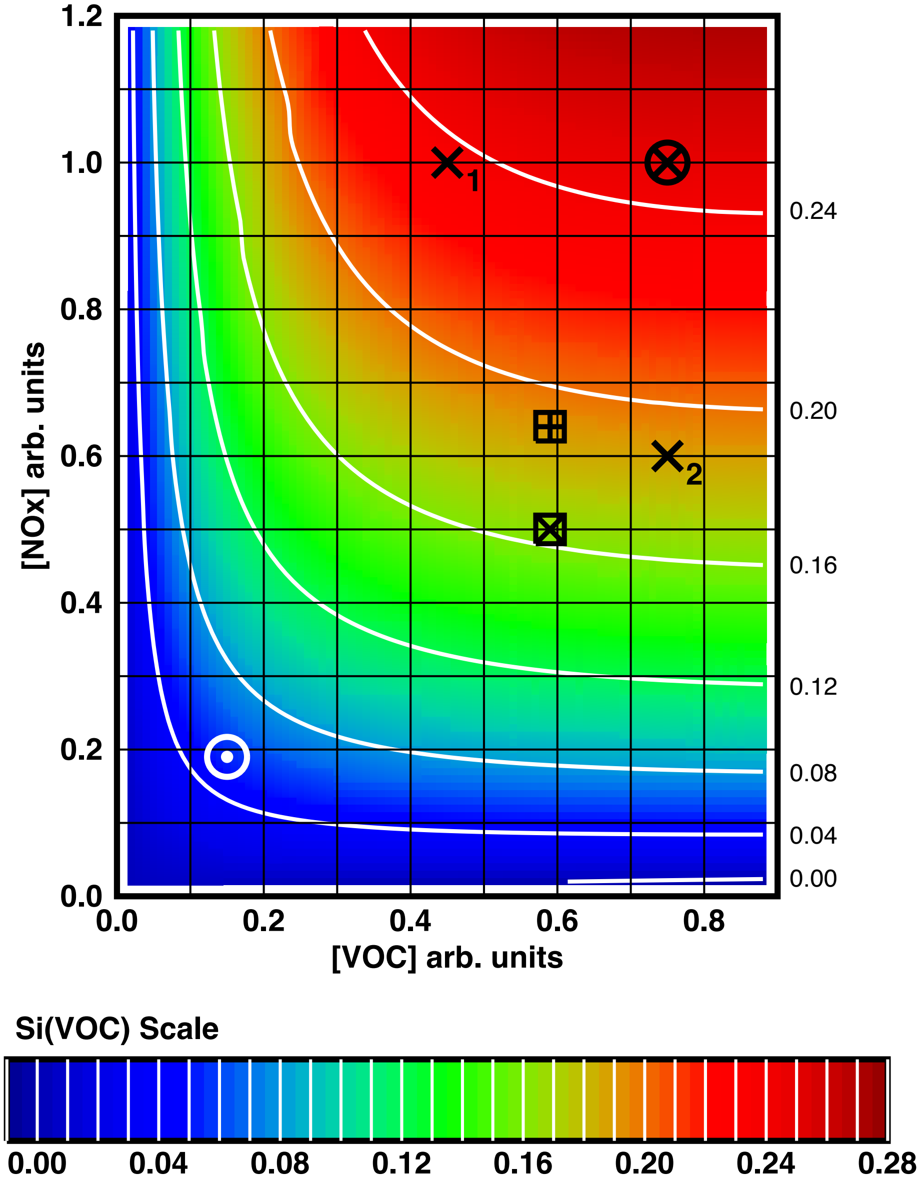

Figure 16. Contour plot showing results of the F0AM box model. Value of estimated VOC sensitivity, S_i(VOC), as a function of input VOC and NO_x concentrations. Values at the indicated points: Base model, $\otimes = 0.248$; 40% reduction in VOC, $\times_1 = 0.235$; 40% reduction in NO_x, $\times_2 = 0.188$; base model without pumpjacks, separators, heaters, $\boxplus = 0.191$; base model without pumpjacks, separators, heaters, and drilling and completion emissions, $\boxtimes = 0.165$; highly diluted CAMx model, $\odot = 0.054$.

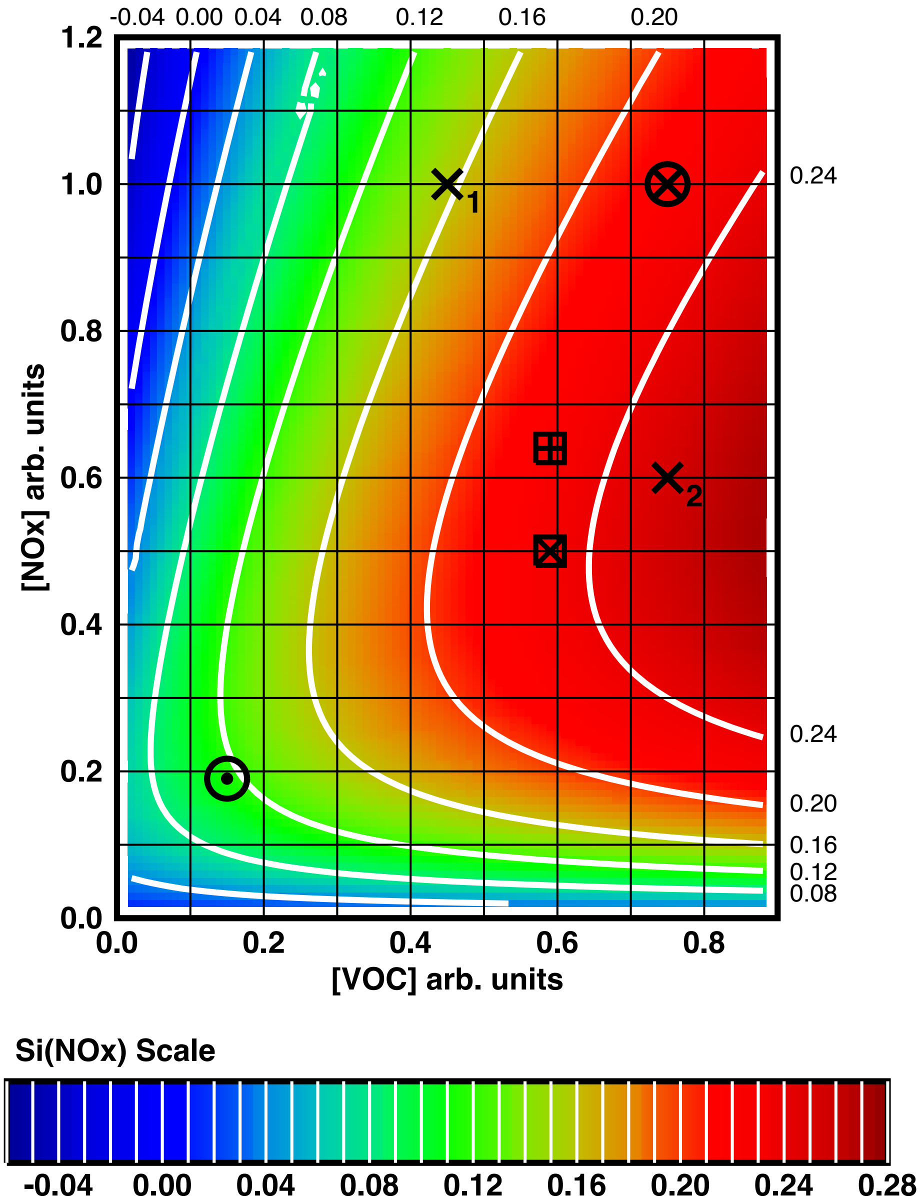

Figure 17. Contour plot showing results of the F0AM box model. Value of estimated NO_x sensitivity, $S_i(NO_x)$, as a function of input VOC and NO_x concentrations. Values at the indicated points: Base model, $\otimes = 0.221$; 40% reduction in VOC, $\times_1 = 0.156$; 40% reduction of NO_x, $\times_2 = 0.253$; base model without pumpjacks, separators, heaters $\boxplus = 0.225$; base model without pumpjacks and drilling and completion emissions, $\boxtimes = 0.231$; highly diluted CAMx model, $\odot = 0.114$. The glitchy behavior in the 0.8-contour near the top of the chart is a result of inaccuracies in the numerical derivative calculation, Eq. 3.

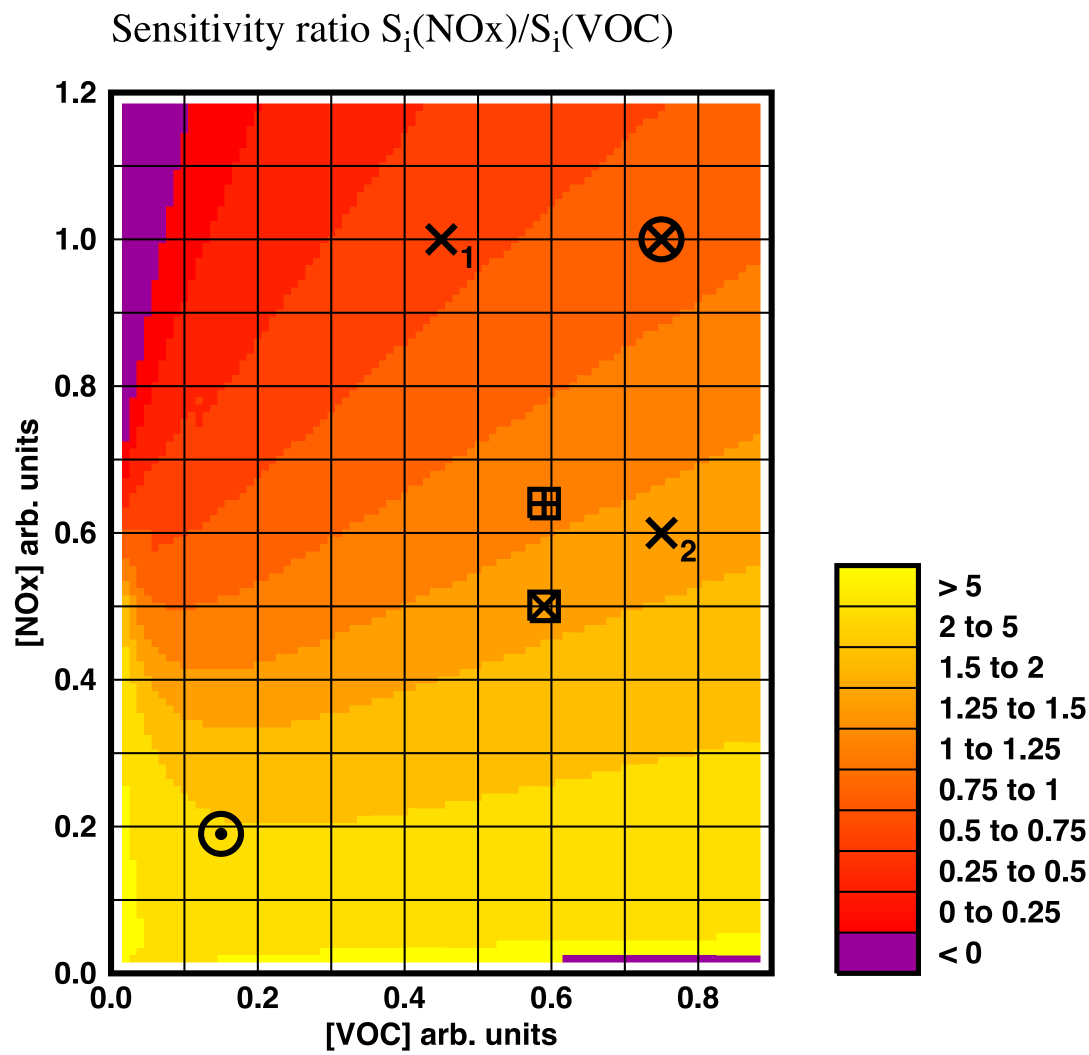

Figure 18. Contour plot showing results of the F0AM box model. Ratio of sensitivities Si(NO_x)/Si(VOC) as a function of input VOC and NO_x concentrations. Values at the indicated points: Base model, $\otimes = 0.891$; 40% reduction in VOC, $\times_1 = 0.663$; 40% reduction of NO_x, $\times_2 = 1.35$; base model without pumpjacks, separators, heaters, $\boxplus = 1.18$; base model without pumpjacks and drilling and completion emissions, $\boxtimes = 1.40$; highly diluted CAMx model, $\odot = 2.11$.

III. B. Results from 3D photochemical grid modeling

We attempted to develop 3D photochemical grid models using the CAMx platform for the same episode, late February and early March 2019, when high ozone measurements were obtained at many monitoring sites throughout the Basin. We used the CB6 chemistry module.

WRF and other meteorological models struggle to represent multi-day thermal inversions: See Tran et al. [2018] and references cited therein. Simulated inversions tend to break up too early, or the model overestimates the thickness and temperature of the inversion layer. Our WRF model suffered from such problems. For example, the simulated inversion layer was accurate at the beginning of the run, but the inversion layer quickly became too thick and then broke up altogether. With an unrealistically thick inversion layer, simulated precursor and ozone concentrations became diluted. This dilution effect is obvious in Figures 19 – 21. Figure 19 compares simulated and measured NO_x concentrations at two sites. Figure 20 compares simulated and measured ozone concentrations at four sites. Figure 21 displays the simulated non-methane hydrocarbon (NMHC) concentration. The mid-day minima in simulated NMHC and NO_x concentrations are the direct consequence of this dilution effect. The overnight spikes in NO_x and NMHC may be a consequence of an overnight inversion setting in, but if so, the inversion does not persist into the daylight hours.

We ran two sets of CAMx runs, one with the drilling and completion NO_x emissions set at the tier 2 approximation, and one at the tier 4 approximation. The tier 2 and tier 4 results are both plotted in Figure 20, but are unresolvable, i.e., the sensitivity of the CAMx runs to NO_x concentrations is small and the two curves overlap. Figure 22 displays another comparison between the two calculations. Note that in the third panel, the ozone concentration difference between the two models is about 0.3 ppb out of a total of ca. 50 ppb, or in the notation of Section I.E.2, $dz/z \approx -0.006$. Assuming that the NO_x concentration is proportional to the NO_x emission, then according to Table 1, $dy/y \approx -0.12$ and $S_i(NO_x) \approx 0.05$, roughly.

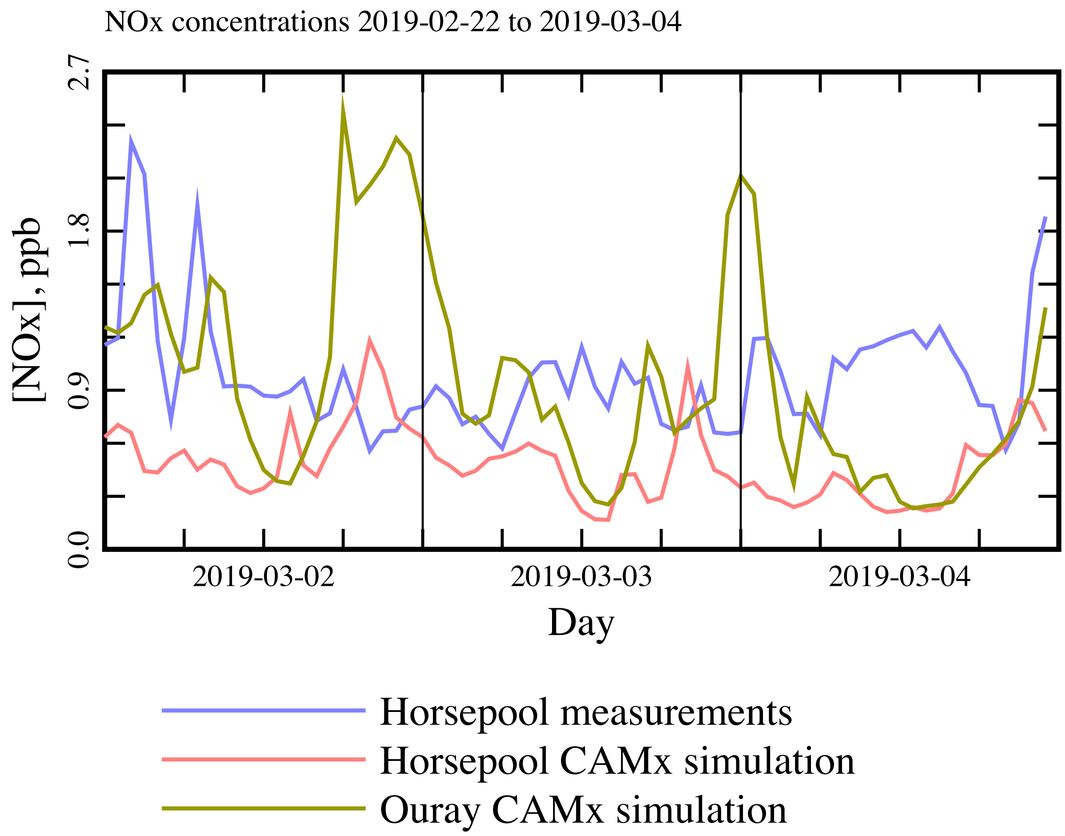

Figure 19. Comparison of simulated NO_x concentrations at Horsepool and Ouray relative to actual measurements at Horsepool.

Unfortunately, we became aware of the poorly simulated meteorology too late to run corrected models, but it turns out that this overly diluted CAMx model confirms two aspects of the box model. First, Figure 19 indicates that the daytime NO_x concentration is about 0.3 ppb. Figure 21 indicates that the daytime NMHC concentration is about 40 ppb. When we compare these values against Figure 14 and Table 7, we see that at the time of the mid-day dilution, the concentrations correspond to about 0.15 VOC units and 0.19 NO_x units in the box model. This overly diluted CAMx model is indicated by the ⊙ symbol in Figures 15 – 18. The box-model value of the ozone concentration, 60 ppb, is in good agreement with the average at Horsepool in Figure 20. Second the incremental NO_x sensitivity of the model CAMx model, ≈ 0.05, is reasonably close to the F0AM model result, ≈ 0.1, within the accuracy of this crude estimation. In general, the sensitivities are low because of the high dilution in the model.

At such high dilutions and low sensitivities, we were unable to obtain any useful source apportionment results from the pumpjacks in any of the four geographic sectors (Appendix A). This is not surprising, since according to Table 1, the pumpjacks were responsible for only about 1-2% of NO_x emissions. Removing those NO_x emissions can only have an impact on ozone concentrations of about one part in 10^4.

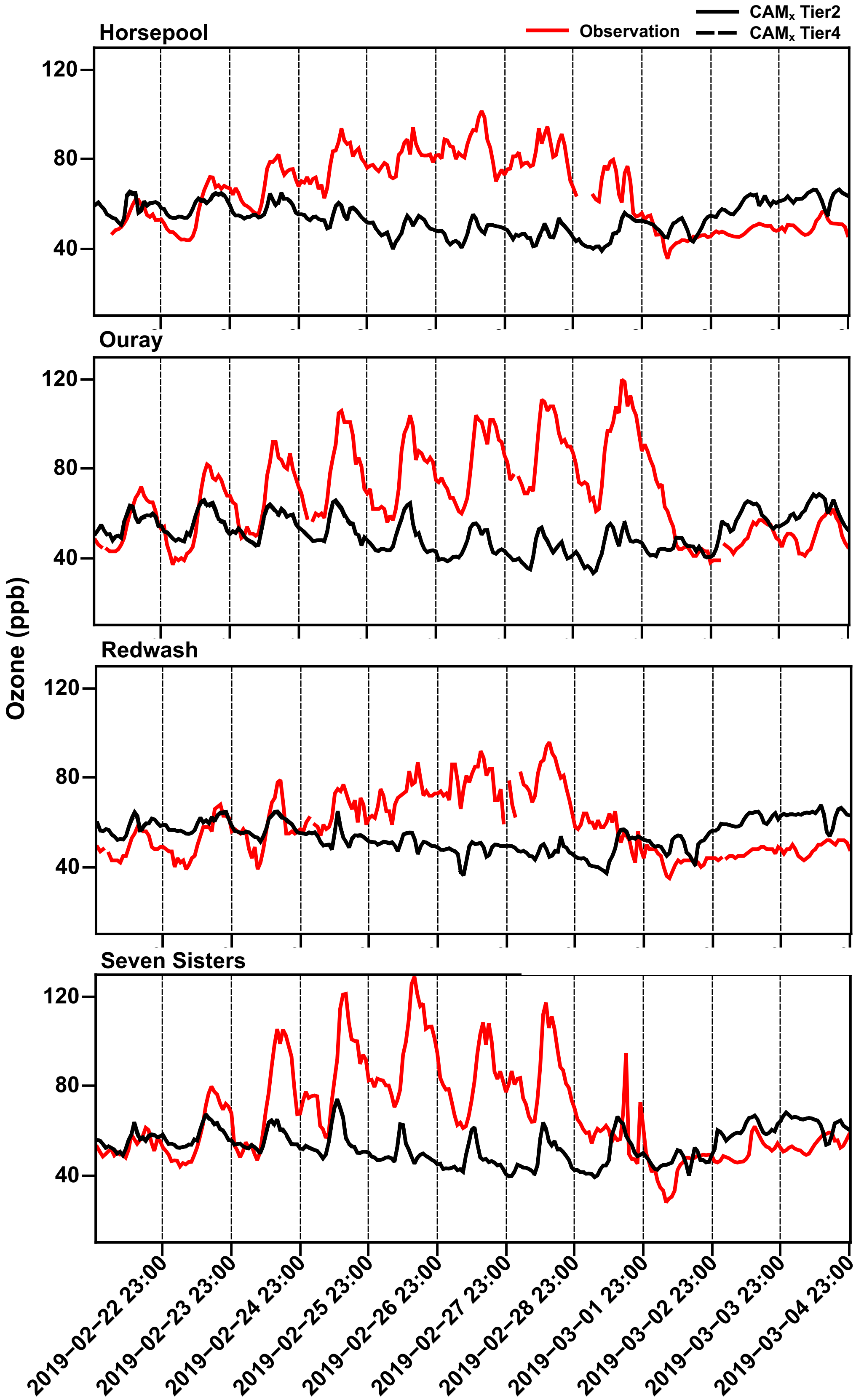

Figure 20. Comparison between CAMx-simulated and observed ozone concentrations.

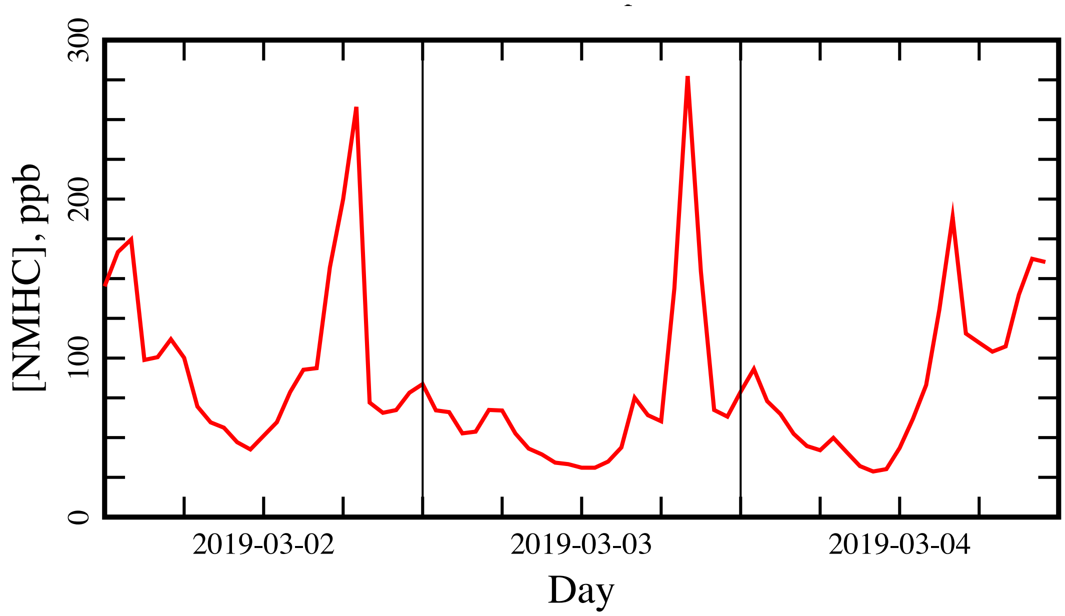

Figure 21. Simulated non-methane hydrocarbon concentrations at Horsepool.

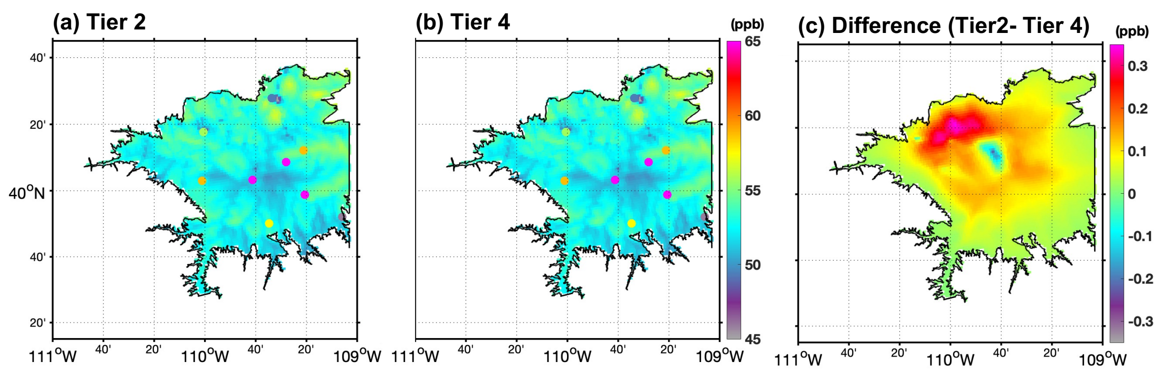

Figure 22. Simulated ozone concentrations in the Uinta Basin with either the tier 2 (a) or tier 4 (b) estimates of drilling and completion NO_x emissions. The difference between the two is on the order of 0.3 ppb.

There is one instance in the literature of a successful WRF model of persistent multi-day thermal inversions. [Tran et al. 2018] WRF possesses a feature, "nudging," in which actual observational data are used to constrain the model. Inversions occur when the air aloft is warmer than air at the surface and are detected through "tethersonde" measurements: A tethered balloon is used to carry a thermocouple aloft and measure the temperature-altitude profile above the surface. Tran et al. [2018] used tethersonde measurements to nudge their WRF model, effectively forcing WRF to build in a tight thermal inversion. Unfortunately, tethersonde measurements do not occur routinely in the Uinta Basin. Our results indicate that such measurements are required in the Uinta Basin if we ever hope to construct successful photochemical grid models.

III. C. Estimates of the impact of electrification

Using the estimates found in Table 1 and the results of the box model presented in Section III.A, we can make predictions about ozone reduction that would occur if electrification were to occur. Table 1 shows estimates for calendar year 2017, while the box model was optimized for an ozone episode in February 2019, so the following predictions assume that values in either year are generically appropriate.

The base box model corresponds to 0.75 VOC units and 1.00 NO_x units. According to Table 2, removing all pumpjack engines, separators, and heaters would reduce VOC emissions by about 21% and all NO_x emissions by about 36%. If we assume that the same reductions will occur in the concentration inputs to the base model, we arrive at about 0.59 VOC units and 0.64 NO_x units, corresponding to the ⊞ symbol in Figures 15 – 18. Removing all pumpjacks, separators, heaters, and electrifying all drilling and completion activities would reduce VOC to about 0.59 units and NO_x to 0.50 units, corresponding to the ⊠ symbol in Figures 15 – 18. In other words, had all emissions from pumpjacks, separators, and heaters been absent in February 2019, the peak ozone would have been reduced from about 110 ppb to about 86 ppb, a reduction of 24 ppb. Furthermore, had all drilling and completion activities also been absent, the peak ozone would have been reduced from about 110 ppb to about 82 ppb, a 28-ppb reduction.

Of course, even with extensive electrification throughout the oil and gas fields, it may not be possible to completely eliminate all internal combustion engines from these emissions categories. The predictions here are only intended to be suggestive.

IV. ECONOMICS AND FEASIBILITY OF ELECTRIFICATION

One of the primary objectives of this study is to examine whether electrification of the Uinta Basin would have a considerable effect on ozone formation in the Basin. This section evaluates the feasibility of making significant changes to oil and gas operation NO_x emissions. The feasibility is examined from an engineering and implementation perspective as well as the socio-economic effects to the Uinta Basin should electrification of well pads become required.

This engineering and implementation evaluation examines the following:

- Existing Uinta Basin transmission grid
- Types of beneficial infrastructure changes
- Known infrastructure development plans
- Existing internal combustion engine characteristics and emissions
- Challenges faced by electrification expansion
- Reliability of electrification
- Complimentary emission reductions from electrification

Potential socio-economic considerations for the Uinta Basin are outlined should wide-spread use of electricity to replace internal combustion engines be required but sufficient electric power for supporting the oil and gas industry be infeasible.

Significantly reducing NO_x emissions would require implementation of substantial control measures or elimination of NO_x emission sources. This section evaluates the feasibility of expanding electrification in the Uinta Basin as a possible means of reducing NO_x emissions. The feasibility evaluation considers the logistics and economics of requiring electrification and the significant impact on the oil and gas industry and thus local socioeconomics, should sufficient infrastructure expansion be infeasible.

Oil and gas industry drivers for development of electrification include a) environment and social, governance (ESG), b) limiting risk, and c) economics. [Steph, 2022] Limiting risk includes providing a sufficient and reliable source of power, such as from a utility grid or onsite generation. This study examines engineering, environmental, and economic aspects of electrifying the oil and gas fields in the Uinta Basin.

Key sources of NO_x and volatile organic compound (VOC) emissions in the Uinta Basin that might be affected by electrification include:

- Pumpjack engine NO_x and VOC emissions
- Separators and heaters NO_x emissions
- Pneumatic controller VOC emissions
- Pneumatic pump VOC emissions
- Storage tank VOC emissions

- Drilling and completions NO_x and VOC emissions

There are additional sources of NO_x and VOC emissions, but the source categories above were deemed as having the best potential to be significantly affected by electrification. The focus of this study is on reducing NO_x emissions by expanding the availability of electricity.

The area being studied is the Uinta Basin as depicted in Figure 23 and the associated existing electrical grid. The Basin, for the purposes of this analysis and when referred to in this study, includes Duchesne and Uintah counties and subparts thereof. References to the Basin are not intended to extend into other counties. The shaded areas in Figure 23 depict locations of oil and gas wells.

IV. A. Engineering

Part of determining the feasibility of reducing NO_x emissions by way of replacing NO_x sources with electrical power is evaluating:

- Complimentary emission reductions from electrification
- The current status of the electrical grid
- The types of electrical infrastructure changes needed
- The types of electrical infrastructure changes being planned
- The areas that would most benefit from electrification
- The feasibility of electrifying various parts of the Basin
- The reliability of an electrical grid as a primary power source

Reducing NO_x emissions could involve replacing combustion sources used for mechanical processes such as pumping oil and instead using electricity. The level of power required at a well pad can vary depending on a variety of factors, but is believed to be in the neighborhood of 0.25 MW to 2.5 MW for a well pad. [Steph, 2022]

IV. A. 1. The existing electrical infrastructure

There are three basic types of electric utilities, 1) electric cooperatives, 2) investor-owned utilities, and 3) public power systems. An electric cooperative is owned by the members and the members are also the electric power consumers. All the owner members live within the cooperative's service area. An investor-owned utility is just that, owned by stockholder investors. The investor-owners do not necessarily live in the service area and are not necessarily stockholders but may be either or both. A public power system is owned by a governmental entity such as a city, state, or federal government.

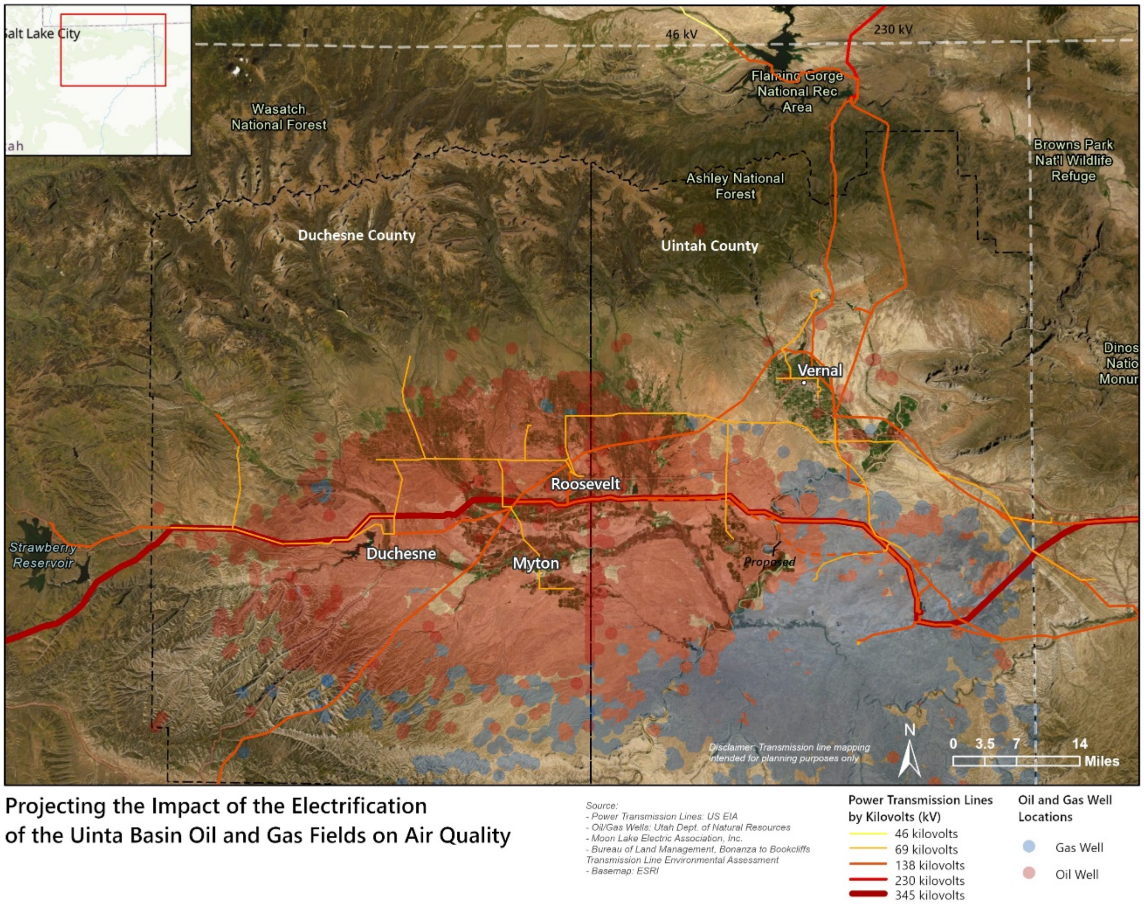

Figure 23. Uinta Basin electrification study area transmission grid

The Uinta Basin is primarily separated into two distinct service areas, as shown in Figure 24, with one area being served by Rocky Mountain Power (RMP) and the other served by Moon Lake Electric Association, Inc. (MLEA). RMP is an investor-owned utility and a division of PacifiCorp. MLEA is a rural electric cooperative. There is another retail electric service provider indicated in Figure 24, Bridger Valley Electric Association, Inc., positioned on the North side of the Uinta Mountains, whose service area is largely outside of Duchesne and Uintah counties and not within this electrification study area. The remainder of this analysis will focus on RMP and MLEA service areas in Duchesne and Uintah counties.

There are three power plants currently in operation in Utah in this region, the Flaming Gorge hydroelectric plant, located about 30 miles north of Vernal, the Uintah Hydroelectric Plant, located about 17 miles north of Roosevelt, and the Bonanza power plant, located about 25 miles southeast of Vernal. There are other powerplants in the region, but the Flaming Gorge, Uintah, and Bonanza facilities are the only ones located within the Uinta Basin study area.

The existing Uinta Basin electric transmission system is depicted in Figures 25 through 28, which display the Uinta Basin region separated into four distinct quadrants, northwest, northeast, southwest, and southeast, respectively. Note that Figures 25 through 28 overlap one another. Figures 25 through 28 do not cover the entire Uinta Basin or the entirety of Duchesne and Uintah counties but focus on the portion of the Uinta Basin electric grid serving the area with most of the oil and gas operations. The figures representing the local electric grid depict 69 kilovolt (kV), 138 kV, and 345 kV powerlines. Local service is provided via local distribution lines that carry lower voltages, reduced via transformers, suitable for end users. The figures do not depict the local service grid for which the larger infrastructure provides power.

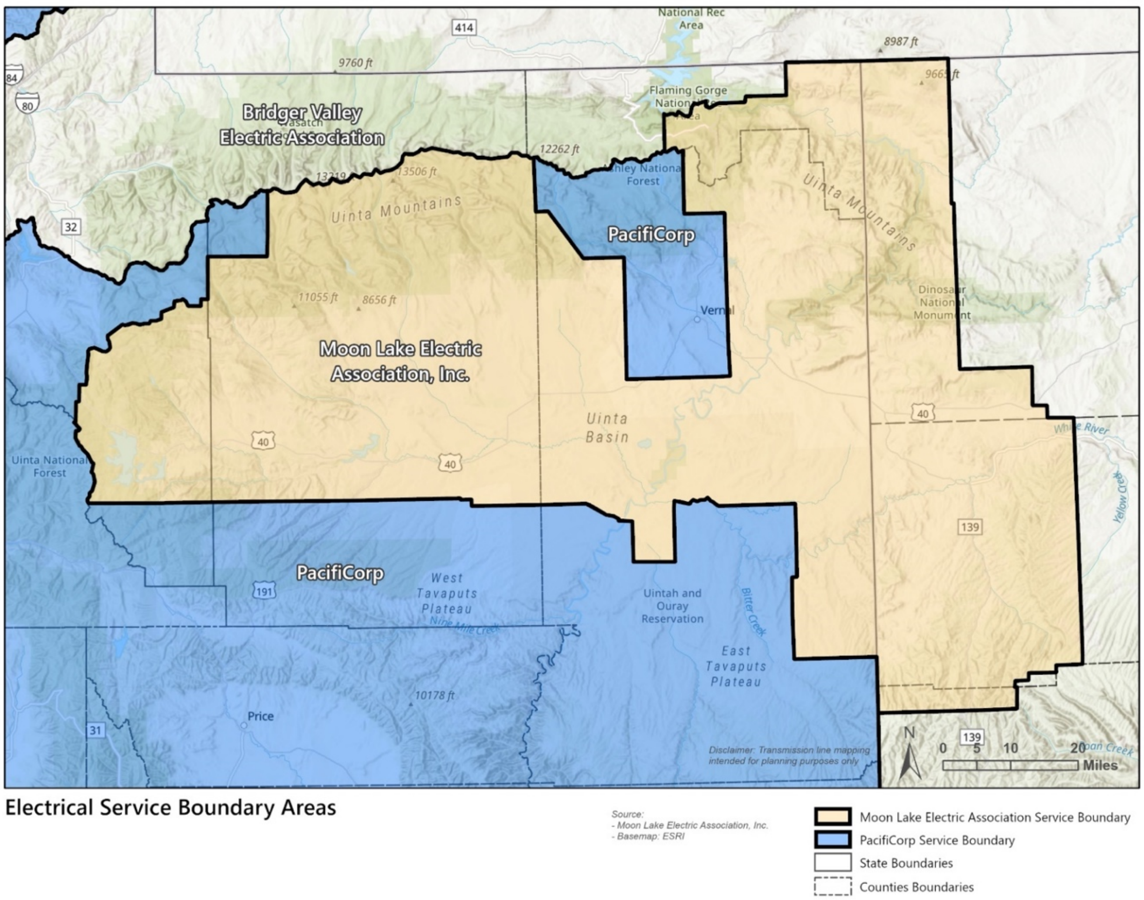

Figure 24. Uinta Basin electrical service area boundaries

As shown in Figures 25 and 28, there is a 345 kV east-west running powerline through the midsection of the Uinta Basin, originating at the Bonanza powerplant. The same 345 kV line can be seen in all four of the Figures 25 through 28 since these maps overlap. There is also a network of substations and 138 kV and 69 kV lines, primarily located north of the 345 kV powerline. The area north of the 345 kV line is the more populated part of the Uinta Basin, which is generally along and north of U.S. Highway 40 which runs from the Utah-Colorado state line north of Bonanza westward through the Basin communities of Vernal, Roosevelt, and Duchesne.

As shown in Figure 24, RMP primarily serves the southern part of the Uinta Basin in Duchesne and Uintah counties as well as an area around and north of Vernal. Vernal itself is located within RMP's service area. RMP's southern Uinta Basin service area is sparsely populated. There is nominal availability of electric power distribution in the area served by RMP in the southern parts of the Uinta Basin, limiting the electric power available to oil and gas development in RMP's southern Uinta Basin service area.

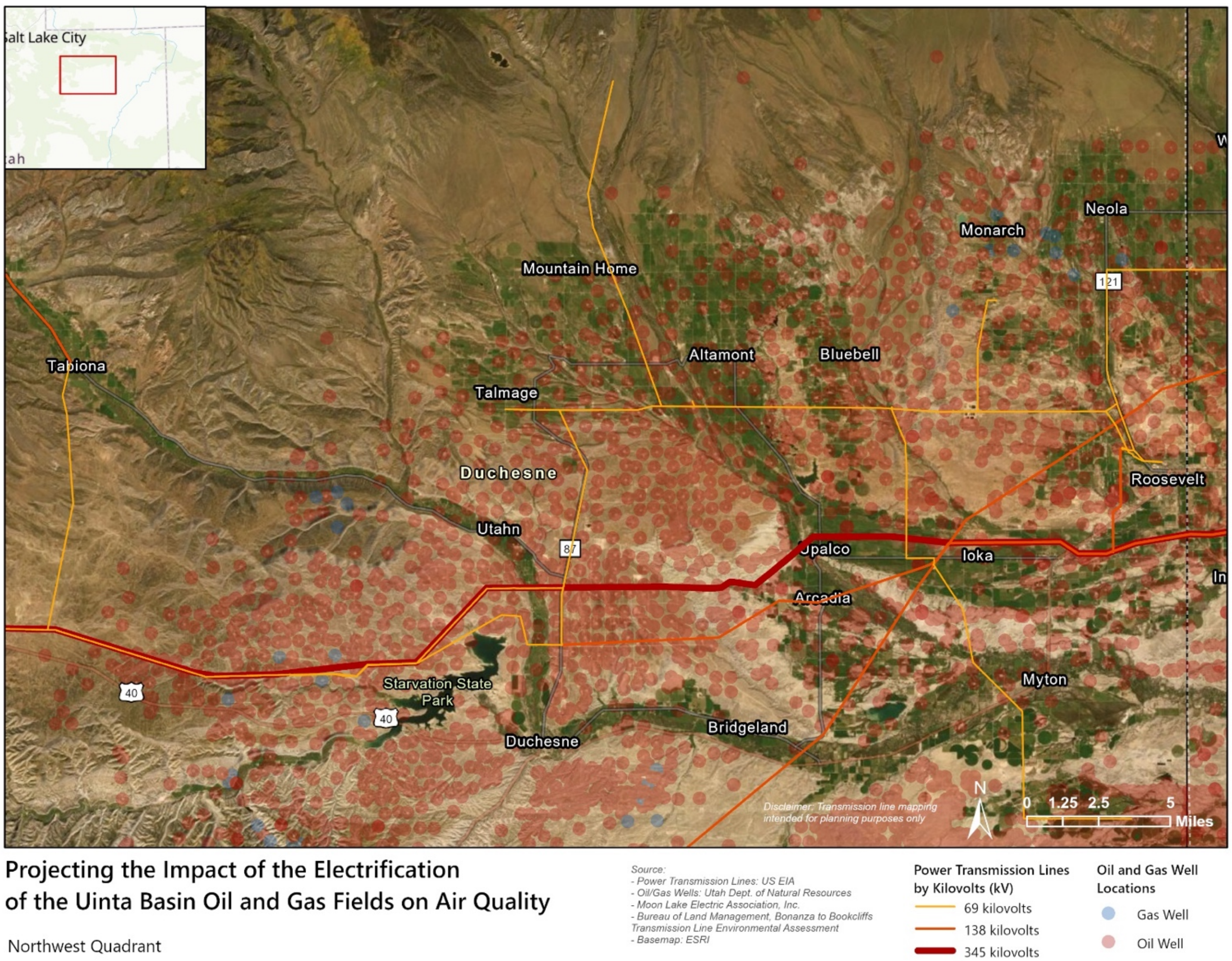

Figure 25. Uinta Basin Northwest Quadrant Transmission Grid

MLEA is a member-owned electric service cooperative where each customer is a member-owner, and the cooperative is tasked with the delivery of electricity to the members. The more heavily populated regions of the Uinta Basin, and thus customers, are in the northern parts of Duchesne and Uintah counties. As can be seen in the transmission system maps, the established electrical grid largely coincides with the more populated northern parts of the Uinta Basin, as would be expected.

MLEA has characterized their portion of the Uinta Basin electrical grid as being “in a stable condition.” [MLEA 2021b] MLEA has been maintaining the Uinta Basin grid to keep it “reliable” by regularly replacing old poles and conductors while upgrading lines as needed. [MLEA 2021b] MLEA has characterized their operations as being a “stable and reliable source of power” based on a partnership with Deseret Power and Transmission [MLEA 2021b] who operates the Bonanza powerplant and serves as a wholesale source of electricity for them.

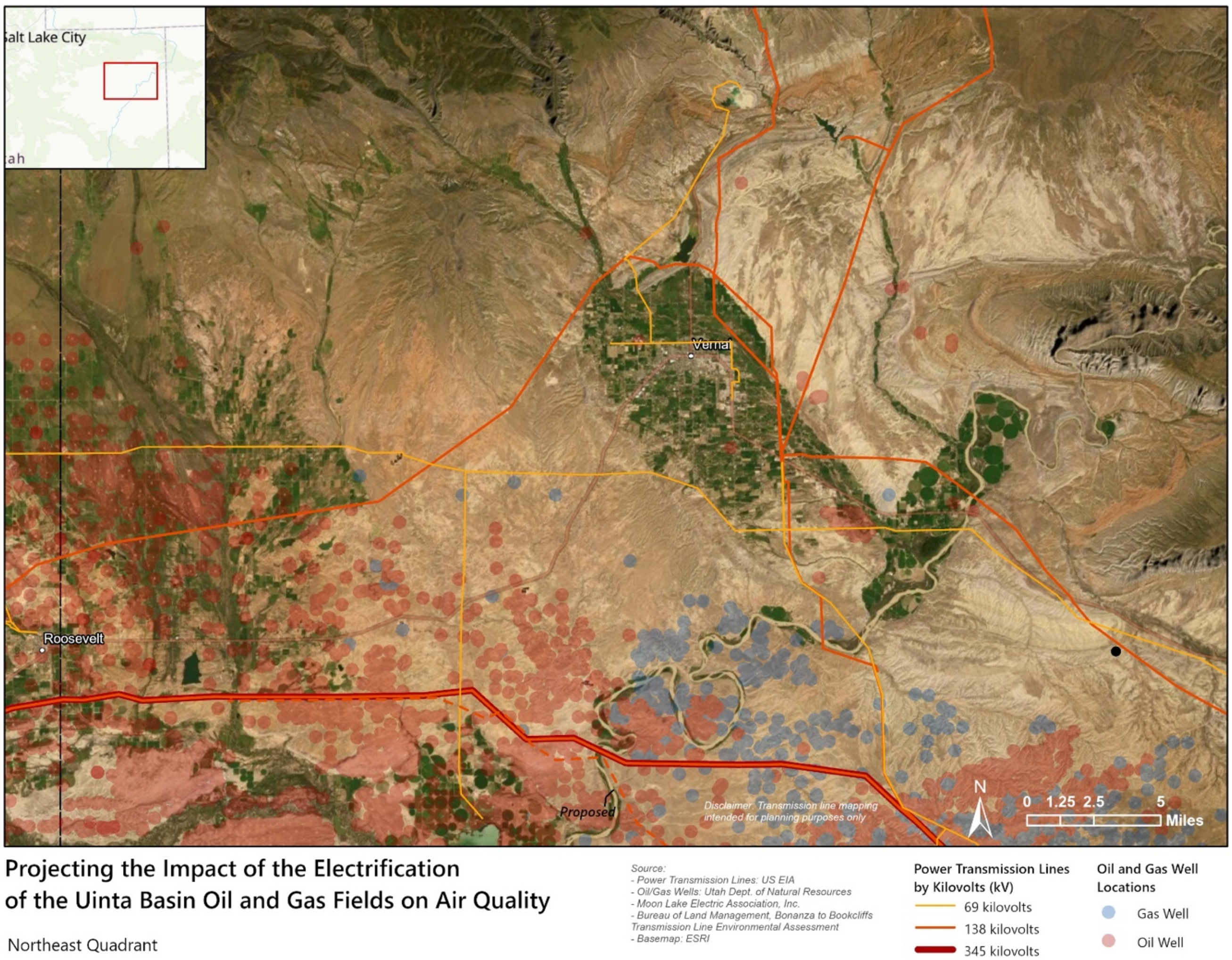

Figure 26. Uinta Basin Northeast Quadrant Transmission Grid

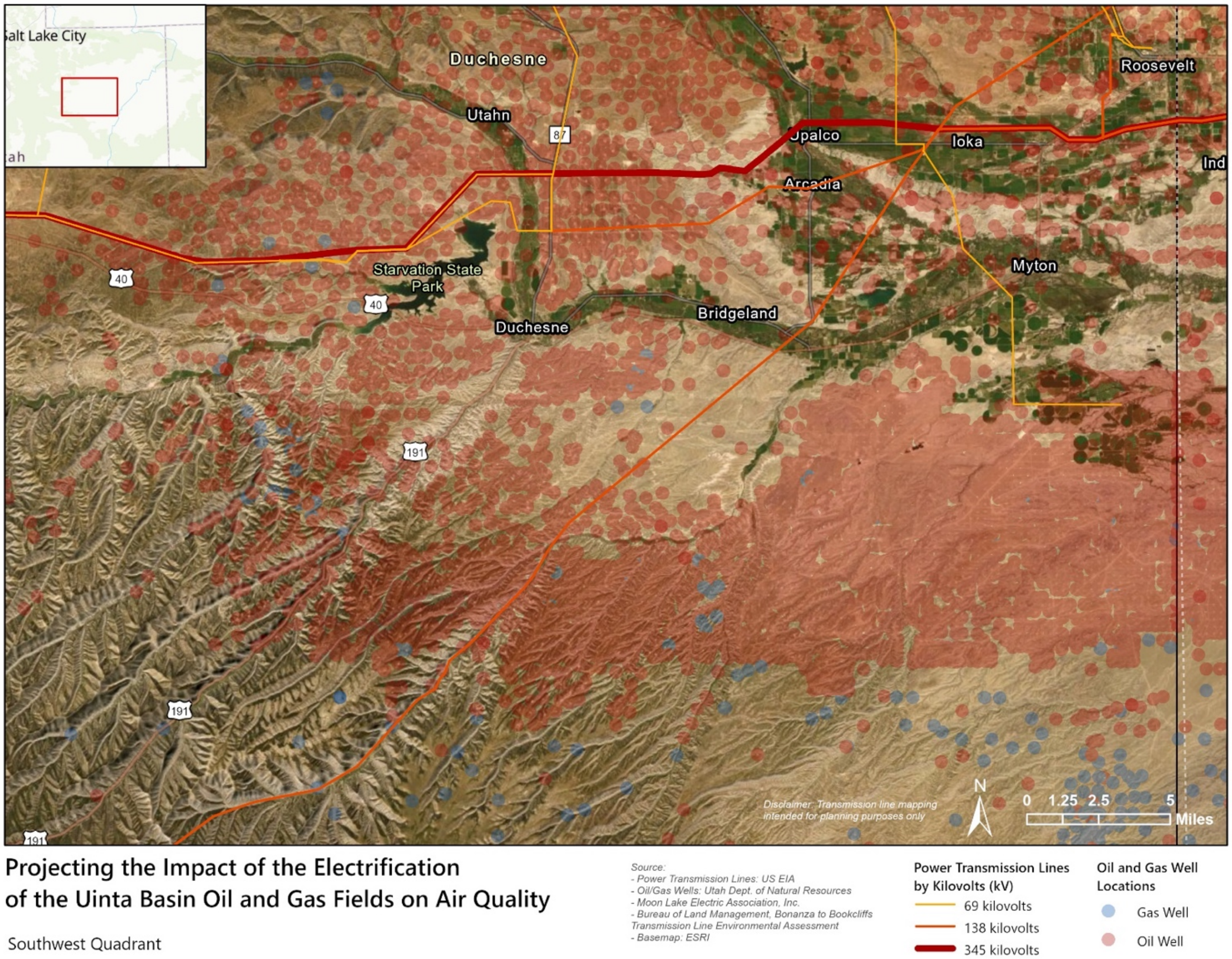

Figure 27. Uinta Basin Southwest Quadrant Transmission Grid

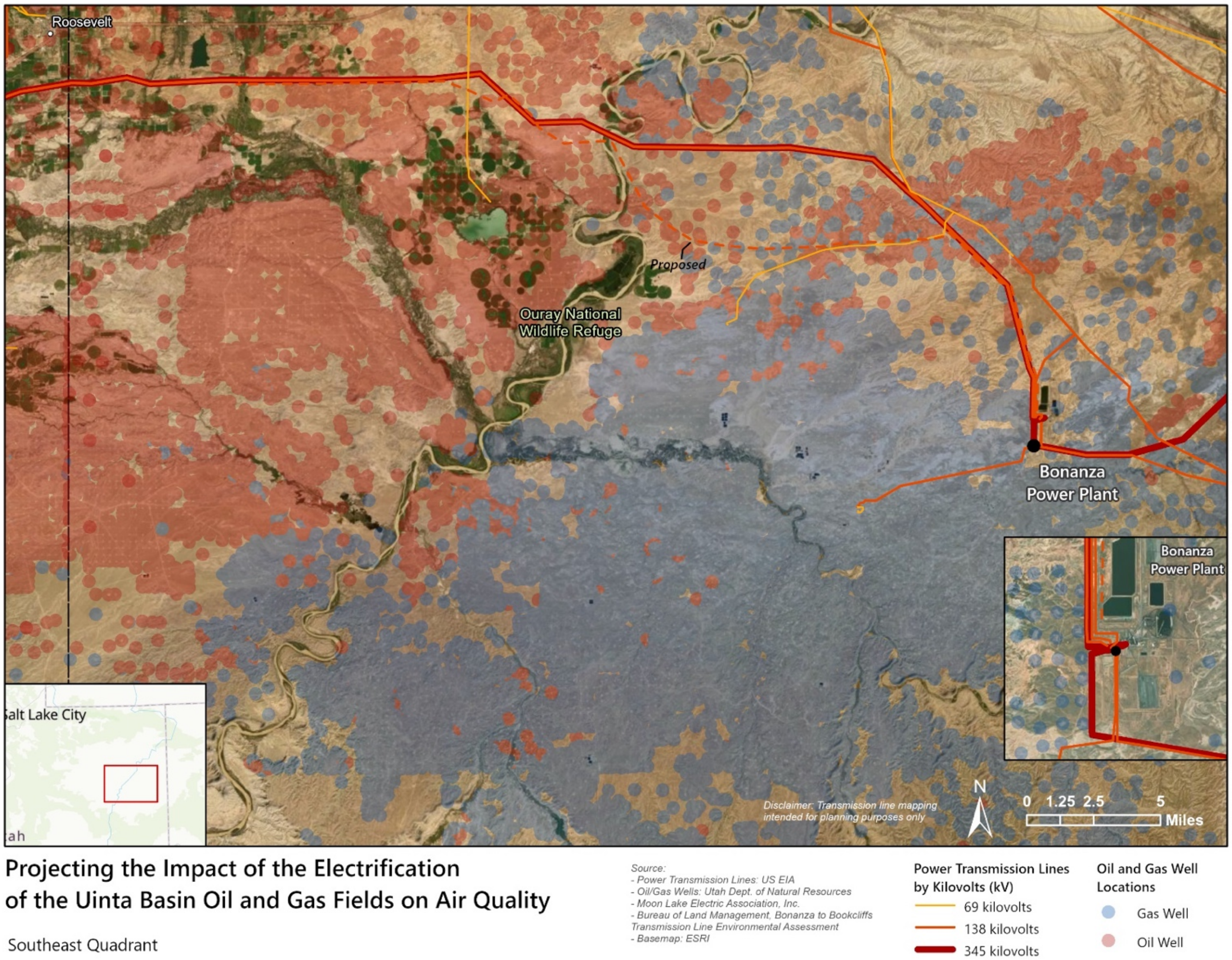

FIGURE 28. Uinta Basin Southeast Quadrant Transmission Grid

IV. A. 2. Needed Electrical Infrastructure Changes.

This study is evaluating potential air quality benefits from electrifying oil and gas production operations. “There is no real disagreement over the benefits of electrifying production operations.” [Urquidez, 2022a] Some of the biggest electric transmission infrastructure changes needed involve upgrading transmission lines, substations and switch yards of the existing infrastructure. [MLEA 2021b] In addition to addressing the existing system in the Uinta Basin, expansion into rural unserved areas to support oil and gas wells is important to look at reducing NO_x emissions.

As can be seen in Figure 23 and Figures 25 through 28, much of the oil and gas development in the Uinta Basin has taken place in regions that are not extensively covered by the existing electrical grid. As a result of the lack of electrical service in portions of the Uinta Basin where significant oil and gas development has occurred, it has been necessary for oil well operators to depend on onsite natural-gas-fired pumpjack engines for oil wells. Significant expansion of the electric grid would be required to provide power on a meaningful level to areas where oil wells are dependent upon pumpjack engines and make a significant reduction in pumpjack engine NO_x emissions.

Given the existing electric grid and types of oil and gas development that occur in the Uinta Basin, this study has broken the evaluation of electrification into four study regions to evaluate the effects of NO_x emission reductions, as shown in Figure 29. The four study areas depicted in Figure 29 are evaluated for the potential for electrification and the effect of electrifying well sites and replacing natural-gas-fired reciprocating internal combustions engines used for oil production. According to MLEA the part of their service area that would most benefit from expanding electrification would be Area C. [MLEA 2021b]

The feasibility of having local utilities provide power to meet the needs of the oil and gas industry depends in part on the timing to get power from the distribution lines to the specific location, such as a well site, where the power is needed. [NM-EMNRD 2019] There are circumstances when onsite generation is required, at least temporarily if not permanently, due to a large distance to the needed power distribution system and the scheduling of installing the needed lines to provide the power. [NM-EMNRD 2019] Therefore, such line power may not always be the answer.

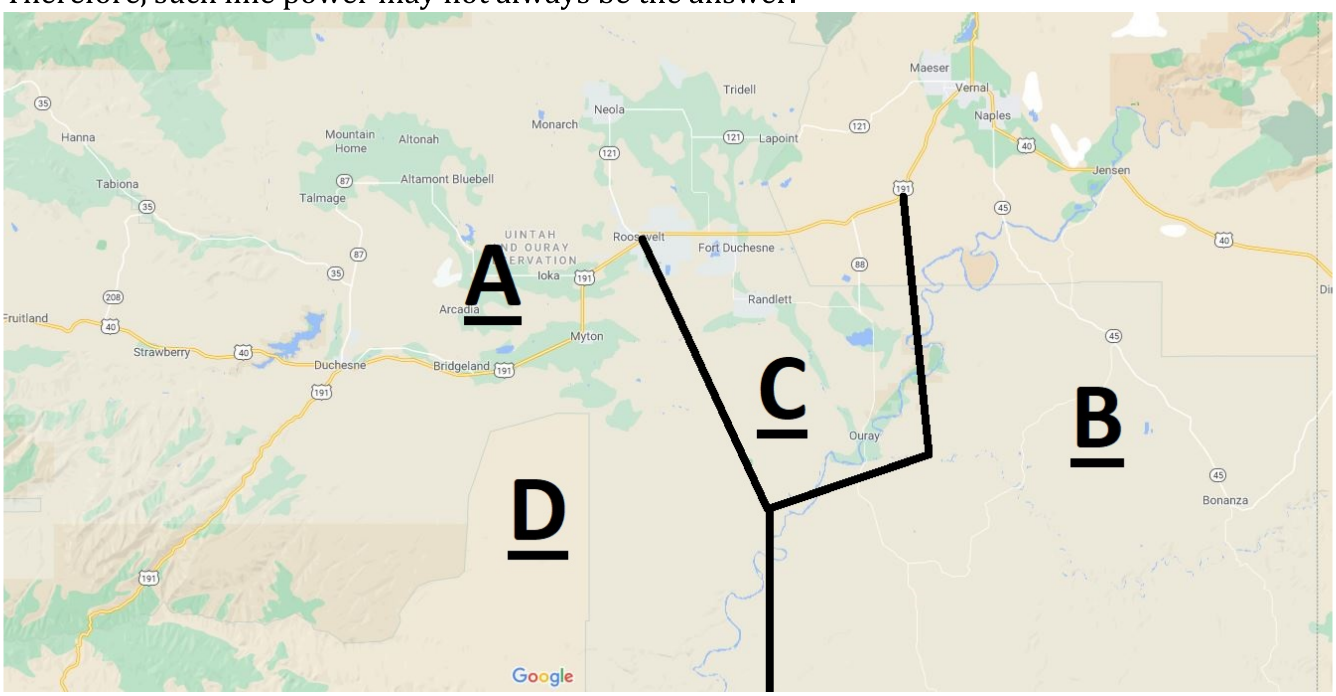

Figure 29. Study Regions

Because it can be challenging to provide adequate, reliable power to remote locations, and because of the relatively short life span of wells and fluctuations in demand for oil and gas, onsite generation can be a preferred approach when distribution from utilities is not available. [NM-EMNRD 2019] It is not uncommon for well sites to use onsite generation. [NM-EMNRD 2019]

IV. A. 3. Planned Infrastructure Changes

Bonanza to Upalco 138 kV Transmission Line

As a result of load growth forecasting, MLEA is planning a significant transmission project to allow them “to continue to supply reliable power into the future.” [MLEA 2021b] MLEA has identified plans to build a new 138 kV transmission line from the Bonanza substation, adjacent to the Bonanza powerplant, which would proceed in a northwesterly direction, eventually terminating approximately 9 miles southwest of Roosevelt at the Upalco substation. [MLEA 2021b] The first phase of the planned transmission line will be from the Bonanza powerplant to the Bookcliffs substation located about one mile south of the community of Fort Duchesne. The proposed Bonanza to Bookcliffs section of the transmission line is shown as a dashed line in Figure 28. The new transmission line will be approximately 38 miles long and traverse the north ends of study Areas B and C as shown in Figure 29.

The proposed new MLEA Bonanza to Bookcliffs transmission line is intended to provide reliability upgrades and additional capacity to the transmission system in areas west of Vernal. [MLEA 2021a] The new transmission line is also intended, in part, to accommodate major load increases for planned load additions for the oil and gas industry in the area. According to MLEA, “a new transmission line is needed to improve reliability, allow for planned future growth, and support conversion of local industry emitting sources to electricity to improve air quality.” [MLEA 2021a] MLEA’s service growth in Area C of the study map shown in Figure 29 is primarily the result of electricity needs of the oil and gas industry. [MLEA 2021b]

The Bureau of Land Management (BLM) issued a Finding of No Significant Impact (FONSI) for the proposed Bonanza to Bookcliffs Transmission Line on September 16, 2021. Also on September 16, 2021 the BLM issued a Decision on the Bonanza to Bookcliffs Transmission Line giving MLEA authorization to construct the powerline. MLEA has proposed completion of the Bonanza to Bookcliffs Transmission Line within five years of the BLM decision, [MLEA 2021a] thus by September of 2026. The remaining portion of the entire planned Bonanza to Upalco transmission line, the section from the Bookcliffs substation to the Upalco substation, is still going through steps associated with establishing a final route to be followed up by permitting and approvals.

Enefit American Oil Utility Corridor Project

Enefit American Oil (EAO) and MLEA have proposed a project that includes 30 miles of 138 kV transmission line in addition to a water pipeline, natural gas pipeline, oil pipeline, and road upgrades. [BLM 2018] The proposed transmission line would go from the Bonanza powerplant then southeast to terminate at EAO’s South Project Mine site.

The proposed new transmission line is for the proposed purpose of providing power to the EAO facility. Once constructed the transmission line would pass through the eastern part of Area B and might hold the potential to provide electrical service to what are primarily natural gas operations in the area. The Enefit American Oil Utility Corridor Project received BLM approval as the result of a September 26, 2018 Record of Decision. [BLM 2018] Expanded electrical service in the natural gas fields in and around this EAO project are not expected to provide significant reductions in pumpjack engine NO_x emissions in large part because the area is predominantly involved with natural gas development rather than oil production.

TransWest Express Transmission Project

The TransWest Express Transmission Project (TWETP) [FR 2016] consists of a planned 600 kV direct current transmission line that would cross Duchesne and Uinta counties along an east-west line approximately 20 miles south of Vernal, UT. The proposed TWETP transmission line would parallel the existing 345 kV transmission line in the central Uinta Basin as shown in Figures 25 through 28 for all but approximately the first 30 miles from the Utah-Colorado border, proceeding west. The last 30 miles crossing the east end of Uinta County would also run east-west, rather than southeast toward Bonanza with the existing 345 kV line, from a point some 20 miles south of Vernal.

The stated purpose of the TWETP is to deliver wind-generated electricity from south-central Wyoming to a substation in southern Nevada. It would deliver approximately 3,000 megawatts of "zero-carbon" electricity. There are no known plans for TWETP to deliver power to the Uinta Basin, and it would not serve to improve electricity distribution to the Basin.

Energy Gateway South Transmission Line Project

The Energy Gateway South Transmission Line Project (EGSTLP) [BLM 2016] consists of a RMP-proposed 500 kV transmission line that would begin near Medicine Bow, WY and extend west and south to terminate near Mona, Utah, south of Provo. The EGSTLP would pass through Duchesne and Uinta counties from a point approximately 6 miles south of where U.S. Highway 40 crosses the Utah-Colorado border and run southwest through the Uinta Basin, passing through the natural gas fields of Area B and continuing southwest in a trajectory located about 8 miles south of the primary cluster of oil wells in Area D.

The purpose of the EGSTP is to improve the transmission network. The Environmental Impact Statement identifies the following as needs to be fulfilled by the EGSTLP [BLM 2016]:

- Meet the electric demands across the service area that includes California, Idaho, Oregon, Utah, Washington, and Wyoming.

- Provide transmission service to third-party customers who are required to meet the needs of their own customers.
- Improve the reliability of electric service and provide redundancy and operational flexibility in the network.
- Provide transport of generation from third parties to meet their own customer demands while accommodating future energy needs and plans.
- Interconnect with the west-wide electric grid as part of an interconnected system of electric power transmission.

Providing electricity to oil and gas customers in the RMP service area is likely to be a business decision to be made by RMP. RMP is an investor-owned utility that must answer to stockholder investors, which is expected to be a key factor in deciding what to do with transmission in the Uinta Basin. Much of Area B that the EGSTLP transmission line will cross is in the MLEA service area. Once the transmission line passes back into the RMP service area in Area D the brunt of the wells with pumpjack engines are north of PacifiCorp in the MLEA service area. Construction of the EGSTLP transmission line is expected to start in the first quarter of 2022 and line service is expected to be available to customers by October of 2024. [PacifiCorp 2022]

IV. A. 4. Areas that Would Benefit from Electrification

Table 13 provides information on oil wells with pumpjack engines that were producing in February of 2017 for each of the four production areas identified in Figure 29. February 2017 was chosen as the period being evaluated in the air quality assessment portion of this study. The well count in Table 13 represents the number of producing wells with engines as reported in the Utah Division of Environmental Quality's 2017 emissions inventory [UDAQ 2021] and February 2017 production data from the Utah Division of Oil, Gas and Mining. [UDOGM 2021a]

Area A

Area A shown in Figure 29 is the northwest-most region of the study area and can be generally characterized as lighter Uinta Basin crude oil and having high producing long horizontal oil wells, with very few natural gas wells. Area A largely consists of the area North of U.S. Highway 40. As can be seen by the distribution of powerlines in Figure 25, Area A is one of the better electrified areas in the Uinta Basin.

As shown in Table 13, Area A is a relatively high oil producing area for the Uinta Basin but the total NO_x emissions from production sites in Area A are very low. The low number of production site engines and subsequently the low NO_x emissions for Area A is believed to reflect a relatively accessible electric grid resulting in a relatively low use of pumpjack engines in Area A.

The electric grid in Area A is relatively good, as shown in Figure 25, but can benefit from continued expansion as new wells and production in the area grows. There are currently site-specific generators used at well pads in Area A for the purpose of providing electric power to electric well pumps when the local grid doesn't reach the site. There are parts of Area A that could benefit from further electric grid development and replacement of existing site-specific generators which produce NO_x emissions. Given the existence of some existing infrastructure already, and the use of onsite generators already, expansion of the grid in Area A as development continues will have a benefit to reducing NO_x emissions.

Table 13. February 2017 Well and Emissions Statistics for the Modeled Sources

Region	Location	Average Well Age (years)	Average Well Oil Production (bbl/day)	Percent of Total NOx	Total NOx (g/hr)	Number of Producing Wells
A	NW	5	19	0.7%	91	17
B	E	17	7	13.7%	1,823	160
C	Mid	5	26	24.4%	3,235	567
D	SW	7	8	61.2%	8,121	2144

Area B

Area B is the eastern part of the Uinta Basin that is dominated by natural gas production and less so by oil production. Area B is where the Bonanza powerplant is located and there is some electric power available from an established grid in the northern portion of this area, as shown in Figure 26. Given the overwhelming presence of natural gas wells in Area B and the low demand for onsite natural gas combustion at such sites, Area B was established as one of the standalone study areas to evaluate effects of electrification.

According to the data in Table 13 representing February 2017, the production sites using engines in Area B have relatively low production. This reflects the area being dominated by natural gas production. There were more engines in Area B than Area A, but the number of engines operating in February 2017 in Area B, 160 engines, were still relatively low compared to the Uinta Basin-wide count of 2,888 engines. Area B oil production site NO_x emissions represented only 14% of the February 2017 total NO_x used in the study. However, Area B production engine count represented only 6% of the Uinta Basin production engine count. The ratio of NO_x emissions per well in Area B, 11.4 grams of NO_x per well (g-NO_x/well), compared to 5.3 g-NO_x/well in Area A, 5.7 g-NO_x/well in Area C, and 3.8 g-NO_x/well in Area D, could be a reflection of the age of the wells operating on engines in the area and the corresponding low production rate. Older engines are expected to have higher emission rates.

Area B has existing electrical infrastructure in the northern and eastern portions of the area. However, spending extensive resources on significant expansion of the grid in Area B is unlikely to have as significant an impact in lowering Uinta Basin NO_x emissions as compared to other areas given the relatively low level of Area B NO_x emissions.

Area C

Area C represents the middle portion of the Uinta Basin where drilling had been picking up in recent years and there were relatively newer crude oil producing wells. As show in Figure 25 and Figure 26, there is some electric infrastructure in the northern reaches of Area C but the availability is not extensive.

Table 13 shows that Area C has some of the higher producing wells in the Uinta Basin that have engines, which is not surprising given that Area C wells are some of the newer wells and the electric grid in the area is not extensive. Area C has 24% of the NO_x emissions and 20% of the wells operating in February of 2017 and using engines. Area C produces about 2,986 grams of NO_x per barrel of oil (g-NO_x/bbl), as compared to 115 g-NO_x/bbl for Area A, 6,250 g-NO_x/bbl in Area B, and 24,363 g-NO_x/bbl in Area D. Area C has the lowest ratio of NO_x/bbl of the three areas with the least electrification, Areas B, C, and D, which could mean that Area C wells are relatively newer with newer engines operating overall compared to Areas B and D.

The following are attractive electrification characteristics of Area C:

- Relatively light existing electric powerline coverage
- The proximity to nearby transmission lines
- MLEA has plans to increase electric transmission in the area (see section III.D.1.a.iii)
- Wells are relatively new and produce at a high rate
- Second highest well pumpjack engine count
- Second highest NO_x emissions
- Proximity to the Ouray ozone monitoring site which tends to measure the highest ozone levels in the Uinta Basin

The characteristics noted above might make Area C electrification the most cost-effective area to reduce a significant amount of NO_x emissions through replacing pumpjack engines with electricity. This would need to be further evaluated prior to making plans and taking action.

Area D

Area D is the Southwest portion of the Uinta Basin generally consisting of slightly older vertical wells producing lower volumes of heavier oil. Area D is somewhat more developed with wells than Areas A and C. The well count in Area D is much higher than the other areas. Area D was isolated as a standalone region for this study because of the relative age of wells and the tendency of the wells to have lower production. The electric grid is rather undeveloped in Area D, as shown in Figures 27 and 28.

Table 13 shows that in February 2017 Area D had the most production engine NO_x emissions along with the highest number of wells using engines. Area D has 74% of the well engines in February of 2017 and 61% of the engine emissions. Area D had 51% of the Uinta

Basin production associated with production engines while Area C had 44%, as compared to 74% and 20% of the engine count for Area D and C, respectively, and 61% and 24% of the emissions for Area D and C, respectively. The higher ratio of NO_x emissions per barrel of production in Area D is likely a reflection of the characteristically lower production rate and the age of wells.

The wells in Area D are somewhat older than those in Areas A and C, as showin in Table 13. Production from the wells in Area D is much lower than those in Area A and Area C, on a per-well basis, as shown in Table 13. There are almost 4 times as many pumpjack engines in Area D as in Area C but only about 15% more total production, as a result of Area D having older low producing vertical wells. The broad expanse of the area covered by Area D and its relatively low existing electric infrastructure, being very undeveloped, and the type of wells in Area D, relatively low producing and aged, make it appear less attractive for spending significant resources for building out an Area D electric grid.

IV. A. 5. Expansion Challenges

It is important that local infrastructure be considered concerning implementing the use of electricity in oil and gas fields. The density of the well sites that could be considered for electrification are a key factor and help drive the types of electrification infrastructure to be considered. [Urquidez, 2022b] Choosing to electrify often depends on well density and the timing of getting power to where it's needed. [Urquidez, 2022a] California oil and gas fields have relatively good access to utility grids [NM-EMNRD 2019] which can make the implementation of electricity in oil and gas there somewhat more feasible than other areas, but not in all instances.

Knowing that wells are likely to be developed in close proximity, when that is the case, they characteristically need to have long lead times for infrastructure development to become more manageable. [Urquidez, 2022a] If there is sufficient and reliable utility owned power grid infrastructure within a few miles of where the power is needed there can be good options to building out the grid to support oil and gas operations, depending on the circumstances involved. [Urquidez, 2022a]

If the plan would be to have a location with natural gas fired generators and distribute the electricity offsite through a local grid serving numerous well sites, the challenges in obtaining a needed air permit would be significant under the current status of the Uinta Basin. The Uinta Basin is currently not meeting the AAQS for ozone concentrations that have been established by EPA and the State of Utah. Key factors in meeting ozone AAQS are the emissions of NO_x in the area from sources such as natural gas fired generators. Obtaining a permit to install a generator, which would increase NO_x emissions, for the purpose of providing electric power to a local micro-grid would face major hurdles that can be difficult to surmount given the current regulatory circumstances in the Uinta Basin. There are regulations that can streamline air quality approvals for oil and gas equipment NO_x emissions site-by-site, however such regulations don't cover sites not directly involving oil and gas equipment.

A key challenge to expanding electrification in the Uinta Basin pertains to easements and rights-of-way as well as the government permitting and approval processes involved. Challenges presented by easements, rights-of-way, permitting, and approvals make electrifying remote parts of the Uinta Basin, where much of the oil and gas development has occurred and continues to develop, "nearly impossible or extremely slow at best." [MLEA 2021b]

Getting electricity with the required electrical parameters from an electric utility to an oil and gas site will require infrastructure between the main utility powerline and the oil and gas site equipment. The infrastructure between the electric utility and the site equipment can be characterized in the following general categories.

- Custody transfer and metering equipment
- Protective equipment
- Transformers
- Primary powerlines
- Secondary powerlines

Electrical infrastructure can be characterized as primary or secondary. Primary lines are typically high voltage lines and secondary lines provide the power to the site equipment at a much lower voltage. The main difference in infrastructure between primary and secondary lines is where protective equipment from the power custody transfer and the transformers occurs in the process and who is responsible for the operation and maintenance of different parts of the system.

In primary metering the custody transfer and metering is owned by the utility company at the front end of the infrastructure and is the only part beyond the utility line that is owned by the utility. In primary metering the infrastructure beyond the utility's custody transfer and metering equipment is the responsibility of the customer who is responsible for installing, operating, and maintaining primary infrastructure feeding protective equipment and transformers as well as the secondary powerlines that then feed facility equipment.

With primary metering the customer must provide the staff and technical expertise to install, operate and maintain all electrical equipment, both primary and secondary. An advantage to primary metering is that there can be shorter lead times for power drops since it can take less wait time for scheduling to get service equipment installed by the utility. Primary metering can run at a higher cost per facility with smaller operations but can be at a lower cost per facility for companies with a high number of sites. However, primary metering can be a major challenge dealing with land issues like easements and rights-of-way.

With secondary metering the electric utility company installs, owns, and operates the infrastructure upstream of the secondary powerline directly feeding the facility equipment. Secondary metering means the utility company is responsible for installation, operation, and maintenance of transformers, custody transfer and metering, protective equipment and the associated primary powerlines. The facility owner/operator installs, operates, and maintains secondary lines in secondary metering.

Secondary metering costs can run higher than primary metering in some areas. With secondary metering, companies are dependent on the schedule and resources available to the electric utility meaning that the process is driven by the utilities since most of the infrastructure is theirs. Secondary metering is not always an option.

The realities involved with timing of planning and approvals for electric infrastructure expansion may not be consistent with the timing needs for oil and gas development. [Urquidez, 2022a] Whether installing high voltage utility lines, high voltage primary lines, or secondary lines, expansion of the grid in the Uinta Basin will take a significant amount of time to go through the whole process from permitting, to obtaining easements and rights-of-way, followed by the build out of the infrastructure. The National Environmental Policy Act (NEPA) process alone for the proposed Bonanza to Bookcliffs transmission line took two years to obtain a decision and approval to begin construction. The NEPA process for the Bonanza to Bookcliffs transmission line occurred during a period of a few years when there were federal requirements limiting the amount of time that the NEPA process was to take and those requirements to speed up the NEPA process are going away under the following presidential administration and as such the time to complete the NEPA process is expected to lengthen. Buildout of the Bonanza to Bookcliffs transmission line is scheduled to be done within five years.

Getting through the process of obtaining easements and rights-of-way for the transmission line route prior to filing for permitting and approvals can take a year or two, and be a tremendous challenge. Oil and gas operators wanting to or considering electrification must consider the fact that planning, preliminary studies, and approvals can take years to complete prior to beginning construction. [Urquidez, 2022a]

The California Air Resources Board (CARB) examined the technical feasibility of options for reducing NO_x, VOCs, and other pollutants from internal combustion engines associated with oil and gas production in California. [CARB 2001] The CARB study concluded that electrification was a technically feasible method for reducing NO_x emissions and would have significant benefits to improving air quality in that region, but that electric power needed to be “reasonably accessible.” [CARB 2001]

The Colorado Department of Public Health and Environment (CDPHE) pointed out that one key consideration in evaluating the feasibility of electrification is the proximity of high voltage transmission lines. [CDPHE 2020] As discussed further in the economics section of this study, the cost effectiveness of electrification, with proximity to a power supply being a driving factor, was a concern as to feasibility depending on the availability of nearby power. [CARB 2001]

There are factors that can make privately owned power distribution systems appealing. Private ownership can minimize regulatory hurdles and make the distribution system buildout faster than if handled by a utility. [Urquidez, 2022a] Perhaps there could be commitment to transfer ownership and operation of parts of the private infrastructure to a utility once it goes into operation. [Urquidez, 2022a]

Partnering can be a welcome approach to electrification in areas served by electric power cooperatives if it is possible. [Urquidez, 2022a] Short term demands such as can be presented by electrifying oil wells in rural areas can present power cooperatives with unique difficulties such as staffing and operation. [Urquidez, 2022a] Building out private electric distribution grids and obtaining the electricity from a local cooperative can be advantageous for the cooperative by providing more paying customers, sustainable or growing economic activity and reduce some of the burden of operating parts of the private grid. [Urquidez, 2022a]

Oil and gas companies have been increasingly considering the use of renewable energy as a source of electricity as they expand. [Bernardi 2021] Available technology for renewable energy such as wind and solar has made substantial progress in recent years, [Stromsta 2020] improving the feasibility of renewables.

IV. A. 6. The Reliability of Electrification

The proper management and resulting stability of the electric grid that upstream oil and gas operations must depend on is critical to the required reliability of sources of electricity. [NM-EMNRD 2019] Electrification has been demonstrated to increase the operational “resiliency and de-risking” of oil and gas field operations, under set conditions including [Steph, 2022]:

- The availability of a reliable grid
- Producers having well designed infrastructure that are their responsibility
- Utility transmission, primary and secondary infrastructure is reliable
- Utility transmission, primary and secondary infrastructure is well maintained
- There are plans for restoring power when inevitable failures occur

Operating an electrical infrastructure meeting the characteristics above have resulted in operators experiencing improved reliability with less downtime and decreased maintenance. [Steph, 2022]

The reliability of electricity for the needs of the oil and gas industry can be dependent upon whether the infrastructure being used was built and maintained for the purpose of providing the high demand that could result from extensive use of the electrical grid. [NM-EMNRD 2019] Unreliable or insufficient grids, perhaps not designed or built for the purpose of supporting oil and gas, can result in unnecessary shutdowns. [NM-EMNRD 2019] Outages can result in damage to equipment and wells. [NM-EMNRD 2019]

The reliability of adequate voltage to a well site can be an important determining factor in using electricity. [NM-EMNRD 2019] Power interruption brings the risk of sending control equipment into “a fail-safe condition.” [NM-EMNRD 2019] Being dependent upon the reliability of electricity can be especially risky in rural areas. Without sufficient infrastructure to provide nearby levels of reliable power it may take months of working with the local utility to obtain just a portion of the level of power that might be needed. [NM-EMNRD 2019]

The quality of the power supply is a factor. Dense oil fields can affect the types of infrastructure needed to properly regulate and control the quality of electric supply. [Urquidez, 2022b] Use of equipment that frequently start and stop can cause issues with power quality. [Urquidez, 2022b] There are solutions available to minimize the negative effect of operations on power quality, but they should be identified and dealt with as early as possible. [Urquidez, 2022b]

If there is excess power beyond what is needed for an isolated location, if the power is sufficiently reliable and is allowed to be used in the larger grid, then distributed generation may help alleviate excess demand on the wider utility grid [NM-EMNRD 2019] potentially enhancing reliability of the grid. Relatively quick approvals of rights-of-ways for the distribution system would be required to make effective use of distributed generation, [NM-EMNRD 2019] however going through the process of obtaining rights-of-way is not always a quick process and takes advanced planning. [MLEA 2021b]

Improved reliability of renewables may be resulting in oil and gas operators to be implementing wind and solar energy use more frequently. [Stromsta 2020] Given the challenges faced with the reliability of “over-stressed” electrical grids renewable energy has appeared as an alternative in West Texas. [Stromsta 2020]

It is important that the integration of renewables into oil and gas production include sufficient planning to cover those times that the renewable resources are not available. [Bernardi 2021] Relying on renewable energy such as solar or wind power typically involves some manner of backup generation. [NM-EMNRD 2019] The intermittent nature of renewable energy requires companies to have backup electricity for those times that the renewables are not available, which will occur. [Bernardi 2021] Backup power is most likely to come in the form of onsite generation or the local power grid.

IV. A. 7. Complimentary Emission Reductions

Expanding electric power distributed generation could be economically beneficial under the right circumstances. [NM-EMNRD 2019] Electricity generated using produced gas from well sites with limited gas takeaway presents the opportunity to both limit flaring and provide distributed generation by combusting the gas in generators. Onsite generation presents opportunities to conduct methane reducing functions such as using electric equipment to replace dehydrators, heater treaters, pneumatic controllers, and pneumatic pumps [NM-EMNRD 2019] and perhaps send generated power offsite for additional beneficial use.

Having sufficient electricity available presents the opportunity to install additional controls on non-combustion sources such as vapor recovery units (VRUs) on storage tanks for VOC emission controls. VRUs can be more effective to control tank VOC emissions than combustors. However, if power were to fail the emissions being controlled would be diverted to combustors and possibly even vented directly to the atmosphere from pressure relief equipment. [NM-EMNRD 2019]

Renewable energy such as wind and solar have also been addressed in this report. Emissions from renewable energy backup in the form of engines driving backup generators can diminish some of the environmental benefits [NM-EMNRD 2019] although backup system emissions would still represent reductions from onsite generation alone.

Potential environmental benefits from well site electrification include methane reduction. [NM-EMNRD 2019] Natural-gas-fired engines are reported to be one of the largest sources of methane emissions in oil and gas production [Kolwey, 2020] and thus electrification could help make a significant reduction in methane emissions. ESG is a high-profile issue in the oil and gas industry.

Natural gas combustion for pumpjacks is a prevalent practice at well pads in the Uinta Basin and converting over to electrification would have the benefit of substantially reducing greenhouse gas (GHG) emissions as well and be accompanied by a positive impact on ESG. [Steph, 2022] GHG emissions reductions have become an important consideration in oil and gas operations. [Urquidez, 2022a] Having a regulatory system that allows oil and gas operators to get electricity in a timely manner will help reduce GHG emissions. [API 2020] Electrification has become a way to demonstrate commitment to ESG and GHG emission reductions.

IV. B. Economics

Electricity from a regional grid has been shown to be a very cost-effective source of power for oil and gas fields when there is sufficient capacity in an existing infrastructure where the power is needed. [Steph, 2022] The denser the regional sites needing power and the steadier the required load on the sites, then the more justifiable it becomes for investment into infrastructure for a distribution system to provide the required power. [Steph, 2022] Significant investment in electric infrastructure to provide power for oil and gas fields has occurred across the oil and gas industry as a whole. [Steph, 2022]

Employing electric power at oil and gas operations can provide significant cost savings under the right conditions. Using onsite gas for onsite power generation can lower operational costs beyond the cost of the generation and even create electricity revenues by selling power, if there is the ability to distribute the power onto the grid nearby. [NM-EMNRD 2019] However, depending on the quantity of generation occurring and thus the size of generating equipment, onsite generation could require a large quantity of gas to be collected from multiple wells and brought to a single site for use, [NM-EMNRD 2019] increasing costs and other challenges.

Should reductions in NO_x emissions be implemented through regulatorily forced elimination or sweeping reductions in the use of natural-gas-fired pumpjack engines on a large scale, such changes could require significant increases in the need for electric power in the Uinta Basin in order to maintain the level of service provided by the engines. Should the regional electric grid be unable to keep up with the demand for replacing the function of pumpjack engines, the economic impact in the Uinta Basin would be significant. Economic factors involving the replacement of natural-gas-fired engines with electricity via a regional electric grid to support the oil and gas industry is examined in this assessment. The economics of developing distributed generation grids is also assessed.

IV. B. 1. Electrification Costs

Consideration of the condition of local infrastructure on a site-by-site basis needs to be part of the evaluation of the cost of electrification. [NM-EMNRD 2019] Proximity of primary power will play a key role in the cost of getting the needed electricity to a site and thus the economic feasibility. [NM-EMNRD 2019]

Expanding electric service can require extensive infrastructure build out. [NM-EMNRD 2019] The cost of constructing utility distribution lines, excluding other costs, can be $50,000 to $90,000 per mile, depending on the location. [Cook et al. 2017a] For oil wells with low production rates, such as are not uncommon especially in study Area B and Area D, adding electricity costs to operating costs can be a significant operating burden. The cost of electrifying, especially a region with low production rates and without existing electrical infrastructure, can force wells to be shut-in when they might otherwise be able to operate. [Cook et al. 2017a]

Dips in oil prices can cause upstream oil and gas companies to retreat from capital investment plans that could have included getting utility line power to well sites. By oil and gas companies pulling back on capital investments associated with costly utility power, bringing in onsite generation as opposed to using line power can be more attractive from a financial perspective. [Cook et al. 2017a]

In a 2017 study [Cook et al. 2017a] the Enhanced Oil Recovery Institute (EORI) at the University of Wyoming examined costs of using electricity for oil lift and the associated impact on the economic life of a well. In addition, the 2017 EORI study evaluated whether, as a result of expanding use of distributed generation, utility provided power was a low-cost option for new oil and gas development. The EORI study concluded that the cost of electricity in their Wyoming study area ranged from $7 to $18 per barrel of oil. According to the study, most marginal wells were “far exceeding” those values and as a result being shut in. Shutting wells in will result in production decreases, lost revenue for governments and other public entities dependent upon taxes and fees and lost revenue for the utility, all of which will subsequently detrimentally affect the local economy.

The EORI study [Cook et al. 2017a] also evaluated the cost of using utility power lines versus using onsite natural gas fired generators. The study used data from 93 counties in six states involving 40 different utilities. In the case of greenfield development not located near existing power systems it was cheaper to utilize onsite generation when natural gas was available to operate the generators. Sixty-six percent of the scenarios evaluated gave a cost advantage to onsite generation versus utility provided power for the entire study.

A 2016 study by a team of researchers from the University of Wyoming characterized the prominent use of line power as opposed to onsite generation as being a result of a "justification and, possibly, misconception" that line power was cheaper and more reliable than onsite generation. [Cook et al. 2017b] The 2016 study [Cook et al. 2017b] concluded that utility provided power is "not necessarily" the lowest cost option for electrifying new oil and gas development. The use of utility line power can be cheaper than onsite generation when the well pads are in close proximity to one another and the new development consists of a large number of wells with high production rates. [Cook et al. 2017b] When evaluating the cost of utility line power in comparison to onsite generation, it is important to consider the capital costs for building and maintaining the power grid. As pointed out in the study, [Cook et al. 2017b] regulatory considerations and the growing importance of ESG are also very important factors beyond just costs associated with installation, operation, and maintenance.

Using onsite gas to generate onsite power can be "portable, scalable, and low or negative cost." [NM-EMNRD 2019]

The cost of renewable energy is such that wind and solar are becoming more cost-effective [Stromsta 2020] in that the cost of renewables have fallen substantially over time. [Tuttle 2020] Renewables have the potential to provide offsets to taxable earnings. [Bernardi 2021]

Solely relying on the intermittent nature of renewables is not an option for oil and gas operations since they require power on a full-time basis. [Bernardi 2021] The need for emissions generating backup can significantly affect the economic feasibility of using renewables. [NM-EMNRD 2019]

California has a relatively well-developed electric grid which has a positive effect on the application of electricity in oil and gas fields. [NM-EMNRD 2019] According to the CARB study, the cost-effectiveness of using electrification was highly dependent on the proximity of power. [CARB 2001] The study pointed out that electrification is an effective approach to reducing NO_x emissions if electricity is "reasonably accessible." CARB pointed out that engines located in remote areas could be limited due to the cost of bringing electricity to remote locations and that cost effectiveness should be considered before requiring electrification. According to CARB, electrification might be considered for engines of 50 horsepower (hp) to 500 hp but outside that range electrification may not be cost effective. CARB points out that electrification faces issues due to installation costs, the availability of power, and rates for electricity. [CARB 2001]

A CDPHE Four Factor Analysis [CDPHE 2020] deduced that replacing internal combustion engines with line power would cost $100 to $4,700 per ton of NO_x emissions reduced, depending on the size of the engine, the length and capacity of the required power line, without consideration of any impacts that might occur from increased load demand at the powerplant. The CDPHE study pointed out that the true cost of electrifying sites to replace internal combustion engines would have to consider distance to a power plant and the amount of power needed. [CDPHE 2020] The focus of the CDPHE analysis was larger engines such as might be used in compression.

Connecting more well sites to an electric grid can reduce operating costs in the form of less fuel used and less equipment maintenance. Utilities get the benefit of having more customers. [Kolwey, 2020] Sites that are connected to the electric grid can have opportunities to save money through effectively managing and reducing power consumption. [Kolwey, 2020]

IV. B. 2. Socioeconomics

If significant reductions in NO_x emissions were to become a requirement in the Uinta Basin, one possible target for reductions would be natural-gas-fired pumpjack engines. Electrification of wells has been used by the upstream oil and industry as an alternative to natural-gas-fired pumpjack engines in some regions, including some parts of the Uinta Basin. This section of the study report addresses some socio-economic factors associated with large scale elimination of natural gas fired pumpjack engines should such actions be needed.

This report provides information on the business and socioeconomic role associated with the oil and gas industry in the Uinta Basin. The report identifies types of business and socioeconomic effects that could potentially occur should widespread significant reduction in the use of natural gas fired engines become necessary and the electric grid be incapable of replacing the power needed to operate wells. A requirement to eliminate natural gas fired engines, should electric power be incapable of providing a timely and affordable alternative, could result in a downturn in the oil and gas production business in the Uinta Basin, having a significant socioeconomic ripple effect.

In this report, the Uinta Basin is treated as the whole of Duchesne and Uintah counties of Utah.

IV. B. 2. a. Population

Population is an important factor in assessing potential effects should elimination or sweeping reductions in the use of pumpjack engines occur at a rate that the growth of electric power availability, as an alternative oil pumping method, cannot keep pace. Table 14 presents the population of Duchesne and Uintah counties from 2010 to 2020, according to the Utah Department of Workforce Services (UDWS). The 2020 combined population of the two counties is 58,102. Duchesne county represents 36% of the 2020 combined population and Uintah County represents 64%. According to the data from the UDWS, Duchesne, Uintah and the combined Uinta Basin population grew by 12%, 14%, and 13%, respectively, from 2010 to 2020.

IV.. B. 2. b. Business sectors

Table 15 contains a breakdown of UDWS Uinta Basin businesses sector employment statistics for 2010 through 2020. Oil and gas extraction and associated support activities is the largest category of employers in both Duchesne and Uinta Counties, and thus the Uinta Basin as a whole. Note that the UDWS data identified as support activities are a combination of support to oil and gas extraction as well as mining. The UDWS data collected did not separately identify workforce support categories for oil and gas versus mining, however it could be reasonably expected that oil and gas would play a prominent role in the support activities data, given the nature of oil and gas operations and the fact that UDWS data demonstrate that the oil and gas extraction employment has been quadruple that of the mining industry over the period of 2010 through 2020.

Table 14. Uinta Basin population trends, 2010 – 2020 [UDWS-2022]

COUNTY	YEAR										
	2010	2011	2012	2013	2014	2015	2016	2017	2018	2019	2020
Duchesne	18,665	19,111	19,572	20,106	20,380	20,862	20,337	19,915	20,850	20,846	20,894
Uintah	32,619	33,315	34,435	35,690	36,867	37,928	36,373	35,219	36,921	36,972	37,208
Total	51,824	52,426	54,007	55,796	57,247	58,970	56,710	55,134	57,771	57,818	58,102

Tables 16 and 17 show trends in Uinta Basin oil and gas industry employment and wages, respectively, over the period of 2010 through 2020. The oil and gas industry directly represents 18% of Uinta Basin employment over the 2010-2020 period, peaking at 23% in 2014. Not only does the oil and gas industry play a vital role in Uinta Basin employment, but even more prominently, oil and gas plays an important role in the local economy because of the dollar value of salaries that can be put back into the local economy. In an even more notable fashion than employment alone, oil and gas industry salaries represented 30% of Uinta Basin salaries from 2010 through 2020, peaking at 36% in 2014 before dropping off from 2015 through 2020. The drop in employment and wages after 2014 corresponds with the end of a parallel five years of relatively good oil and gas prices as shown in Table 18.

Because of the critical role of the oil and gas industry to the regional economy, changes to the industry will have a corresponding impact on the Uinta Basin's other employment sectors. As outlined in the General Plans for both Duchesne and Uintah [DC 2019; UC 2021] counties and as supported by the UDWS data in Tables 15 through 17, the oil and gas industry is vital to the Uinta Basin economy. A 2013 reported titled "The Role of Oil and Gas and Amenities in County Economic Development" [Yonk & Simmons 2013] characterizes "natural resource exploration and development" as the "lifeblood of the region's economy."

Table 15. Uinta Basin Employment Sectors, 2010 – 2020 [UDWS-2022]

	Average 2010 - 2020					
	County					
	Duchesne		Uintah		Total	
Employment Sector	Employees	Percent of Total Employees	Employees	Percent of Total Employees	Employees	Percent of Total Employees
Oil and Gas Extraction and Support for Mining, Oil and Gas	1753	21.1%	2104	15.3%	3858	17.5%
Retail Trade	837	10.1%	1639	12.0%	2476	11.3%
Health Care and Social Assistance	1072	13.0%	1095	8.0%	2167	9.9%
Public Administration	476	5.8%	1557	11.4%	2033	9.3%
Education Services	780	9.5%	984	7.2%	1763	8.1%
Transportation and Warehousing	839	10.1%	862	6.3%	1701	7.7%
Accommodation and Food Services	414	5.0%	1147	8.4%	1560	7.1%
Construction	585	7.0%	912	6.6%	1497	6.8%
Wholesale Trade	244	2.9%	567	4.1%	811	3.7%
Other Services (except Public Admin.)	180	2.2%	417	3.0%	596	2.7%
Professiona.l Scientific & Technical Svc	118	1.4%	365	2.6%	482	2.2%
Real Estate and Rental and Leasing	69	0.8%	351	2.5%	419	1.9%
Information	222	2.7%	172	1.3%	395	1.8%
Admin., Support, Waste Mgmt, Remediation	107	1.3%	252	1.8%	359	1.6%
Manufacturing	163	2.0%	172	1.2%	334	1.5%
Arts, Entertainment, and Recreation	62	0.8%	254	1.9%	316	1.4%
Finance and Insurance	122	1.5%	184	1.3%	306	1.4%
Mining (except Oil and Gas)	10	0.1%	239	1.8%	249	1.2%
Utilities	55	0.7%	193	1.4%	248	1.1%
Agriculture, Forestry, Fishing & Hunting	91	1.2%	145	1.2%	236	1.2%
Management of Companies and Enterprises	40	0.5%	0	0.0%	40	0.2%

Oil and gas prices subsequently play a major role in oil and gas production in the Uinta Basin. Table 18 presents the 2010 through 2020 oil and gas prices. According to the Uintah County General Plan the local "economy seems to be more impacted by the cycles of energy prices than it is by general recessions." In the report "The Role of Oil and Gas and Amenities in County Economic Development" the following statement is made concerning the connection between production and maintaining local resources: "New wells lead to more tax dollars that pay for improvements like new roads or improvement and maintenance of old ones." [Yonk & Simmons 2013]

The oil and gas industry provides economic benefit in the Uinta Basin for more than just local employees and businesses. The oil and gas industry serves as a significant source of

Duchesne and Uintah County tax base. [DC 2019, UC 2021] As a result of the importance of the oil and gas industry in the Uinta Basin the counties "work closely with regulators, interest groups, and companies to find ways to manage the land for multiuse purposes." [Yonk & Simmons 2013]

Air quality regulations, including major pending regulatory changes affecting restrictions on emissions from oil and gas sources, are under development by regulators and are tied to production and emissions from 2017. Because of the pivotal regulatory implications of oil and gas production and associated emissions in 2017, due to ozone air quality, and the direct connection with oil and gas production, the oil and gas production for 2017 are examined here. In 2017 Duchesne and Uintah Counties were the first and second largest oil producing counties in the State of Utah, as shown in Table 19. In 2017 oil production from Duchesne and Uintah counties represented 26% and 30%, respectively, of statewide oil production. As shown in Table 20, Uintah County was the predominant producer of natural gas in 2017, at 65% of Utah's production, while Duchesne County was the third largest in 2017, representing 12% of state natural gas production. In the cases of both oil production and gas production, Uintah County was the top producer in the State of Utah in 2017. Because of the magnitude and position of Uinta Basin oil and gas production from the State of Utah and the revenue that is generated in the state from production, there is a far-reaching economic impact beyond just the Uinta Basin alone. [DC 2019]

Table 16. Oil and Gas Employment [UDWS 2022]

	COUNTY														
	Duchesne					Uintah					Total				
Year	Oil and Gas Extraction Employees	Support Activities for Mining, Oil and Gas Extraction Employees	Combined Oil and Gas Extraction and Support Activities Employees	Total[1] Employees	Combined Oil and Gas Extraction and Support Percent of Total Employees	Oil and Gas Extraction Employees	Support Activities for Mining, Oil and Gas Extraction Employees	Combined Oil and Gas Extraction and Support Activities Employees	Total[1] Employees	Combined Oil and Gas Extraction and Support Percent of Total Employees	Oil and Gas Extraction Employees	Support Activities for Mining, Oil and Gas Extraction Employees	Combined Oil and Gas Extraction and Support Activities Employees	Total[1] Employees	Combined Oil and Gas Extraction and Support Percent of Total Employees
2010	689	811	1,500	7,328	20.5%	230	2,129	2,359	13,332	17.7%	919	2,940	3,859	20,660	18.7%
2011	735	1,021	1,756	8,003	21.9%	472	2,303	2,775	13,439	20.6%	1,207	3,324	4,531	21,442	21.1%
2012	914	1,260	2,174	9,035	24.1%	514	2,357	2,871	14,993	19.1%	1,428	3,617	5,045	24,028	21.0%
2013	900	1,352	2,252	9,270	24.3%	581	2,174	2,755	14,633	18.8%	1,481	3,526	5,007	23,903	20.9%
2014	963	1,556	2,519	9,703	26.0%	621	2,299	2,920	14,154	20.6%	1,584	3,855	5,439	23,857	22.8%
2015	803	1,124	1,927	8,468	22.8%	602	1,566	2,168	13,966	15.5%	1,405	2,690	4,095	22,434	18.3%
2016	662	819	1,481	7,670	19.3%	501	936	1,437	12,403	11.6%	1,163	1,755	2,918	20,073	14.5%
2017	607	899	1,506	7,829	19.2%	413	1,123	1,536	12,563	12.2%	1,020	2,022	3,042	20,392	14.9%
2018	580	945	1,525	7,783	19.6%	265	1,282	1,547	12,914	12.0%	845	2,227	3,072	20,697	14.8%
2019	550	919	1,469	7,879	18.6%	275	1,391	1,666	13,067	12.7%	825	2,310	3,135	20,946	15.0%
2020	472	707	1,179	7,623	15.5%	129	982	1,111	12,030	9.2%	601	1,689	2,290	19,653	11.7%

[1]Represents sum of all individual primary "Industry Sectors" categories of "Average Employment" data.

Table 17. Oil and Gas Wages [UDWS 2022]

	COUNTY														
	Duchesne					Uintah					Total				
Year	Oil and Gas Extraction Wages (Millions)	Support Activities for Mining, Oil and Gas Extraction Wages (Millions)	Combined Oil and Gas Extraction and Support Activities Wages (Millions)	Total[1] Employment Wages (Millions)	Combined Oil and Gas Extraction and Support Percent of Total Wages	Oil and Gas Extraction Wages (Millions)	Support Activities for Mining, Oil and Gas Extraction Wages (Millions)	Combined Oil and Gas Extraction and Support Activities Wages (Millions)	Total[1] Employment Wages (Millions)	Combined Oil and Gas Extraction and Support Percent of Total Wages	Oil and Gas Extraction Wages (Millions)	Support Activities for Mining, Oil and Gas Extraction Wages (Millions)	Combined Oil and Gas Extraction and Support Activities Wages (Millions)	Total[1] Employment Wages (Millions)	Combined Oil and Gas Extraction and Support Percent of Total Wages
2010	$56.0	$48.6	$104.6	$301.9	34.7%	$19.2	$132.6	$151.8	$560.4	27.1%	$75.2	$181.3	$256.5	$862.4	29.7%
2011	$62.8	$60.9	$123.7	$343.3	36.0%	$44.4	$157.2	$201.6	$633.8	31.8%	$107.3	$218.1	$325.3	$977.1	33.3%
2012	$78.5	$77.0	$155.5	$408.7	38.0%	$49.4	$166.0	$215.4	$699.0	30.8%	$127.9	$243.0	$370.9	$1,107.7	33.5%
2013	$81.0	$84.2	$165.1	$430.1	38.4%	$60.7	$156.3	$217.0	$695.0	31.2%	$141.6	$240.5	$382.1	$1,125.1	34.0%
2014	$91.1	$105.9	$197.0	$477.6	41.3%	$69.1	$166.9	$236.1	$721.9	32.7%	$160.3	$272.8	$433.1	$1,199.5	36.1%
2015	$75.0	$70.1	$145.1	$394.7	36.8%	$69.2	$105.8	$175.0	$634.9	27.6%	$144.1	$175.9	$320.1	$1,029.6	31.1%
2016	$61.3	$47.6	$108.9	$339.7	32.0%	$58.4	$56.7	$115.1	$527.0	21.8%	$119.7	$104.2	$223.9	$866.8	25.8%
2017	$52.8	$56.7	$109.5	$350.7	31.2%	$46.4	$69.9	$116.3	$554.7	21.0%	$99.1	$126.6	$225.8	$905.4	24.9%
2018	$53.4	$60.2	$113.6	$352.7	32.2%	$25.1	$85.2	$110.3	$574.3	19.2%	$78.5	$145.4	$223.9	$927.0	24.2%
2019	$54.6	$59.1	$113.6	$366.2	31.0%	$25.9	$92.3	$118.2	$578.0	20.4%	$80.5	$151.4	$231.8	$944.2	24.6%
2020	$58.8	$43.7	$102.5	$362.6	28.3%	$12.4	$62.6	$75.0	$526.4	14.2%	$71.2	$106.3	$177.5	$889.0	20.0%

[1]Represents sum of all individual primary "Industry Sectors" categories of "Average Employment" data.

IV. B. 2. c. Socioeconomic summary

The oil and gas industry plays integral roles in economic growth in areas such as the Uinta Basin throughout the western United States [Yonk & Simmons 2013] including Duchesne and Uintah counties. [DC 2019, UC 2021] There is a solid tie between the strength of the oil and gas industry and the strength of the Uinta Basin economy. [DC 2019, UC 2021] There is an important tie between Uinta Basin oil and gas production and the State of Utah's overall economy. [DC 2019, UC 2021] Given the important roles of the oil and gas industry to the Uinta Basin and State of Utah's economies [DC 2019, UC 2021] it is imperative that if electrification and replacement of natural gas fired pumpjack engines were to be considered as a requirement on a wide spread basis in the Uinta Basin that it be done with significant forethought toward the importance of the oil and gas industry to the economy. As shown earlier in this report a large part of the Uinta Basin where significant oil and gas development occurs is currently without developed electrical infrastructure. If wide-spread replacement of internal combustion engines with electricity were required but infeasible, which could be for reasons such as logistical and economic challenges, a critical part of the Uinta Basin economy [DC 2019, UC 2021] would be negatively affected, extending far beyond the oil and gas industry itself.

Table 18. Oil and Natural Gas Prices, 2010 – 2021

Year	Utah Crude Oil First Purchase Price (Dollars per Barrel) [EIA 2022(a)]	Henry Hub Natural Gas Spot Price (Dollars per Million BTU) [EIA 2022(b)]
2010	$68.10	$4.39
2011	$82.70	$4.00
2012	$82.97	$2.75
2013	$84.70	$3.73
2014	$79.11	$4.39
2015	$40.12	$2.63
2016	$37.00	$2.52
2017	$44.31	$2.99
2018	$56.95	$3.17
2019	$48.30	$2.57
2020	$34.64	$2.03
2021	$60.11	$3.91

Table 19. Oil Production by County, 2000 and 2017 [UDOGM 2021b]

County	Oil			
	2000		2017	
	Oil Production (BBLs)	Percent of State Total Oil Production	Oil Production (BBLs)	Percent of State Total Oil Production
DUCHESNE	4,772,096	30.6%	16,986,437	49.33%
UINTAH	2,788,078	17.9%	11,278,096	32.75%
SAN JUAN	6,152,940	39.4%	4,112,573	11.94%
SEVIER			1,196,170	3.47%
GRAND	197,559	1.3%	407,603	1.18%
SUMMIT	1,477,075	9.5%	169,161	0.49%
GARFIELD	214,266	1.4%	139,199	0.40%
SANPETE			88,428	0.26%
CARBON	211	0.0%	57,792	0.17%
DAGGETT	2,696	0.0%	803	0.00%
EMERY	3,279	0.0%	571	0.00%
JUAB			236	0.00%
Total	15,608,200	100.0%	34,437,069	100.00%

Table 20. Natural Gas Production by County, 2000 and 2017 [UDOGM 2021b]

County	Natural Gas			
	2000		2017	
	Natural Gas Production (MCF)	Percent of State Total Natural Gas Production	Natural Gas Production (MCF)	Percent of State Total Natural Gas Production
UINTAH	83,100,123	29.6%	205,419,493	65.17%
CARBON	72,586,085	25.8%	46,883,601	14.87%
DUCHESNE	13,934,444	5.0%	38,971,837	12.36%
SAN JUAN	23,965,074	8.5%	8,876,914	2.82%
EMERY	4,042,810	1.4%	7,466,663	2.37%
GRAND	5,287,347	1.9%	3,596,442	1.14%
SUMMIT	76,290,493	27.1%	2,082,449	0.66%
DAGGETT	1,955,920	0.7%	1,078,305	0.34%
SANPETE			812,196	0.26%
GARFIELD	7,650	0.0%	9,125	0.00%
JUAB			-	0.00%
SEVIER			-	0.00%
Total	281,169,946	100.0%	315,197,025	100.00%

V. CONCLUSIONS AND RECOMMENDATIONS

Despite earlier evidence based in part on the Edwards et al. [2014] box model, our box model, when informed with the latest VOC speciation data, predicts that the Uinta Basin wintertime air mass is about equally sensitive to reductions in VOC and NO_x. A 1% reduction in either NO_x or VOC is predicted to yield a reduction in ozone concentration of around 0.2 to 0.3%. A 40% reduction in either NO_x or VOC is predicted to reduce ozone concentrations by about 12 ppb. Pollution controls aimed at reducing either NO_x or VOC are predicted to be about equally effective.

An important finding of this study and of the USU Engine Study [Lyman et al. 2022] is that NO_x and VOC emissions from pumpjack engines are severely over- and under-estimated, respectively. NO_x emissions by pumpjacks in the Uinta Basin had been estimated to constitute about 40% of all NO_x emissions from the oil and gas sector [Gorchov-Negron et al. 2018, UDAQ 2021a], whereas now they appear to be negligible (Table 1). VOC emissions by pumpjacks were thought to be negligible (Table 1), but recent measurements indicate that they are not. NO_x emissions by natural-gas-fired engines appear to be a highly non-linear function of the load on the engine. Estimates of pumpjack NOx emissions are most accurate at new wells when the engines work at near 100% load, but about one-half of all pumpjack engines in the Uinta Basin lift fewer than 14 barrels of oil and water a day and operate well below 100% load. VOC estimates seem to be predicated upon manufacturers' recommendations and do not adequately consider engine adjustments (e.g., the air-fuel ratio) made by operators in the field.

More research into natural-gas-fired engines is called for. For example, we have been unable to find any definitive explanation in the literature for the non-linear behavior of NO_x emissions. The recommended techniques for estimating pumpjack emissions also need sorely to be revised to consider actual operating conditions in the field. In the future, we plan to develop improved techniques to develop load-based pumpjack VOC emissions estimates.

Wintertime satellite measurements of the NO2 column correlate more strongly with new-well development than with oil and water production. This also suggests that drilling and completion activities are a more significant NO_x source than are pumpjack engines.

Electrification of the oil and gas fields would eliminate significant ozone precursor emissions. We estimate that if all emissions from pumpjacks, separators, and heaters had been removed in February 2019 through electrification, the peak ozone concentration would have been reduced by about 24 ppb. Moreover, had all drilling and completion activities also been removed through electrification, an additional 4-ppb ozone reduction would have occurred. These estimates are based on complete removal of the emissions categories, while electrification will probably occur in stages.

Electrification of the Uinta Basin oil and gas fields is expected to be costly. Just the cost of running new utility distribution lines has been estimated at $50,000 to $90,000 per mile, [Cook et al. 2017a] and this does not include the cost of switching pumpjack engines or other equipment. It is also likely that existing power generation facilities will need to be augmented. However, the economy relies directly or indirectly on the oil and gas sector. 18% of Uinta Basin jobs and 31% of Uinta Basin wages between 2010 and 2019 were directly related to the industry, and these percentages were even larger before 2015. Many residents of the Basin endured economic hardship when the industry declined in 2015. The overall cost-benefit analysis needs to consider the societal costs that might occur if the Basin is not electrified, including the ripple effect that would extend to the rest of the state and region.

Given the high cost of electrification, another possible, although also costly, interim solution might be to call a moratorium on certain activities for four to eight weeks in any winter when the risk for ozone is deemed to be high. Since ozone measurements began at the Ouray monitoring station in 2010, almost 80% of all exceedances of the 70 ppb NAAQS occurred in two months, 30% in January and 48% in February. Excluding January and February exceedances, only three years, 2010, 2011 and 2013, would have had more than three exceedances (the threshold for non-attainment designations) and today the Basin would not be in non-attainment for ozone.

We considered four different sectors of the oil and gas field (Figure 29) and evaluated separately the impact of electrification in each of the sectors. Sector A to the north of US Highway 40 is already electrified. Regions of sector B not already electrified are dominated by natural gas production, hence expanded electrical service there is not expected to have a significant impact on air quality. Both sectors C and D are dominated by oil production, while well pads in sector C are closer to existing or planned transmission lines.

Because meteorological modeling of persistent, multi-day thermal inversions is so challenging, we were unable to develop an adequate 3D photochemical grid model of the Uinta Basin winter airshed. This is a crucial problem, because pollution-control strategies mandated by the Clean Air Act will be based on such models. Successful models will require use of the nudging feature in WRF. [Tran et al. 2018] However, this will require more frequent tethersonde measurements of the temperature-altitude profile in the Uinta Basin. We plan to continue this work in the future, focusing on episodes when the required tethersonde measurements are available.

APPENDIX A. GEOGRAPHICAL GROUPINGS OF PUMPJACKS

The following map shows the distribution of well pads in the Uinta Basin: Gas and oil wells predominate, respectively, east and west of the Green River.

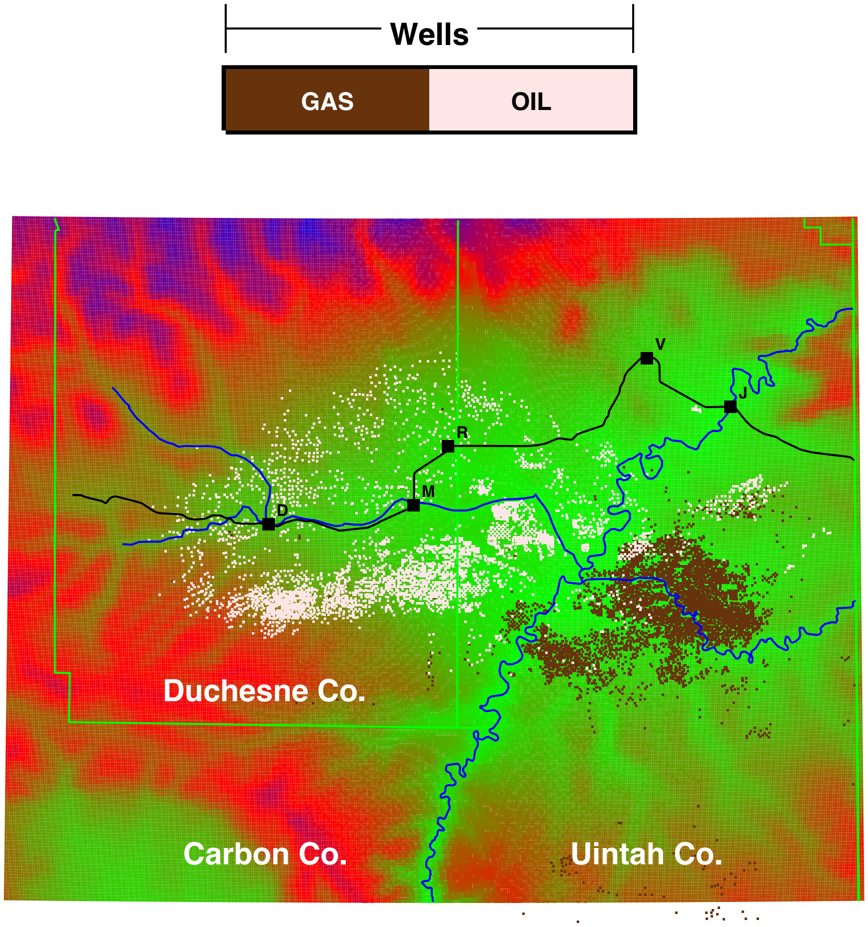

Figure A1. Map of the Uinta Basin, showing locations of oil and gas wells. U.S. Highway 40 appears as a black trace. Five towns, Duchesne, Myton, Roosevelt, Vernal, and Jensen are shown.

In Figure A2, the positions of pumpjack internal combustion engines have been overlain onto Figure A1. The pumpjacks have been assigned to one of four geographic areas. See Section IV.A.4 for added explanations of the four areas. Because practically every oil well has a pumpjack, most of the oil wells shown in Figure A1 have been obscured by the symbols for pumpjacks. Natural gas wells continue to appear in Figure A2 because, typically, gas wells do not need artificial lifting.

Area A Lies in the northwest part of the Basin, entirely north of US Highway 40, while all remaining sectors lie south of the highway. Dashed lines define the boundaries of areas B, C, and D to the south of the highway. Oil wells in area A are younger on average, and because electricity is available, there are only a few pumpjacks. Area B to the southeast has, on average, older, lower-producing oil wells, and some limited electricity. Area C lies in the south-central basin, with, on average, newer, higher-producing oil wells, and little electricity. Area D lies to the southwest. Many of its wells are also older and low producers. Area D contains about three-quarters of producing wells.

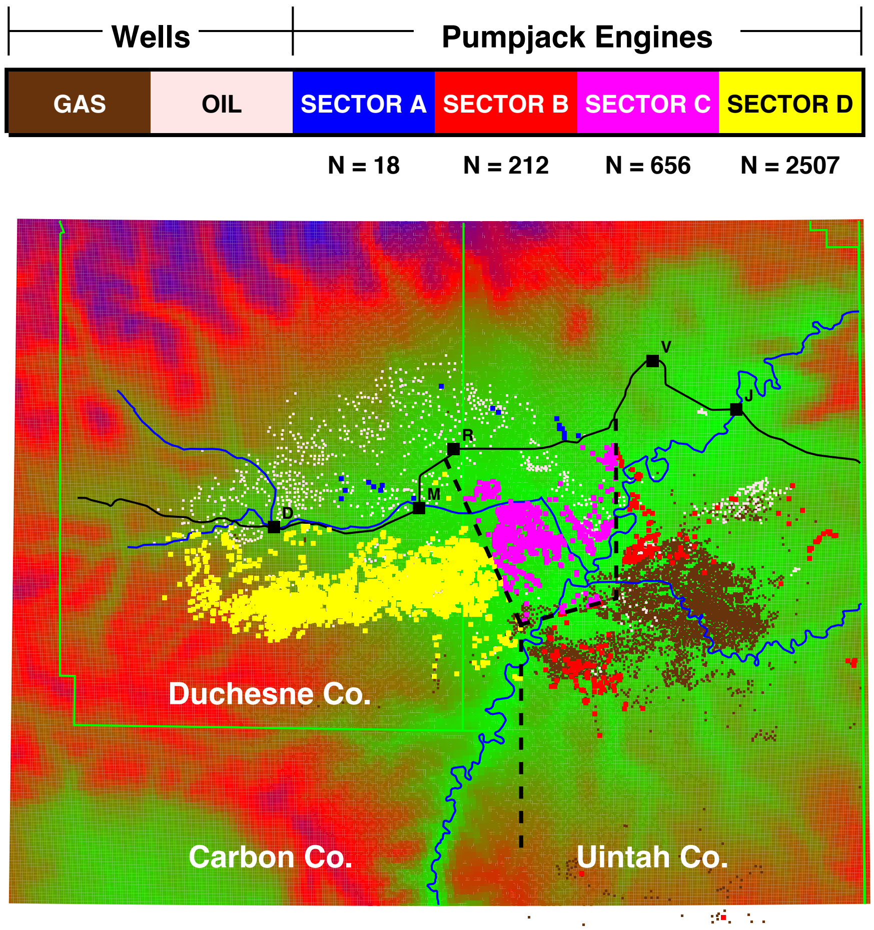

Figure A2. Same map as Figure A1, with pumpjack locations superimposed. Pumpjacks are colored by geographical sector.

APPENDIX B. SAMPLE CALCULATIONS OF ENGINE LOAD AND NO_x EMISSION

Table A1 summarizes three sample calculations of engine emissions, given here to illuminate our procedures for QRod calculations. The oil, water, and production days data were obtained from the UDOGM database [UDOGM 2021a] for February 2017, and have been used to calculate the liquids lifted in bbl/day. The SER was obtained by interpolation or extrapolation from the JJJJ certification tests. (The estimate is SER = 0.45 g/(hp-hr) for any engine rated at 40 hp, and 0.62 for any at 65 hp.) The liquids lifted are the most important variable used by QRod to determine the horsepower load on the engine. Screen shots of the three QRod calculations appear below (Figures A3 – A5). Because it was impossible to run QRod for thousands of engines, we performed enough QRod runs at different input variables to obtain a calibration curve, Eq. (9) to estimate the load from the liquids lifted (LL). Eq. (9) agrees within about 10% or better with the actual QRod run. Then the estimated emission in g/hr is in the last row.

Table A1. Three sample calculations of engine emissions. The three columns correspond to the three screen shots in Figures A3 – A5.

	Low load	Medium load	High load
API	4304751649	4301351994	4301334161
Make/Model	Arrow L-795	Ajax E-565	Ajax E-42
Oil production bbl	58	168	1888
Water production bbl	45	225	128
Days of operation	28	28	28
SER [g/(hp-hr)]	0.62	0.45	0.45
Liquids lifted, LL, bbl/day	3.6786	14.04	72.00
QRod estimate of load (hp)	0.671	2.60	15.61
Load estimate, Eq. (9) (hp)	0.719	2.90	15.91
Emission estimate, Eq. (10) (g/hr)	0.446	1.304	7.160

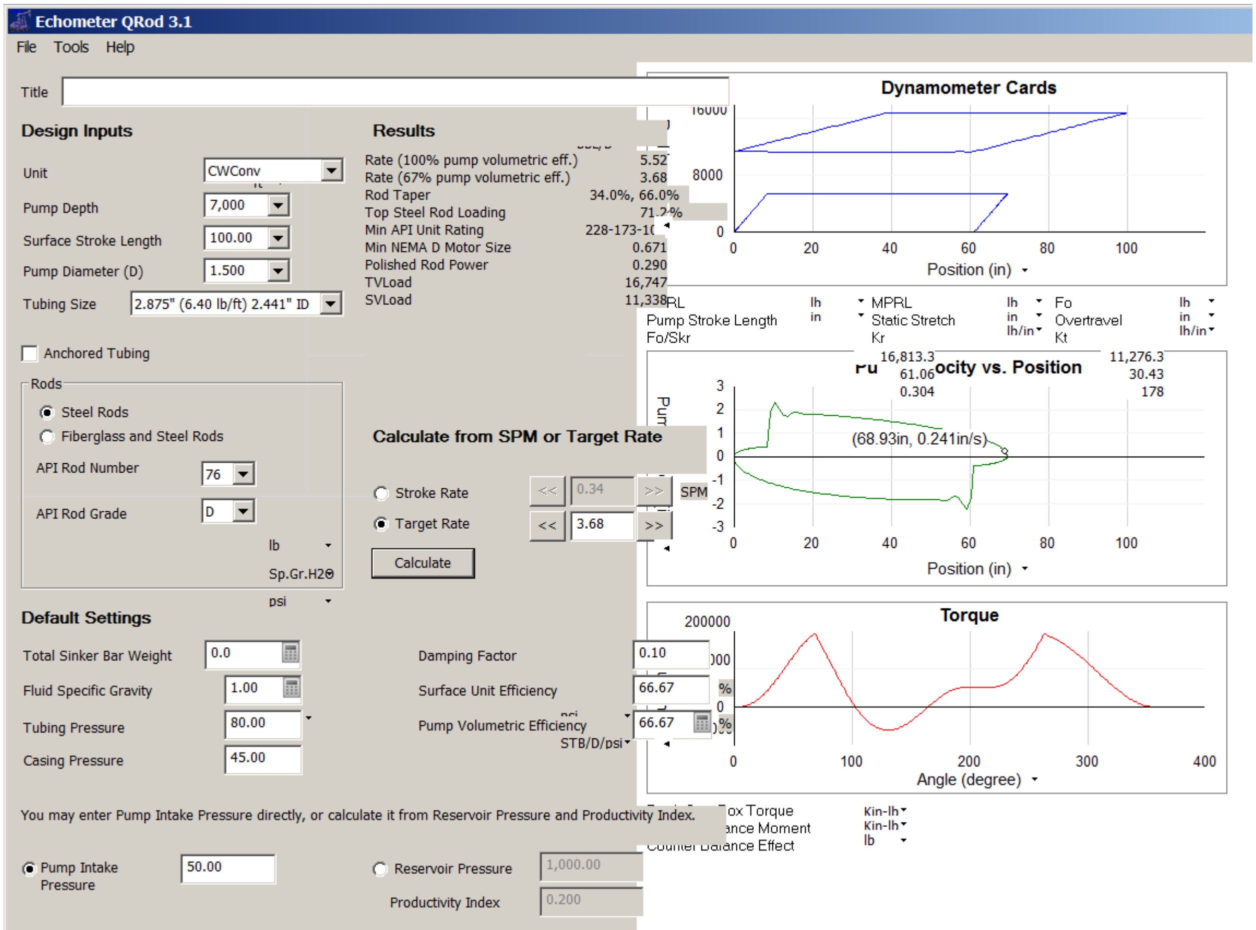

Figure A3. QRod calculation at rate = 3.68 bbl/day. Load = 0.671 hp.

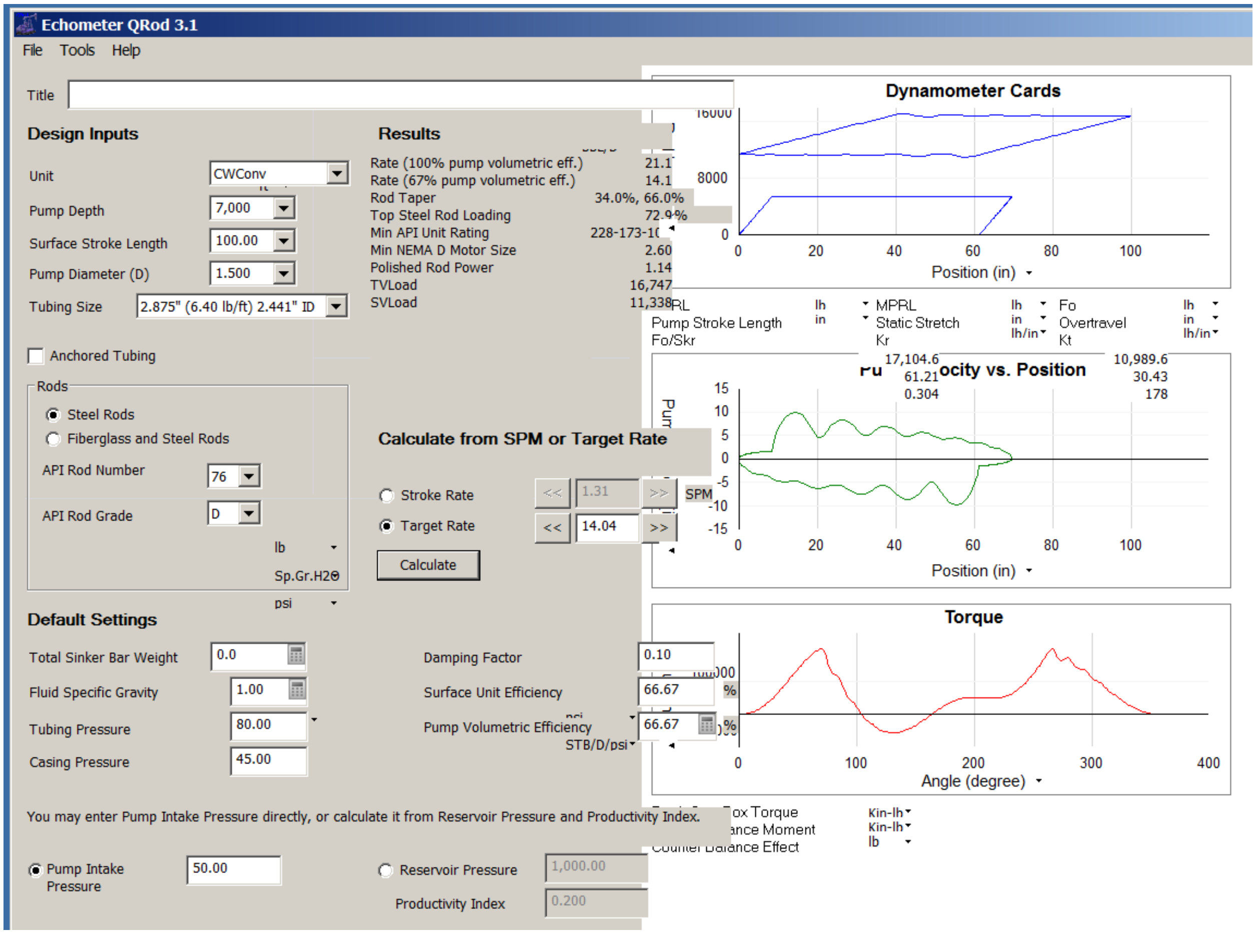

Figure A4. QRod calculation at rate = 14.04 bbl/day. Load = 2.60 hp.

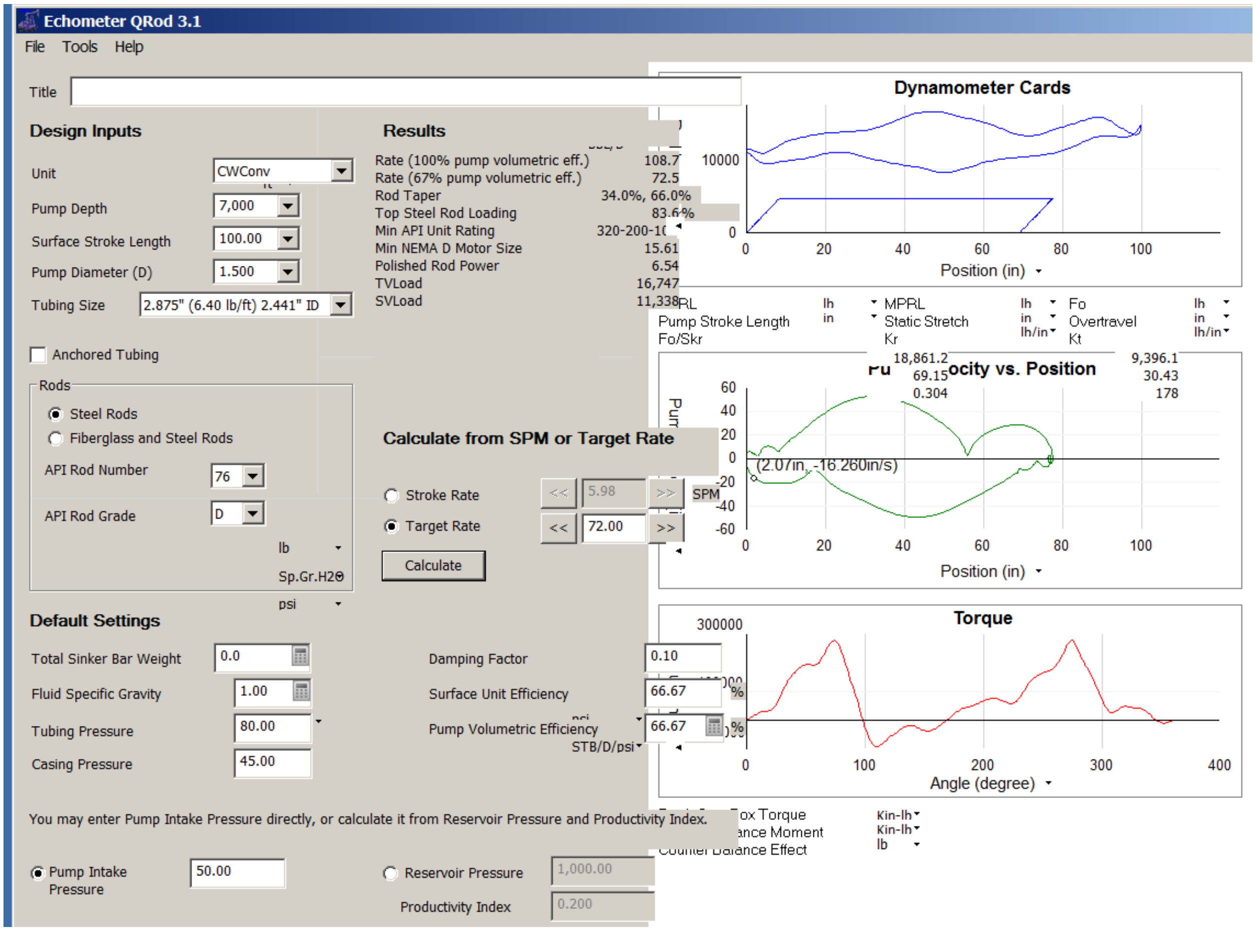

Figure A5. QRod calculation at rate = 72.00 bbl/day. Load = 15.61 hp.

APPENDIX C. DISTRIBUTIONS OF IMPORTANT PUMPJACK ESTIMATES

The calculations in Appendix B are representative of the pumpjack estimates, but to get a better idea of how some of the input, output and intermediate variables are distributed in those calculations, we have prepared the following tables and histograms. The inventory contains 3393 engines, but according to the DOGM database, several hundred of these had zero production in February 2017. Therefore, the following distributions only include 2888 engines having non-zero production.

C1. Distribution in liquids lifted, LL.

Table A2. Statistics on liquids lifted by each pumpjack engine. Units are bbl/day. Compare this with Figure 5.

Mean	28.12
Std. Dev.	75.40
Minimum	0.0357
10%-tile	3.107
25%-tile	6.184
50%-tile	13.75
75%-tile	28.49
90%-tile	56.07
Maximum	1793.8214

C2. Distribution in specific emission rates, SER, estimates.

Table A3. Statistics on estimated SER values. Units are gm/(hp-hr).

Mean	1.21
Std. Dev.	1.444
Minimum	0.18
10%-tile	0.34
25%-tile	0.45
50%-tile	0.62
75%-tile	0.62
90%-tile	4.4
Maximum	13.4

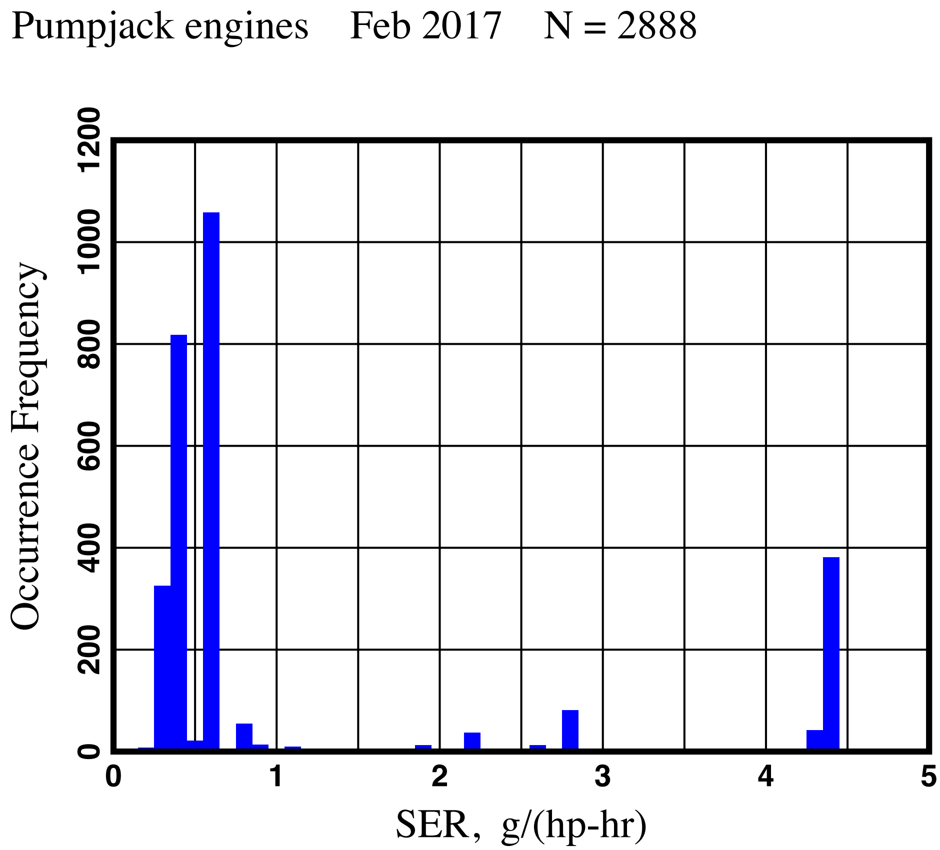

Figure A6. Distribution in SER values applied to each engine. Six outliers lie off the right side of the chart (five at 6.9 g/hp-hr and one at 13.4 g/hp-hr). Statistics for the distribution appear in Table A3. The cluster below 1 g/(hp-hr) belongs to the post-JJJJ engines. The clusters around 2.8 and 4.4 belong to the pre-JJJ engines.

C3. Distribution of estimated loads.

Table A4. Statistics on estimated loads. Units are hp.

Mean	5.22
Std. Dev.	7.58
Minimum	0.0058
10%-tile	0.588
25%-tile	1.233
50%-tile	2.389
75%-tile	6.051
90%-tile	12.316
Maximum	96

C4. Distribution of estimated NO_x emissions.

Table A5. Statistics on estimated NO_x emissions. Units are g/hr.

Mean	4.595
Std. Dev.	8.807
Minimum	0.00
10%-tile	0.419
25%-tile	0.913
50%-tile	2.0495
75%-tile	4.495
90%-tile	10.259
Maximum	158.9

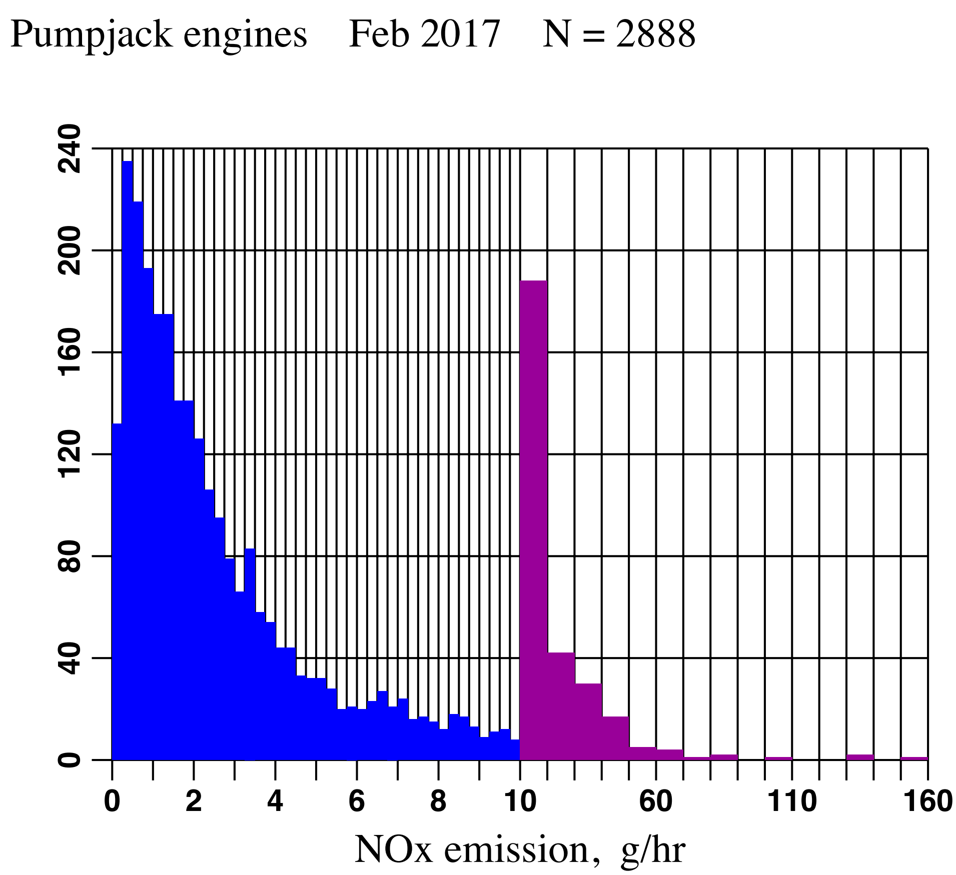

Figure A7. Distribution of estimated NO_x emissions. Note the change in scale between the right and left halves, with the right accounting for only about 10% of all wells. Statistics on this distribution are given in Table A5.

REFERENCES

[API 2020] American Petroleum Institute, "API Comments on the Colorado Greenhouse Gas Pollution Reduction Roadmap," https://www.api.org/news-policy-and-issues/letters-or-comments/2020/11/13/api-comments-on-the-colorado-greenhouse-gas-pollution-reduction-roadmap, November 13, 2020, last referenced 02-2022.

A. Bernardi, Burns & McDonnell, "Applying Renewable Generation to Oil and Gas Facilities," https://blog.burnsmcd.com/applying-renewable-generation-to-oil-and-gas-facilities, January 4, 2021. Last referenced 02-2022.

[BLM 2016]. Bureau of Land Management "Energy Gateway South Transmission Line Project." Last referenced 02/2022.
https://eplanning.blm.gov/eplanning-ui/project/53044/510
https://eplanning.blm.gov/public_projects/nepa/53044/92847/111847/EGS-RecordofDecision.pdf

[BLM 2018] Bureau of Land Management, "Record of Decision for the Enefit American Oil Utility Corridor Project," and "Final Environmental Impact Statement for the Enefit American Oil Utility Corridor Project." Last referenced 02/2022.
https://eplanning.blm.gov/public_projects/nepa/37462/158127/193295/001_ROD_for_the_Enefit_Utility_Corridor_Project_-_Signed_9.24.18.pdf
https://eplanning.blm.gov/public_projects/nepa/37462/145046/178753/2_Volume_I.pdf
https://eplanning.blm.gov/public_projects/nepa/37462/145047/178754/3_Volume_II_Appendices_A-C.pdf

[CAMx 2022] https://www.camx.com/ Last referenced 02/2022.

[CARB 2001] California Environmental Protection Agency, Air Resources Board, "Determination of Reasonably Available Control Technology and Best Available Retrofit Control Technology for Stationary Spark-Ignited Internal Combustion Engines," November 2001, https://ww3.arb.ca.gov/ractbarc/rb-iceall.pdf, last referenced 02-2022.

L.J. Carpenter, T.J. Green, G.P. Mills, S. Bauguitte, S.A. Penkett, P. Zanis, E. Schuepbach, N. Schmidbauer, P.S. Monks, C Zellweger, "Ozidized nitrogen and ozone production efficiencies in the springtime free troposphere over the Alps," J. Geophs. Res., 105 (D11), 14,547-14,559 (2000).

[CDPHE 2020] Colorado Department of Public Health and Environment, "Reciprocating Internal Combustion Engine (RICE) Source Category: NO_x Emission 4-Factor Analysis for Reasonable Progress (RP), downloaded from https://www.researchgate.net, last referenced 02-2022.

[CMAS 2022] https://cmascenter.org/ Last references 02/2022.

Code of Federal Regulations (CFR), https://www.ecfr.gov/current/title-40/chapter-I/subchapter-C/part-60/subpart-JJJJ, last referenced 01/2022.

C.C.-K. Chou, C.-Y. Tsai, C.-J. Shiu, S.C. Liu, T. Zhu, "Measurement of NO_y during Campaign of Air Quality Research in Beijing 2006 (CAREBeijing-2006): Implications for the ozone production efficiency of NO_x," J. Geophys. Res., 114, D00G01 (2009).

B. Cook, Z. Soukup, G. Buckingham, "Electricity in the Oil Patch: The Power Costs of Production, CO2-EOR, Electric Lines and Onsite Generators," AIChE Carbon Management Technology Conference, July 18, 2017, *(2017a),* https://www.aiche.org/fscarbonmanagement/cmtc/2017/proceeding/paper/electricity-oil-patch-power-costs-production-co2-eor-electric-lines-and-onsite-generators, last referenced 02-2022.

B. Cook, Z.A. Soukup, G.P. Buckingham, "Electrifying the Oilfield: The Comparative Economics of Grid Power and Onsite Gas Generators (Draft Jan 30 2017)" Enhanced Oil Recovery Institute, (2017b) https://www.eoriwyoming.org/library/economics/electrifying-the-oilfield-the-comparative-economics-of-grid-power-and-onsite-gas-generators-draft-30jan2017, last referenced 02-2022.

B. Dix, J. de Bruin, E. Roosenbrand, T. Vlemmix, C. Francoeur, A. Gorchov-Negron, B. McDonald, M. Zhizhin, C. Elvidge, P. Veefkind, P. Levelt, J. de Gouw, "Nitrogen Oxide Emissions from U.S. Oil and Gas Production: Recent Trends and Source Attribution," Geophys. Res. Lett. DOI: 10.1029/2019GL085866.

[DC 2019] "Duchesne County General Plan," November 18, 2019, https://www.duchesne.utah.gov/wp-content/uploads/2019/11/General-Plan-2019-update.pdf, last referenced 02-2022.

"Echometer QRod 3.1," https://www.echometer.com/Software/QRod, last referenced 09/2021.

P.M. Edwards, S.S. Brown, J.M. Roberts, R. Ahmadov, R.M. Banta, J.A. deGouw, W.P. Dubé, R.A. Field, J.H. Flynn, J.B. Gilman, M. Graus, D. Helmig, A. Koss, A.O. Langford, B.L. Lefer, B.M. Lerner, R. Li, S.-M. Li, S.A. McKeen, S.M. Murphy, D.D. Parish, C.J. Senff, J. Soltis, J. Stutz, C. Sweeney, C.R. Thompson, M.K. Trainer, C. Tsai, P.R. Veres, R.A. Washenfelder, C. Warneke, R.J. Wild, C.J. Young, B. Yuan, R. Zamora, "High winter ozone pollution from carbonyl photolysis in an oil and gas basin," Nature, 514, 351-354 (2014).

[EIA 2022(a)] U.S. Energy Information Administration, https://www.eia.gov/dnav/pet/hist/LeafHandler.ashx?n=PET&s=F004049__3&f=M, last referenced 02/2022.

[EIA 2022(b)] U.S. Energy Information Administration, https://www.eia.gov/dnav/ng/hist/rngwhhdm.htm, last referenced 02/2022.

[FR 2016] Federal Register, "Notice of Availability of the Record of Decision for the TransWest Express Transmission Project in Wyoming, Colorado, Utah and Nevada." Last referenced 02/2022.
https://www.federalregister.gov/documents/2016/12/16/2016-30345/notice-of-availability-of-the-record-of-decision-for-the-transwest-express-transmission-project-in

W.S. Goliff, W.R. Stockwell, C.V. Lawson, "The regional atmospheric chemistry mechanism, version 2," Atmospheric Environment, 68, 174-185 (2013).

A.M. Gorchov Negron, B.C. McDonald, S.A. McKeen, J. Peischl, R. Ahmadov, J.A. de Gouw, G.J. Frost, M.G. Hastings, I.B. Pollack, T.B. Ryerson, C. Thompson, C. Warneke, M. Trainer, "Development of a Fuel-Based Oil and Gas Inventory of Nitrogen Oxides Emissions," Environmental Science and Technology, 52, 10175-10185 (2018).

A.A. Griffin, *Combustion Characteristics of a Two-Stroke Large Bore Natural Gas Spark-Ignited Engine*, Masters Thesis, Texas A&M University (2015).

A.A. Griffin, T.J. Jacobs, "Combustion Characteristics of a 2-Stroke Large Bore Natural Gas Spark-Ignited Engine," Proceedings, ASME ICEF2015, 1-9 (2015).

D.J. Jacob, L.W. Horowitz, J.W. Munger, B.G. Heikes, R.R. Dickerson, R.S. Artz, W.C. Keene, "Seasonal transition from NO_x- to hydrocarbon-limited conditions for ozone production over the eastern United States in September," J. Geophys. Res., 100 (D5), 9315-9324 (1995)

M.E. Jenkin, S.M. Saunders, V. Wagner, M.J. Pilling, "Protocol for the development of the Master Chemical Mechanism, MCM v3 (Part B): tropospheric degradation of aromatic volatile organic compounds," Atmos. Chem. Phys., 3, 181-193 (2003).

M.E. Jenkin, J.C. Young, A.R. Rickard, "The MCM v3.3.1 degradation scheme for isoprene," Atmos. Chem. Phys., 15, 11433-11459 (2015).

L.I. Kleinman, "Low and high NO_x tropospheric chemistry," J. Geophys. Res., 99 (D8), 16,831-16,838 (1994a).

L. Kleinman, Y.-N. Lee, S.R. Springston, L. Nunnermacker, X. Zhou, R. Brown, K. Hallock, P. Klotz, D. Leahy, J.H. Lee, L. Newman, "Ozone formation at a rural site in the southeastern United States," J. Geophys. Res., 99 (D2), 3469-3482 (1994b).

L.I. Kleinman, P.H. Daum, J.H. Lee, Y.-N. Lee, L.J. Nunnermacker, S.R. Springston, L. Newman, J. Weinstein-Lloyd, S. Sillman, "Dependence of ozone production on NO and hydrocarbons in the troposphere," Geophys. Res. Lett., 24 (18), 2299-2302 (1997).

N. Kolwey, "Energy Efficiency and Electrification Best Practices for Oil and Gas Production," Southwest Energy Efficiency Project and Colorado Energy Office, Aug. 2020, https://swenergy.org/pubs/energy-efficiency-and-electrification-best-practices-for-oil-and-gas-production, last referenced, 02/2022.

S.N. Lyman, M. Holmes, H. Tran, T. Tran, T. O'Neil, "High ethylene and propylene in an area dominated by oil production," Atmosphere, 12, 1 (2021).

S. Lyman, M. Mansfield, H. Shorthill, "Final Report: 2013 Uintah Basin Winter Ozone & Air Quality Study," pp. 23-31, https://www.usu.edu/binghamresearch/files/2013-final-report-uimssd-R.pdf

S. Lyman, M. Mansfield, H. Tran, T. Tran, "2018 Annual Report: Uinta Basin Air Quality Research," pp. 33-35, https://www.usu.edu/binghamresearch/files/reports/UBAQR-2018-AnnualReport.pdf

S. Lyman, H. Tran, T. O'Neil, M. Mansfield, "Air Pollutant Emissions from Natural Gas-Fueled Pumpjack Engines in the Uinta Basin (2022). In preparation, to be available at https://www.usu.edu/binghamresearch/.

M.L. Mansfield, S.N. Lyman, "Winter Ozone Pollution in Utah's Uinta Basin is Attenuating," Atmosphere, 12, 4 (2021).

[MCM 2022] "The Master Chemical Mechanism," http://mcm.york.ac.uk/, last referenced 02/2022

J.B. Milford, D. Gao, S. Sillman, P. Blossey, A.G. Russell, "Total reactive nitrogen (NO_y) as an indicator of the sensitivity of ozone to reductions in hydrocarbons and NO_x emissions," J. Geophys. Res. 99 (D2), 3533-3542 (1994).

Minnesota Pollution Control Agency [MPCA], "Internal combustion engines air emissions calculator," https://www.pca.state.mn.us/regulations/air-emissions-calculators, last referenced 08/2021.

[MLEA 2021a] Moon Lake Electric Association, Inc., *Draft Plan of Development, Bonanza to Bookcliffs 138 kV Transmission Line, Revision 2.0*, February 2021.

[MLEA 2021b] Moon Lake Electric Association, Inc., correspondence with Robert Hammer, SLR International, November 21, 2021.

[NASA 2021] https://aura.gsfc.nasa.gov/science/data.html, last referenced 10/2021.

[NM-EMNRD 2019]. New Mexico Environment Department and New Mexico Energy, Minerals and Natural Resources Department, "New Mexico Methane Advisory Panel Technical Report," https://www.emnrd.nm.gov/ocd/wp-content/uploads/sites/6/MAP-Technical-Report-December-19-2019-FINAL.pdf, last referenced 02/2022.

L.J. Nunnermacker, L.I. Kleinman, D. Imre, P.H. Daum, Y.-N. Lee, J.H. Lee, S.R. Springston, L. Newman, NO_y lifetimes and O_3 production efficiencies in urban and power plant plumes: Analysis of field data," J. Geophys. Res., 105 (D7), 9165-9176 (2000).

Oklahoma Department of Environmental Quality [ODEQ], "2011 Oil and Gas Emission Inventory Enhancement Project for CenSARA States," December 21, 2012, https://www.deq.ok.gov/wp-content/uploads/air-division/EI_OG_Final_Report_CenSara_122712.pdf.

[PacifiCorp 2022] https://www.pacificorp.com/transmission/transmission-projects/energy-gateway/gateway-south.html, last referenced 02/2022.

S.M. Saunders, M.E. Jenkin, R.G. Derwent, M.J. Pilling, "Protocol for the development of the Master Chemical Mechanism, MCM v3 (Part A): tropospheric degradation of non-aromatic volatile organic compounds," Atmos. Chem. Phys., 3, 161-180 (2003).

J.H. Seinfeld & S.N. Pandis, *Atmospheric Chemistry and Physics: From Air Pollution to Climate Change,* 2nd ed., Wiley (2006).

X. Shi & G.P. Brasseur, "The response in air quality to the reduction of Chinese economic activities during the COVID-19 outbreak," Geo. Phys. Res. Let., 47, e2020GL088070 (2020).

S. Sillman, "The use of NO_y, H_2O_2, and HNO_3 as indicators for ozone-NO_x-hydrocarbon sensitivity in urban locations," J. Geophys. Res., 100 (D7), 14,175-14,188 (1995).

S. Sillman, D. He, M.R. Pippin, P.H. Daum, D.G. Imre, L.I. Kleinman, J.H. Lee, J. Weinstein-Lloyd, "Model correlations for ozone, reactive nitrogen, and peroxides for Nashville in comparison with measurements: Implications for O_3-NO_x-hydrocarbon chemistry," J. Geophys. Res., 103 (D17), 22,629-22,644 (1998).

S. Sillman, "The relation between ozone, NO_x and hydrocarbons in urban and polluted rural environments," Atmos. Env., 33, 1821-1845 (1999).

S. Sillman, D. He, "Some theoretical results concerning O_3-NO_x-VOC chemistry and NO_x-VOC indicators," J. Geophys. Res., 107 (D22), 4659 (2002).

D. Steph, Burns-McDonnel, "The Business Case for Electrification of the Oilfield," https://info.burnsmcd.com/white-paper/business-case-for-electrification-of-the-oil-field, last referenced 02/2022.

A.F. Stein, E. Mantilla, M.M. Millán, "Using measured and modeled indicators to assess ozone-NO_x-VOC sensitivity in a western Mediterranean coastal environment," Atmos. Env., 39, 1767-7180 (2005).

W.R. Stockwell, F. Kirchner, M. Kuhn, S. Seefeld, "A New Mechanism for Regional Atmospheric Chemistry Modeling," J. Geophys. Res. Atm., 102 (D22), 25847-25879 (1997).

K.-E. Stromsta, “Chevron to Build 500MW of Renewables to Power Oil and Gas Facilities – and It’s Considering More,” Green Tech Media, https://www.greentechmedia.com/articles/read/chevron-to-build-500mw-of-renewables-globally-to-power-oil-and-gas-facilities, July 30, 2020, last referenced 02/2022.

Texas Commission on Environmental Quality [TCEQ], “Characterization of Oil and Gas Production Equipment and Develop [sic] a Methodology to Estimate Statewide Emissions – Final Report,” https://www.tceq.texas.gov/assets/public/implementation/air/am/contracts/reports/ei/5820784003FY1026-20101124-ergi-oilGasEmissionsInventory.pdf

M. Trainer, D.D. Parish, M.P. Buhr, R.B. Norton, F.C. Fehsenfeld, K.G. Anlauf, J.W. Bottenheim, Y.Z. Tang, H.A. Wiebe, J.M. Roberts, R.L. Tanner, L. Newman, V.C. Bowersox, J.F. Meagher, K.J. Olszyna, M.O. Rodgers, T. Wang, H. Berresheim, K.L. Demerjian, U.K. Roychowdhury, “Correlation of ozone with NOy in photochemically aged air,” J. Geophys. Res., 98 (D2), 2917-2925 (1993).

M. Trainer, B.A. Ridley, M.P. Buhr, G. Kok, J. Walega, G. Hübler, D.D. Parrish, F.C. Fehsenfeld, “Regional ozone and urban plumes in the southeastern United States: Birmingham, a case study,” J. Geophys. Res., 100 (D9), 18,823-18,834 (1995).

T. Tran, H. Tran, M. Mansfield, S. Lyman, E. Crosman, “Four dimensional data assimilation (FDDA) impacts on WRF performance in simulating inversion layer structure and distributions of CMAQ-simulated winter ozone concentrations in the Uintah Basin,” Atmospheric Environment, 177, 75-92 (2018).

R. Tuttle, “Chevron Powering Oil Pumps with Solar Panels,” Rigzone, July 23, 2020, https://www.rigzone.com/news/wire/chevron_powering_oil_pumps_with_solar_panels-23-jul-2020-162807-article/, last referenced 02/2022.

[UC 2021] Uintah County General Plan, http://co.uintah.ut.us/document_center/CommunityDevelopment/General%20Plan%202017%20Update%202-1-2021.pdf, last referenced 02/2022.

[UCAR 2022] https://www.mmm.ucar.edu/weather-research-and-forecasting-model Last referenced 02/2022.

O. Urquidez, 1898 & Co., “Five factors form the basis for wellfield electrification decisions,” https://1898blog.burnsmcd.com/five-factors-form-the-basis-for-wellfield-electrification-decisions, March 22, 2021, last referenced 02-2022 (b).

O. Urquidez, Burns & McDonnell, “Oilfield Electrification: Collaboration between producers and utilities can result in a win-win,” https://www.burnsmcd.com/insightsnews/1898/white-papers/oilfield-electrification-collaboration-win-win, last referenced 02/2022 (a).

Utah Division of Air Quality, [UDAQ 2021a] last referenced 08/2021. https://documents.deq.utah.gov/air-quality/planning/technical-analysis/research/oil-and-gas/DAQ-2017-011495.pdf

Utah Division of Oil, Gas, and Mining [UDOGM 2021a], https://oilgas.ogm.utah.gov/oilgasweb/live-data-search/lds-prod/prod-lu.xhtml, last referenced 09/2021.

Utah Division of Oil, Gas, and Mining [UDOGM 2021b], https://oilgas.ogm.utah.gov/oilgasweb/ last referenced 12/2021.

[UDWS 2022] Utah Economic Data Viewer, Department of Workforce Services, https://jobs.utah.gov/jsp/utalmis/#/, last referenced 02-2022.

K.S. Varde, N. Patro, K. Drouillard, "Lean Burn Natural Gas Fueled S.I. Engine and Exhaust Emissions," SAE Technical Paper Series, 952499, Fuels & Lubricants Meeting & Exposition, Toronto, Ontario, October 16-19, 1995.

Y. Wang, J.A. Logan, D.J. Jacob, "Global simulation of tropospheric O_3-NO_x-hydrocarbon chemistry: 2. Model evaluation and global ozone budget," J. Geophys. Res., 103 (D9), 10,727-10,755 (1998b).

Western Regional Air Partnership [WRAP], https://www.wrapair2.org/phaseiii.aspx, "Development of Baseline 2006 Emissions from Oil and Gas Activity in the Uinta Basin," (2009).

G. M. Wolfe, M. M. Marvin, S. J. Roberts, K. R. Travis, and J. Liao, The Framework for 0-D Atmospheric Modeling (F0AM) v3.1, Geoscientific Model Development, doi: 10.5194/gmd-2016-175, 2016.

E.C. Wood, S.C. Herndon, T.B. Onasch, J.H. Kroll, M.R. Canagaratna, C.E. Kolb, D.R. Worsnop, J.A. Neuman, R. Seila, M. Zavala, W.B. Knighton, "A case study of ozone production, nitrogen oxides, and the radical budget in Mexico City," Atmos. Chem. Phys., 9, 2499-2517 (2009). "acp-9-2499-2009.pdf"

Wyoming Air Quality Division, "State of Wyoming Air Quality Division Portable Analyzer Monitoring Protocol," (2006). https://deq.wyoming.gov/aqd/compliance/inspections/

G. Yarwood, "Carbon Bond Mechanism: CB6," https://acm.aqrc.ucdavis.edu/sites/g/files/dgvnsk3471/files/inline-files/ACM2020_Yarwood_CB6.pdf

R.M. Yonk, R.T. Simmons, “The Role of Oil and Gas and Amenities in County Economic Development,” https://www.api.org/news-and-media/docs/~/media/files/news/2013/13-august/liberty%20final%20report%205.pdf, last referenced 02/2022.

R. Zong, L. Xue, T. Wang, W. Wang, “Inter-comparison of the Regional Atmospheric Chemistry Mechanism (RACM2) and Master Chemical Mechanism (MCM) on the simulation of acetaldehyde,” Atmospheric Environment, 186, 144-149 (2018).